Université de Lille 1 SCIENCES ET TECHNOLOGIES

N° d'ordre:

UNIVERSITÉ LILLE 1 - SCIENCES ET TECHNOLOGIES

**École doctorale :** Ecole doctorale Sciences Pour l'Ingénieur Université Lille Nord-de-France - 072

# THÈSE

pour obtenir le grade de

## docteur

Discipline : Micro et nano technologies, acoustique et télécommunications

présenté par

YAN Xin

# Robustesse aux interférences dans les réseaux de capteurs

Soutenue le 10 décembre 2015

Jury :

| | | | |
|---|---|---|---|
| GELLÉ | GUILLAUME | Professeur, Université de Reims Champagne-Ardenne | Rapporteur |
| POULLIAT | CHARLY | Professeur, ENSEEIHT | Rapporteur |
| GOUPIL | ALBAN | Maitre de conférence, Université de Reims Champagne-Ardenne | |
| MARY | PHILIPPE | Maitre de conférence, IETR INSA de Rennes | |
| COUDOUX | FRANÇOIS-XAVIER | Professeur, Université de Valenciennes et du Hainaut | |
| SIMON | ÉRIC | Professeur, TELECOM Lille 1 | |

Thèse dirigée par :

| | | |
|---|---|---|
| CLAVIER | LAURENT | Professeur, Université de Lille 1/TELECOM Lille |

Université de Lille 1 SCIENCES ET TECHNOLOGIES

N° of order:

LILLE 1 UNIVERSITY - SCIENCE AND TECHNOLOGY

**Doctoral school:** Ecole doctorale Sciences Pour l'Ingénieur Université Lille Nord-de-France - 072

# THESIS

in order to become

# Doctor

Subject: Micro and Nanotechnologies, Acoustics and Telecommunications

defended by

YAN Xin

# Robustness against interference in sensor networks

Defended on 10th December, 2015

Dissertation committee:

| | | | |
|---|---|---|---|
| GELLÉ | GUILLAUME | Professor, University of Reims Champagne-Ardenne | Recorder |
| POULLIAT | CHARLY | Professor, ENSEEIHT | Recorder |
| GOUPIL | ALBAN | Associate professor, University of Reims Champagne-Ardenne | |
| MARY | PHILIPPE | Associate professor, IETR INSA Rennes | |
| COUDOUX | FRANÇOIS-XAVIER | Professor, University of Valenciennes and Hainaut | |
| SIMON | ÉRIC | Professor, TELECOM Lille | |

Ph. D. thesis supervised by:

LAURENT CLAVIER Professor, Lille 1 University/TELECOM Lille

**Keywords:** Sensor networks, Interference, stable distributions, dependence, copulas

**Mots clés :** réseaux de capteurs, interférence, distributions stables, dépendance, copules

This thesis was prepared in


Institut de Recherche sur les Composants logiciels et matériels pour l'Information et la Communication Avancée
Parc Scientifique de la Haute Borne
50, avenue Halley
B.P. 70478
59658 Villeneuve d'Ascq, France
☎ + 33 (0) 3 62 53 15 00
FAX +33 (0) 3 20 71 70 42
✉ secretariat@ircica.univ-lille1.fr
Site http://www.ircica.univ-lille1.fr/

# Acknowledgements

I would first like to express my special appreciation and thanks to my advisor Professor CLAVIER Laurent, for supporting me during these past three years, and for having been a tremendous mentor for me. I would like to thank him for encouraging my research patiently and for allowing me to grow as a research scientist. Your advices on the research were priceless.

Besides my advisor, I would also like to thank my committee members, professor GUILLAUME Gellé, professor CHARLY Poulliat, associate professor ALBAN Goupil, associate professor MARY Philippe, professor COUDOUX François-Xavier and associate professor SIMON Eric for serving as my committee members.

I am also very grateful to professor PETERS Gareth for his scientific advice and knowledge and many insightful discussions and suggestions. I want to thank all the people who have cooperated with me: Nourddine AZZAOUI, François SEPTIER, Ido NEVAT.

I thank all the members of the CSAM group and people I have known in IRCICA: Nathalie, ROLLAND, Christophe LOYEZ, Alexandre BOE, Philippe Mariage, Rédha KASSI, Bernard VERBEKE, Amal ABBADI, Kamel GUERCHOUCHE, Roman IGUAL, Aymeric PASTRE, Viktor TOLDOV, Mauro de FREITAS, Wei GU, Peggy STANKOWSKI, Michel SOULAGE, Ahmed BEN ABDESELAM and etc.

My family is what I want to thank most. Words cannot express how grateful I am to my mother and father for all of the sacrifices that you've made for supporting my study in foreign country. I would also thank my two grandmothers, my aunts and uncles, my cousins. Specially, I want to thank to my two grandfathers who have left away. I hope they can see it from the star.

Last but not the least, I would also like to thank all of my friends who supported me in writing, and incented me to strive towards my goal: Freddy JAFFRE, Yanwen Wu, Yanwen QIN, Didier LEPELTIER, Shiqi CHENG, Sijia GU, Zhifan JIANG, Haoling QI and etc.

I want to rethank to all the people I mentioned above and also to the people whom I didn't mentioned but directly or indirectly helped me during my study. Without your help, I won't be here.

# Abstract

Modern wireless system designs are increasingly involving dense deployment architectures for wireless networks. Such a feature makes interference in these networks an important limitation to the system performance. In several situations, such as wireless ad-hoc or ultra wide band impulse radio, this interference exhibits an impulsive behaviour. Such impulsive behaviour is often badly captured by the classical Gaussian model.

It has been shown that, with such interference, the classical linear receiver, optimal for Gaussian noise, is no longer robust. Many works have proposed solutions to adapt the receiving strategy, showing significant performance gains. However, all those works rely on interference distributions assumptions. Either distributions are empirically proposed, exhibiting a better fit with the interference law in the studied context, or exact analytical expressions are derived but generally lead to infinite series expressions, complex to handle for an efficient receiver design.

Most of the conventional works were done under the premise of an assumption of independent and identically distributed interference random variables. However, space, time or frequency diversity can result in vectors with dependent components. In time hopping ultra wide band the combination of interferers changes at each pulse, a strong interferer will present during a long period in comparison to the bit duration. It will increase the probability of strong interference simultaneously on different repetitions. Another example is in a multiple receive antenna system, a strong interferer will simultaneously be received on several antennas, giving a non zero probability of having several strong interference sample on the same sample. Consequently, this independence assumption is, in many cases, not realistic.

In this thesis, we first give a general system model and give several distributions and models, and we compare them in modelling the impulsive interference. We then evaluate the robustness of different receiver strategies proposed when the noise model changes. We propose to classify the different ways to define receivers. We give also the parameter estimation method and we illustrate their performance under an impulsive interference environment. We also propose a first approach to model the time and/or space dependency of the interference samples. We use the framework of copulas that allows separating the marginal distributions and the dependence structure of the inter-

ference. We use the flexible family of the skew-t copulas and show that it significantly impacts the performance of a receiver.

# Résumé

Le design modern des systèmes sans fil concerne de plus en plus un déploiement dense d'architectures pour des réseaux sans fil. Par conséquence, l'interférence devient une limitation importante à la performance du système de ces réseaux. Dans plusieurs situations, comme ad-hoc sans fil ou transmission de impulsion radio de ultra large bande, les interférences présentent un comportement impulsif. Ce comportement impulsif est souvent mal capté par le modèle Gaussien classique.

Avec telles interférences, le récepteur linéaire classique qui est optimal pour un bruit gaussien n'est plus robuste. Des nombreuses solutions sont proposées pour adapter la stratégie de réception, en montrant des gains significatifs de performance. Cependant, tous ces travaux sont fait sous des hypothèses des distributions d'interférence. Les distributions sont empiriquement proposée, en présentant un meilleur ajustement à la loi de l'interférence dans le contexte étudié, ou des expressions analytiques exactes sont dérivées, mais généralement avec une expression de série infinie, qui est très compliqué à gérer pour l'efficace de récepteur.

La plupart des travaux classiques ont été faites sous une hypothèse de variables aléatoires indépendantes et identiquement distribuées interférence. Cependant, une diversité spatiale, temporelle ou fréquentielle peuvent donner des vecteurs un composant dépendant. Comme dans time hopping ultra large bande où la combinaison de interférence change à chaque impulsion, une interférence forte présentera pendant une longue période par rapport à la durée d'un bit. Il va accroître la probabilité d'une forte interférence simultanément sur différentes répétitions. Un autre exemple est dans un système de réception avec plusieurs antennes, une interférence forte sera simultanément être reçue sur plusieurs antennes. Ça donne plus de probabilité d'avoir plusieurs interférences fortes sur le même échantillon. Par conséquence, cette hypothèse d'indépendance n'est plus réaliste dans de nombreux cas.

Dans cette thèse, nous donnons d'abord un modèle du système général et donner plusieurs modèles de l'interférence impulsive. Nous évaluons ensuite la robustesse de différentes stratégies des récepteur avec differents modèles de bruit. Nous proposons des nouveaux récepteurs basés sur différents principaux. Nous donnons également la méthode d'estimation des paramètres et nous illustrons leur performance dans un environnement d'interférence impulsive. Nous proposons une première approche pour mo-

déliser la dépendance temporelle et spatiale d'interférence. Nous utilisons copule qui permet de séparer les distributions marginales et la structure de dépendance d'interférence. Nous utilisons une famille flexible, skew-t copule, et on montrons son impact significatif sur la performance d'un récepteur.

# Contents

**List of Tables** **xiii**

**List of Figures** **xv**

**Introduction** **xix**

**1 Non Gaussian Interference** **1**
1.1 Wireless Network Interference Model in Spatial Random Fields . . . . . 1
1.2 The independent case . . . . . 5
1.3 Different interference model . . . . . 7

**2 Receiver Design - the independent case** **25**
2.1 System scenario . . . . . 25
2.2 Impact of impulsive interference noise on optimal decision regions . . . . 29
2.3 Robust reception . . . . . 32
2.4 Simulation results . . . . . 51

**3 Dependence** **67**
3.1 System model . . . . . 68
3.2 Sub-Gaussian Model . . . . . 70
3.3 Copula . . . . . 74
3.4 Skew-$t$ copula . . . . . 77
3.5 Result analysis . . . . . 104

**General conclusion** **105**

**A The $\alpha$-stable case** **107**

**Bibliography** **113**

# List of Tables

2.1 Receiver strategies. . . . . 34
2.2 Mean and variance for the estimated values of $\kappa$ in different situations and varying training sequence length. 1000 estimations were used. . . . . 41
2.3 Mean and variance for the estimated values of $p$ in the same situations as Table 2.2 and varying training sequence length. 1000 estimations were used. . . . . 50
2.4 Comparison of different receivers' performance in different noise . . . . . 65

3.1 Different setting of parameter and their dependence . . . . . 87
3.2 Estimation result of Skew-t copula . . . . . 92

# List of Figures

1.1 Gaussian noise $\mu = 0, \sigma^2 = 1$ . . . . . 8
1.2 Gaussian noise pdf $\mu = 0, \sigma^2 = 1$ . . . . . 9
1.3 Gaussian noise A= $0.2$, Ratio= $10^{-1}$ . . . . . 10
1.4 Middleton Class A distribution pdf with different parameter setting . . . . 11
1.5 The probability density function of an $\alpha$-stable distribution with $\mu = 0$, $\gamma = 1$ and different values of $\alpha$ and $\beta$ . . . . . 13
1.6 Comparison of noises for symmetric $\alpha$-stable distribution $(\alpha = 1.5)$ and Gaussian distribution $\alpha = 2$. . . . . 14
1.7 Comparison of probability density function for symmetric $\alpha$-stable distribution $(\alpha = 1.5)$ and Gaussian distribution $\alpha = 2$. . . . . 14
1.8 Zoom of probability density function for symmetric $\alpha$-stable distribution $(\alpha = 1.5)$ and Gaussian distribution $\alpha = 2$. . . . . 15
1.9 Comparison of probability density function for $\epsilon$-contaminated distribution $(\epsilon = 0.1, \kappa = 10, \sigma^2 = 1)$ and Gaussian distribution $\mu = 0, \sigma^2 = 1$. . . . 20
1.10 $\epsilon$-contaminated noise . . . . . 20
1.11 Guassian noise . . . . . 21
1.12 pdf of Gaussian mixture noise ($P = 3$, $\lambda_1 = 0.1$, $\mu_1 = -0.1$, $\sigma_1^2 = 1$, $\lambda_2 = 0.8$, $\mu_2 = 0$, $\sigma_2^2 = 0.1$, $\lambda_3 = 0.1$, $\mu_3 = 0.1$, $\sigma_3^2 = 1$) . . . . . 22
1.13 Gaussian mixture noise ($P = 3$, $\lambda_1 = 0.1$, $\mu_1 = -0.1$, $\sigma_1^2 = 1$, $\lambda_2 = 0.8$, $\mu_2 = 0$, $\sigma_2^2 = 0.1$, $\lambda_3 = 0.1$, $\mu_3 = 0.1$, $\sigma_3^2 = 1$) . . . . . 23
1.14 Gaussian noise . . . . . 23
1.15 Generalized Gaussian distribution noise . . . . . 24
1.16 pdf of Generalized Gaussian distribution with different parameters . . . . 24

2.1 The system SIMO . . . . . 27
2.2 Decode-and forward (DF) relaying communications scheme . . . . . 27
2.3 Relaying communications with interferences . . . . . 28
2.4 Rake receiver with 5 fingers . . . . . 28

2.5 Example realisations for each different impulsive noise processes. The following parameters were used in each case: Gaussian case ($\mu = 0$ and $\sigma^2 = 1$); Generalized Gaussian case ($\alpha = 1$, $\beta = 0.2$); $\epsilon$-contaminated case ($\epsilon = 0.1$, $\kappa = 10$, $\sigma^2 = 1$); Gaussian mixture case ($P = 3$, $\lambda_1 = 0.1$, $\mu_1 = -0.1$, $\sigma_1^2 = 1$, $\lambda_2 = 0.8$, $\mu_2 = 0$, $\sigma_2^2 = 0.1$, $\lambda_3 = 0.1$, $\mu_3 = 0.1$, $\sigma_3^2 = 1$); Sum of Gaussian and $\alpha$-stable in a highly impulsive case ($\alpha = 1.2$, $\gamma = 1$ and $\sigma^2 = 0.1$); Sum of Gaussian and $\alpha$-stable in a moderate impulsive case ($\alpha = 1.5$, $\gamma = 1$ and $\sigma^2 = 0.25$). . . . . 30
2.6 Optimal decision regions for the different noise processes. We use the same parameters defined in Fig. 2.5: the received vector $\mathbf{Y}$ is composed of two received samples (two dimensions, $\mathbf{Y} = [y_1\ y_2]$), the wireless channel is set to $\mathbf{h} = [1\ 1]$, and we consider three possible transmitted values (ie. $\Omega = \{-1, 0, 1\}$). . . . . 31
2.7 Optimal decision regions for the different noise processes. with two possible transmitted values . . . . . 33
2.8 NIG triangle characterizing the flexibility of the skewness and kurtosis properties of the NIG family of models. . . . . 43
2.9 Decision regions for the NIG receiver when $\alpha = 0.3$ or $2.5$ ($\delta = 1$ and $\beta = \mu = 0$). . . . . 45
2.10 NIG and Myriad approximations of a mixture of stable ($\alpha = 1.2$ and $\gamma = 1$) and Gaussian ($\sigma^2 = 0.2$)(high impulsive case) . . . . . 46
2.11 NIG and Myriad approximations of a mixture of stable ($\alpha = 1.2$ and $\gamma = 0.28$) and Gaussian ($\sigma^2 = 0.2$)(low impulsive case) . . . . . 47
2.12 LLR for different noises. The very and slightly impulsive cases are defined as in Table 2.2 with $\gamma = 0.1$ in both case. The $\epsilon$-contaminated as the same parameters as in Fig. 1.10. The value of $p$ is $0.5$. . . . . 51
2.13 Comparison of different noise dominating environments . . . . . 52
2.14 BER of different receivers under Gaussian noise . . . . . 53
2.15 BER of different receivers under slightly impulsive noise environment . . . 55
2.16 Moderate impulsive environment . . . . . 56
2.17 Highly impulsive environment . . . . . 58
2.18 pdf of decision statistics in dominant $\alpha$-stable noise plus Gaussian noise. . 59
2.19 Performance in $\epsilon$-contaminated noise . . . . . 60
2.20 pdf of decision statistics in $\epsilon$-contaminated noise. . . . . 60
2.21 Performance in Gaussian mixture model noise. . . . . 61
2.22 Performance in generalized Gaussian distribution model noise. . . . . 62
2.23 Performance in Middleton Class A noise. . . . . 63

3.1 Case 1: example of interference samples on a TH-PPM-UWB system. . . . 69
3.2 Case 2: example of interference samples on a SIMO system (independent). 70
3.3 Case 2: example of interference samples on a SIMO system (dependent). . 71

3.4 Isotropic Case: Sub-Gaussian samples . . . . . 72
3.5 Anisotropic Case: $\alpha$-stable samples . . . . . 73
3.6 Case 1: independent samples. ($\nu = 5$, $\sigma = 0$, $\beta = 0$) . . . . . 86
3.7 Case 2: tail dependence ($\nu = 1$, $\sigma = 0$ $\beta = 0$) . . . . . 87
3.8 Case 3: linear dependence ($\nu = 3$ $\sigma = 0.9$ $\beta = 0$) . . . . . 88
3.9 Case 4: asymetric dependence ($\nu = 3$ $\sigma = 0$ $\beta = 2$) . . . . . 88
3.10 Effect of the parameters of copula . . . . . 89
3.11 Estimation process of skew-t copula . . . . . 90
3.12 Receivers performance in sub-Gaussian noise under a slightly impulsive environment with temporal dependence $NIR = 10dB$ . . . . . 93
3.13 Receivers performance in sub-Gaussian noise under a moderate impulsive environment with temporal dependence $NIR = 0dB$ . . . . . 94
3.14 Receivers performance in sub-Gaussian noise under a highly impulsive environment with temporal dependence $NIR = -10dB$ . . . . . 95
3.15 Receivers performance in sub-Gaussian noise under a slightly impulsive environment with spatial dependence$SNR = 10dB$ . . . . . 96
3.16 Receivers performance in sub-Gaussian noise under a moderate impulsive environment with spatial dependence$SNR = 0dB$ . . . . . 97
3.17 Receivers performance in sub-Gaussian noise under a highly impulsive environment with spatial dependence$SNR = -10dB$ . . . . . 98
3.18 MRC in Gaussian noise with copula structure . . . . . 100
3.19 $p$-norm receiver in Gaussian noise with copula structure . . . . . 101
3.20 $p$-norm receiver in $\alpha$-stable noise copula structure . . . . . 102
3.21 MRC receiver in $\alpha$-stable noise with copula structure . . . . . 103

# Introduction

A radical change is happening and will grow in the coming years due to the exponential increase of communicating objects in wireless networks: the interconnection of perhaps 100 times more communicating objects than what exists nowadays. The consequence is a denser deployment of wireless networks.

It becomes a hot topics these years. We can quote Stéphane Richard, CEO of Orange, which plans to invest $600$ million euros in Internet of Things (IoT)[1]:

"*[...] the Internet of Things looks like a ground swell in coming years. It is estimated that there will be over* $25$ *billion devices connected worldwide in 2020. As part of our new strategic plan Essentiels2020, Orange aims to become the benchmark operator of the Internet of Things. To meet all the needs, we have decided, in addition to cellular networks, deploying a national network dedicated to objects requiring low speed connectivity and low power consumption. The network, based on LoRa technology, will be gradually opened from the first quarter 2016.*"

And many more companies are investing in this topic like Texas Instrument [2], Bouygues Telecom[3], Google[4], Apple... CISCO, Sagemcom, IBM and others invest in the LoRa alliance[5]. Sigfox[6] is growing very quickly selling low power communication technologies. It also creates many opportunities for start-ups. We can cite World Sensing[7], monitoring infrastructures or parking spaces ; NooliTIC[8], optimizing energy consumption in data centres or monitoring patients in hospitals ; Sen.se[9] proposing wireless sensors for many different personal applications.

[1] http://www.frenchweb.fr/apres-bouygues-telecom-orange-ecarte-sigfox-pour-son-projet-iot/206903#7uaLl4t3BzQzBeS1.99
[2] http://www.ti.com/ww/en/internet_of_things/iot-overview.html
[3] http://www.bouyguestelecom-entreprises.fr/m2m/m2m-potentiel-activites
[4] https://cloud.google.com/solutions/iot/
[5] https://www.lora-alliance.org/
[6] http://www.sigfox.com/fr/
[7] http://www.worldsensing.com/
[8] http://www.noolitic.fr/index.html
[9] https://sen.se/mother/

For the European research actors, we can refer to the COST IC1004 White Paper[10] on *scientific challenges towards 5G mobile communications* to confirm these thoughts:

*In further developments of machine to machine and other types of sensors connectivity [...] future scenarios in radio communications give rise to situations where a huge number of devices are located in physical proximity, generating large amounts of independent traffic with different requirements, and at the same time are to share the same pool of radio resources. The number of contenders for the radio resources in such situations can potentially be much higher than those manageable by traditional wireless architectures, protocols and procedures, so Radio Access Networks have to evolve to new paradigms.*

This suggests that Machine-to-Machine (M2M) and Internet of Things (IoT) communications will have a huge impact on the future telecommunication market with the deployment of billions of communicating objects. Those objects will be low cost and will have strong energy constraints. How will they handle the heavily occupied spectrum, especially in the ISM, license free, bands?

In this context, it is essential that technological solutions can anticipate the environmental evolution. Due to the increase of the density of wireless communications, interference will become one of the main limitations to the system performance.

The interference channel has been studied for long in information theory [20, 47, 78, 17]. If the exact capacity is not known some close approximation have been derived. The question on how to deal with interference is however still an open problem. A lot of works on multiuser detectors for instance have been proposed [87] but also, more recently, some new schemes for interference alignment [17] or even amplifying interference [25]. We think that the limited complexity and energy available on a node will not allow to use sophisticated signal processing solution to fully suppress interference. If the exact amount of this interference is still difficult to predict, some will remain and receivers will have to deal with it.

In several situations, like wireless *ad hoc* networks [84, 89, 88, 19] or ultra wide band impulse radio [36, 30, 39], this interference exhibits an impulsive behaviour, badly captured by Gaussian model.

Recent works tackling the interference in large scale cellular networks have been based on Poisson point process models [7, 8, 88]. However tractable models are still unavailable. They clearly show the impulsive nature of interference[74, 75]. A mathematical analysis leads to the $\alpha$-stable family as a good representative of such interference in many contexts. Its main advantages are the stability property (a sum of $\alpha$-stable

[10] White paper, cost IC1004, "Scientific challenges towards 5G mobile communications", Dec. 2013.

random variable is an $\alpha$-stable random variable) leading to a generalized form of the central limit theorem and the fact that it includes the Gaussian distribution. The difficulty is that, in general, the probability density function, although depending on four parameters only, has no analytical expression. It then raises some difficult mathematical challenges to apply this family to wireless communications.

It has been shown that, with such an interference, the classical linear receiver, optimal for Gaussian noise, is no longer robust. Many works have proposed solutions to adapt the receiving strategy, showing significant performance gains. However, all those works rely on interference distributions assumptions. Either distributions are empirically proposed, exhibiting a better fit with the interference law in the studied context. Or exact analytical expressions are derived but generally lead to infinite series expressions, complex to handle for an efficient receiver design.

**This work tries to anticipate the evolution of telecommunications and to develop robust communication solutions with this simple point of view: many nodes will not have sufficient energy or software capabilities to support complex signal processing techniques to handle interference. They will see it as a noise. The difficulty is that this noise will not necessarily be Gaussian. Consequently, the usual linear receiver is not optimal and new strategies have to be implemented. Besides, these strategies need to be robust against a changing environment (high or low density of nodes, high or low activity, presence or not of competing networks...).**

Our first objective is to evaluate the robustness of different receiver strategies when the noise model changes (Gaussian, $\epsilon$-contaminated, Gaussian Mixture, Generalized Gaussian, $\alpha$-stable+Gaussian). We propose to classify the different ways to define receivers. The first way is based on a linear design. This is optimal if noise is Gaussian and results in very low complexity solutions. However, performance rapidly degrade when impulsiveness is present. A second way is to base the design on a selected parametric distribution. We consider two constraints on the choice of the distribution. First it has to be flexible enough to represent a wide variety of environment. The receiver has to exhibit good performance in Gaussian noise or in highly impulsive environment. The main illustrations of such distributions are given by the Myriad filters and the Normal Inverse Gaussian (NIG) receiver. Second, estimation of the parameters has to be rather easy in order to be implemented online. Finally, a third way is to directly approximate the log-likelihood ratio function. An old idea is to use a linear part for small received value and, for values higher than a given threshold, to limit the decoded value to a maximum or even to null this value. More complex function can also be used. We will also propose to approximate this function using the $p$-norm. Receiver is indeed simply a distance calculation between the received symbol and the possibly transmitted ones. The euclidean norm (corresponding to $p = 2$) is optimal in the Gaussian noise case. Reducing the value of $p$ allows to have distances that are better suited to impulsive interference.

The first part of this manuscript assumes that interference samples are independent. In many context this assumption may not be true. However, due to the impulsive context, the classical correlation used to model dependency may not be sufficient. For example, it does not take into account upper tail dependence, meaning the probability to have simultaneously two large interference events on two samples. We propose in this work a first approach to model the time and/or space dependency of the interference samples. We use the framework of copulas that allows to separate the marginal distributions (that was studied in the first part) and the dependence structure of the interference. We use the flexible family of the skew-$t$ copulas and show that it significantly impact the performance of a receiver.

Chapter 1

# Non Gaussian Interference

## 1.1 Wireless Network Interference Model in Spatial Random Fields

We consider a generic multi-user wireless system model without power control in which we derive the interference model for a received signal observed in the presence of a random number of unknown spatially distributed interferers. We treat the interfering users as spatially Poisson distributed and their transmitted signals are subject to a power-law propagation loss function.

The system model is defined as follows:

1. Consider an unknown number of spatially distributed transmitters denoted by $N$. They are distributed on a circular domain $\Omega(A_{\mathcal{R}}) := \left\{\mathbf{x} \in \mathbb{R}^2 : \|\mathbf{x}\| \leq r_T\right\}$ with area $A_{\mathcal{R}}$, at locations indexed by $\mathcal{L} = \left\{L^{(i)}\right\}_{i=1\ldots N}$ according to an homogeneous spatial Poisson process with intensity parameter $\lambda$. Therefore, the number of transmitters in $\Omega(A_{\mathcal{R}})$ has distribution

$$\mathbb{P}(N = n) = \frac{(\lambda A_{\mathcal{R}})^n}{n!} \exp(-\lambda A_{\mathcal{R}}). \tag{1.1}$$

2. The $i$-th interferer $(i \in \{1, 2, \ldots, N\})$ transmits a signal using a shaping filter $g^{(i)}(t)$. We denote by $X_n^{(i)}$ the unknown $i$-th interferers transmitted symbol. Consequently, in the time domain the representation of the $i$-th interferer symbol is given by:

$$S_n^{(i)}(t) = X_n^{(i)} g^{(i)}(t), \tag{1.2}$$

The central frequency of the transmission is denoted by $f_i$. So that its signal is:

$$s^{(i)}(t) = \left( \sum_{n=-\infty}^{+\infty} S_n^{(i)}(t - nT_s) \right) \exp(2j\pi f_i t) = ( \sum_{n=-\infty}^{+\infty} X_n^{(i)} g_k^{(i)}(t - nT_s)) \exp(2j\pi f_i t) . \tag{1.3}$$

3. The distance of the $i$-th interferer from the receiver, $R^{(i)}$, is a random variable, given by:

$$R^{(i)} = \left\| L^{(i)} - l^R \right\|, \tag{1.4}$$

where $L^{(i)}$ is a random location of the $i$-th potential interferer and $l^R$ is a known location of the receiver in region $\mathcal{R}$. Given $N = n$ total interferers, the location of the $i$-th interferer is uniformly distributed in space over the *circular interference domain* with a distribution given by:

$$f_{R^{(i)}|N}(r|N = n) = \begin{cases} \dfrac{2r}{r_T^2}, \text{ if } 0 \leq r \leq r_T \\ 0, \text{ otherwise,} \end{cases} \tag{1.5}$$

where $r_T$ is the maximal distance in which an interfere can have a non-negligible contribution to the interference.

4. For the $i$-th interferer, the baseband representation of the channel experienced by the symbol $X_n^{(i)}$ is given by $\frac{A^{(i)} e^{j\Phi^{(i)}}}{(R^{(i)})^{\sigma/2}}$. The random variable for the phase, denoted by $\Phi^{(i)}$, is uniformly distributed in $[0, 2\pi]$. The path loss experienced by the $i$-th interferer is given by $(R^{(i)})^{-\frac{\sigma}{2}}$, where $\sigma$ is the attenuation coefficient, a deterministic and known parameter reflecting the physical environment in which transmission is occurring. $A^{(i)} e^{j\Phi^{(i)}}$ is a complex coefficient that contains the shadowing and multipath fading. This representation is general enough to encompass all commonly encountered fading models. We will illustrate three practically important cases corresponding to the Rayleigh, Rice and Nakagami fading scenarios.

5. The total interference experienced by the received signal, for symbol received between $t = 0$ and $t = T_s$, after applying the target users shaping filter $\left(g^{(0)}\right)$ at

the receiver side is given by:

$$\begin{aligned} Y_0^{(i)} &= \int_0^{T_s} r^{(i)}(u) e^{-2j\pi f_0 u} g^0(-u) du \\ &= \int_0^{T_s} \sum_{n=-\infty}^{+\infty} X_n^{(i)} g^{(i)}(u - nT_s - \Delta^{(i)}) \exp\left(2j\pi f_i (u - \Delta^{(i)})\right) \\ &\qquad \times \frac{A^{(i)} e^{j\Phi^{(i)}}}{(R^{(i)})^{-\sigma/2}} e^{-2j\pi f_0 u} g^{(0)}(-u) du \end{aligned} \tag{1.6}$$

If we consider that $g^{(i)}(t)$ is long and at least as long as $g^{(0)}(t)$, at most two consecutive symbols can interfere with the symbol we are trying to detect ($n_1^{(i)}$ et $n_2^{(i)}$). Further extension are possible if interfering bandwidth is larger than the useful one.

$$\begin{aligned} Y_0^{(i)} &= \int_0^{T_s} X_{n_1^{(i)}}^{(i)} g^{(i)}(u - n_1^{(i)} T_s - \Delta^{(i)}) \exp\left(2j\pi f_i (u - \Delta^{(i)})\right) \\ &\qquad \times \frac{A^{(i)} e^{j\Phi^{(i)}}}{(R^{(i)})^{\sigma/2}} e^{-2j\pi f_0 u} g^{(0)}(-u) du \\ &\quad + \int_0^{T_s} X_{n_2^{(i)}}^{(i)} g^{(i)}(u - n_2^{(i)} T_s - \Delta^{(i)}) \exp\left(2j\pi f_i (u - \Delta^{(i)})\right) \\ &\qquad \times \frac{A^{(i)} e^{j\Phi^{(i)}}}{(R^{(i)})^{\sigma/2}} e^{-2j\pi f_0 u} g^{(0)}(-u) du \\ &= \int_0^{T_s} \sum_{n=n_1^{(i)}, n_2^{(i)}} X_n^{(i)} g^{(i)}(u - nT_s - \Delta^{(i)}) \exp\left(2j\pi f_i (u - \Delta^{(i)})\right) \\ &\qquad \times \frac{A^{(i)} e^{j\Phi^{(i)}}}{(R^{(i)})^{\sigma/2}} e^{-2j\pi f_0 u} g^{(0)}(-u) du \\ &= \sum_{n=n_1^{(i)}, n_2^{(i)}} \frac{1}{(R^{(i)})^{\sigma/2}} X_n^{(i)} A^{(i)} e^{j\Phi^{(i)}} \\ &\qquad \times \int_0^{T_s} g^{(i)}(u - nT_s - \Delta^{(i)}) e^{\left(2j\pi f_i (u - \Delta^{(i)})\right)} e^{-2j\pi f_0 u} g^{(0)}(-u) du \\ &= \sum_{n=n_1^{(i)}, n_2^{(i)}} \frac{1}{(R^{(i)})^{\sigma/2}} X_n^{(i)} A^{(i)} e^{j\Phi^{(i)}} \\ &\qquad \times \int_0^{T_s} g^{(i)}(u - nT_s - \Delta^{(i)}) g^{(0)}(-u) e^{\left(-2j\pi (f_0 - f_i) u - 2j\pi f_i \Delta^{(i)}\right)} du \end{aligned} \tag{1.7}$$

Let $\Theta^i = 2\pi f_i \Delta^{(i)}$.

$$\begin{aligned} Y_0^{(i)} &= \sum_{n=n_1^{(i)},n_2^{(i)}} \frac{1}{(R^{(i)})^{\sigma/2}} X_n^{(i)} A_i^{(i)} e^{j\Phi_i^{(i)}} \\ &\qquad \times \int_0^{T_s} g_i^{(i)}(u - nT_s - \Delta^{(i)}) g^{(0)}(-u) e^{-2j\pi(f_0 - f_i)u - j\Theta^{(i)}} du \\ &= \sum_{n=n_1^{(i)},n_2^{(i)}} \frac{1}{(R^{(i)})^{\sigma/2}} X_n^{(i)} A^{(i)} e^{j\left(\Phi^{(i)} - \Theta^{(i)}\right)} \\ &\qquad \times \int_0^{T_s} g^{(i)}(u - nT_s - \Delta^{(i)}) g^{(0)}(u) e^{-2j\pi(f_0 - f_i)u} du \end{aligned}$$

Finally, the resulting total interference is:

$$\begin{aligned} Y_0 &= \sum_{i=1}^{N} Y_0^{(i)} \\ &= \sum_{i=1}^{N} \sum_{n=n_1^{(i)},n_2^{(i)}} \frac{1}{(R^{(i)})^{\sigma/2}} X_n^{(i)} A^{(i)} e^{j\left(\Phi^{(i)} - \Theta^{(i)}\right)} \\ &\qquad \times \int_0^{T_s} g_k^{(i)}(u - nT_s - \Delta^{(i)}) g^{(0)}(-u) e^{-2j\pi(f_0 - f_i)u} du \\ &= \sum_{i=1}^{N} \sum_{n=n_1^{(i)},n_2^{(i)}} \frac{1}{(R^{(i)})^{\sigma/2}} X_n^{(i)} A^{(i)} e^{j\Psi^{(i)}} c_n^{(i)} \end{aligned} \tag{1.8}$$

where:

- $\Psi^{(i)} = \Phi^{(i)} - \Theta^{(i)}$ results from the phase shift induced by multipath ($\Phi^{(i)}$) and the synchronisation difference between the interferer and the useful signal ($\Theta^{(i)}$). It is rather natural to consider it as randomly distributed over $[0, 2\pi]$.
- $c_n^{(i)} = \int_0^{T_s} g^{(i)}(u - nT_s - \Delta^{(i)}) g^{(0)}(-u) e^{-2j\pi(f_0 - f_i)u} du$ is a random variable resulting from the filtering of interferer $i$ and depends on the system parameters: $\exp(2j\pi(f_i - f_0)u)$ results from the frequency down conversion; $\Delta^{(i)}$ is due to the user asynchronism.

Finally we can simplify the notation without impacting the study of this

manuscript:

$$Y = \sum_{i=1}^{N} \sum_{n=n_1^{(i)},n_2^{(i)}} \frac{1}{(R^{(i)})^{\sigma/2}} X_n^{(i)} A^{(i)} e^{j\Psi^{(i)}} c_n^{(i)}$$
$$= \sum_{i=1}^{\kappa_R} Y_I^{(i)} + j \sum_{i=1}^{\kappa_R} Y_Q^{(i)} \tag{1.9}$$

where $\kappa_R$ represents the total number of interfering symbols.

In a first part of this work, we will consider independence between the random variable. All the random factors can let us think that at two different (but even close) points in time or space, the signals should be independent. What then is a good model for $Y$, if there is one, and what should be the receiver strategy?

However, such an assumption is not fully acceptable, especially if we have some strong, line of sights, interferers. A dependency should probably be included, especially the probability of having simultaneous strong events appearing at close instants or points in space.

## 1.2 The independent case

In very general settings, following (1.9) and considering the real part only, we can write $Y$ as:

$$Y_I = \sum_{i=1}^{\kappa_R} \gamma_i \psi_i. \tag{1.10}$$

where $\gamma_i = \frac{1}{(R^{(i)})^{\sigma/2}} A^{(i)} e^{j\Psi^{(i)}}$ are positive, independent identically distributed random variables and $\psi_i = X_n^{(i)} c_n^{(i)}$ are independent, identically distributed and bounded random variables. Their probability density function is even.

Let now suppose that we are placed in a dense traffic: $\kappa_R$ is very large. Since $(\gamma_i)_{i=1,\cdots,\kappa_R}$ have finite variances, it is the same for the products $(\gamma_i\psi_i)_{i=1,\cdots,\kappa_R}$.

One intuitive approach, considering an asymptotic regime where the number of interferers grows to infinity while the contribution of each interferer to the total multiple access interference (MAI) becomes infinitesimal, would be to use the central limit theo-

rem. The MAI, then expressed as the normalized sum:

$$Z^{(\kappa_R)} = \frac{1}{\sqrt{\kappa}_R} \sum_{k=1}^{\kappa_R} \gamma_k \psi_k \tag{1.11}$$

converges in law to a normal distribution with the same variance as $\gamma_k \psi_k$. This means that $Z^{(\kappa_R)}$ is asymptotically Gaussian and by the sequel may be approximated with a normal distribution when $\kappa_R$ is large enough.

However, in the general case, the asymptotic regime is not easily reached. An in-depth study is proposed in [36] for IR-UWB signals and only a large number of users, a large processing gain and a large number of repetitions lead to a Gaussian MAI. Besides, we can discuss the condition of finite variance on $\gamma_k$. If it can seem natural because it represents a channel attenuation, the interference is compared to the desired link attenuation $\gamma_0$. If this link is long but the interfering one is short, the observed relative values of $\gamma_k$ may be "very large". These rare events are very important in our context and give an impulsive nature to attenuations. To capture these situations, heavy tailed distributions with infinite variance can be well suited while models with finite second order will fail to do so. The generalized central limit theorem has then to be used (see [67, p. 22] or [77, p. 9]) and states that the MAI (for large $\kappa_R$) falls in the domain of attraction of a random variable with a stable distribution.

**Theorem 1 (Central Limit theorem).** *In probability theory, the central limit theorem, or briefly CLT, states that, given certain conditions, the arithmetic mean of a large number of iterates of independent random variables, each with well-defined expected value and variance, will be approximately normally distributed.*

This infinite variance hypothesis is equivalent to neglecting the near field[1] when calculating the amplitude attenuation of the signal $\gamma_k$. We suppose that it is given by $\gamma_k = d_k^{-a/2}$, $a$ being the attenuation coefficient and $d_k$ the distance from interferer $k$. If interferers are uniformly distributed inside the circle $C$ of radius $R$, the attenuation probability density function is :

$$f_{\gamma_i}(x) = \frac{4x^{-\frac{4}{a}-1}}{aR^2} \quad \text{for} \quad R^{-\frac{a}{2}} \leq x < +\infty. \tag{1.12}$$

Its variance is infinite for $a > 2$. Even if this hypothesis does not correspond to reality, it is an accurate way to represent the high variability in $\gamma_k$ and the fact that there are many far users with small $\gamma_k$ but few close ones with high $\gamma_k$.

[1] If we do not neglect the near field, for $d$ less than a given distance $d_0$ the received power would not follow the same law as the one we use. A better model would be to then consider that $\gamma_k = d_0^{-a/2} \forall d < d_0$.

Considering the near field case and limiting the received power so that second order moments exist leads in general to infinite series representation of the interference. Such distributions are not easy to handle. That is why many authors have proposed some empirical choices that allow to have analytical expression when designing the receiver and assessing the performance. No model however is known to be general enough and we can expect that different contexts will lead to different models. In the rest of the chapter we will give an overview of the models that have been proposed in the literature.

## 1.3 Different interference model

We will now review some classical noise/interference models, often encountered in literature. Of course the Gaussian noise is the most used model. It is an accurate representation of the thermal noise in receivers. However, its is often no longer valid when we consider interference coming from external sources. In particular, for instance in power line communications, underwater transmissions or networks many works have proposed better adapted models. Most of this models have in common to exhibit an impulsive behaviour. We would define an impulsive behaviour as a random variable having a Probability Density Function (PDF) with a heavy tail. In probability theory, heavy-tailed distributions are probability distributions whose tails are not exponentially bounded: that is, they have heavier tails than the exponential distribution. When such models appear in the interference regime, this heavy tail behaviour significantly degrades performance unless the receiver can account for it. Consequently, models have been proposed to better take the interference behaviour into account. We can identify several approaches:

- Some analytical approaches try to derive the interference distribution. The main contributions are from Middleton and in more recent works based on stochastic geometry. If they allow to understand the impact of the physical underlying phenomena and to link this phenomena to the model parameters, they often result in difficult to tract PDF. Most of the time infinite series are obtained. Some assumption can lead to the $\alpha$-stable model, but this is not necessarily better because in most cases the PDF is not known.

- Other approaches use some mixtures of distributions. Some components of the mixture will increase the weight of the tails for instance the $\epsilon$-contaminated model or the mixture of Gaussian. They can also be seen like truncated Middleton's PDF.

- Another approach is to empirically choose a distribution based on simulation or measurements.

The following of this section will detail some of the most commonly used models.

### 1.3.1 Gaussian model

In any communication system, thermal noise, caused by the vibrations of atoms in conductors, affects the receiver. It can be seen as the sum of many independent and identically distributed contributions. Consequently, resulting from the central limit theorem (with finite variance added random variables), the total noise is Gaussian distributed.

Due to its omni-presence and to the fact that it is in many situations the only significant noise, most of the conventional signal processing research use the Gaussian model.

The Gaussian noise PDF is givent by (1.13):

$$p(x) = \frac{1}{\sigma\sqrt{2\pi}} \exp^{-\frac{(x-\mu)^2}{2\sigma^2}} \tag{1.13}$$

where $x$ represents the random variable, $\mu$ the mean value and $\sigma$ the standard deviation.

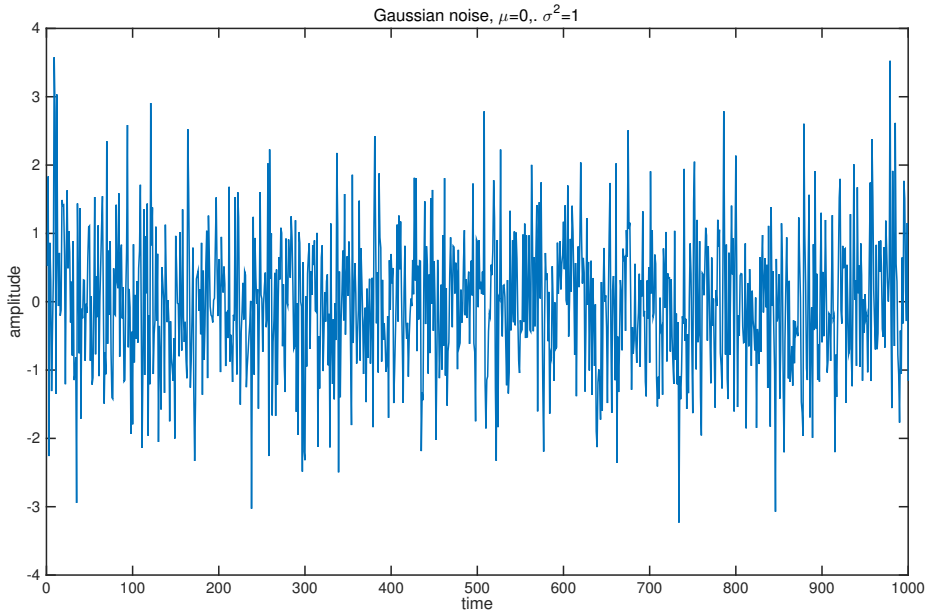


Figure 1.1: Gaussian noise $\mu = 0, \sigma^2 = 1$

Figure 1.1 and 1.2 shows the Gaussian noise and its pdf curve when $\mu = 0$ and $\sigma^2 = 1$.What is important to have in mind here is:

- firstly, looking at the noise plot in Fig. 1.1 that no sample "get out of the frame". In other words there are no outliers and the behaviour of the random process is

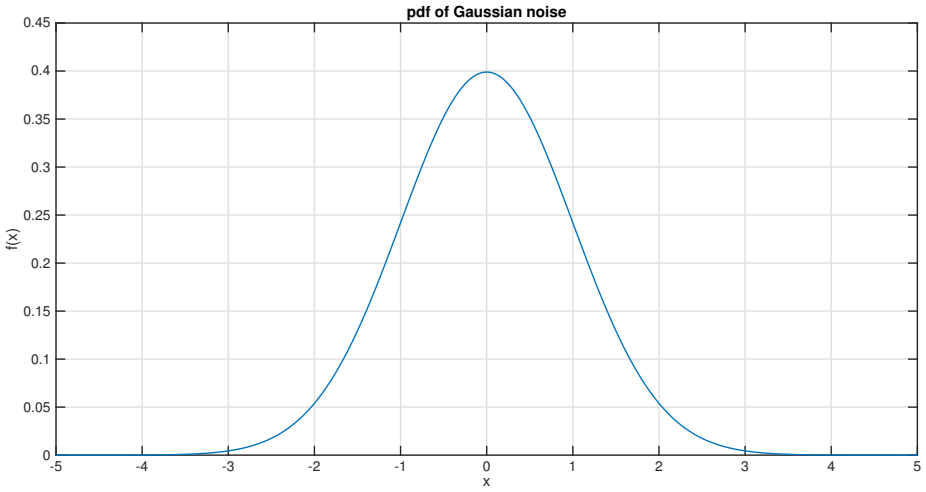


Figure 1.2: Gaussian noise pdf $\mu = 0, \sigma^2 = 1$

not at all peaky. This means that such a model is unable to represent a suddenly appearing large value.

- secondly, looking at the PDF in Fig. 1.2, the decrease in the tail is exponential. This means that it goes towards zero very quickly making highly improbable the appearance of large samples; which is the same conclusion as the first point.

The Gaussian assumption brings a great convenience, because it has often analytical and tractable solutions for signal processing problems.

However in many contexts, large values appear in the interference and are not predicted by the Gaussian model. We illustrate in the following the two main approaches that have lead to impulsive models: (*a*) the theoretical approaches — Middleton Class A, B and C models and the $\alpha$-stable model and (*b*) the empirical approaches — the Gaussian-mixture model, generalized Gaussian model, and $\epsilon$-contaminated model. Of course this is not an exhaustive list of the different models but we think it covers the main solutions.

### 1.3.2 Middleton Class A

We can trace back some works on non Gaussian noise to 1960 [37] and 1972 [40] about atmospheric noise. Assuming Poisson distributed sources, the CF of the impulsive noise can be obtained. Furthermore, appropriate assumptions on the transmission medium and source waveforms allow one to obtain the interference PDF. A similar approach

based on CF was used by Middleton [64, 63] who obtained more general expressions based on series expansions. He classified interference in two main categories depending if the noise bandwidth is less than the useful signal (class A) or greater (class B). Class C is a sum of class A and B. Canonical expressions of the distribution functions are obtained. For instance the PDF for class A can be written as,

$$\mathbb{P}(x) = e^{-A} \sum_{m=0}^{+\infty} \frac{A^m}{m!\sqrt{2\pi\sigma_m^2}} e^{-\frac{x^2}{2\sigma_m^2}}, \tag{1.14}$$

where

$$\sigma_m^2 = \left(\sigma_G^2 + \sigma_I^2\right) \frac{\left(\frac{m}{A} + \frac{\sigma_G^2}{\sigma_I^2}\right)}{1 + \frac{\sigma_G^2}{\sigma_I^2}},$$

$\sigma_G^2$ denotes the Gaussian noise power and $\sigma_I^2$ the impulsive noise power. The ratio of the intensity of the independent Gaussian component to the intensity of the impulsive non-Gaussian component in general belongs to $[10^{-6}, 1]$. $A$ is the overlap index, which defines the number of noise emissions per second multiplied by the mean duration of the typical emission, in general belongs to $[10^{-2}, 1]$.

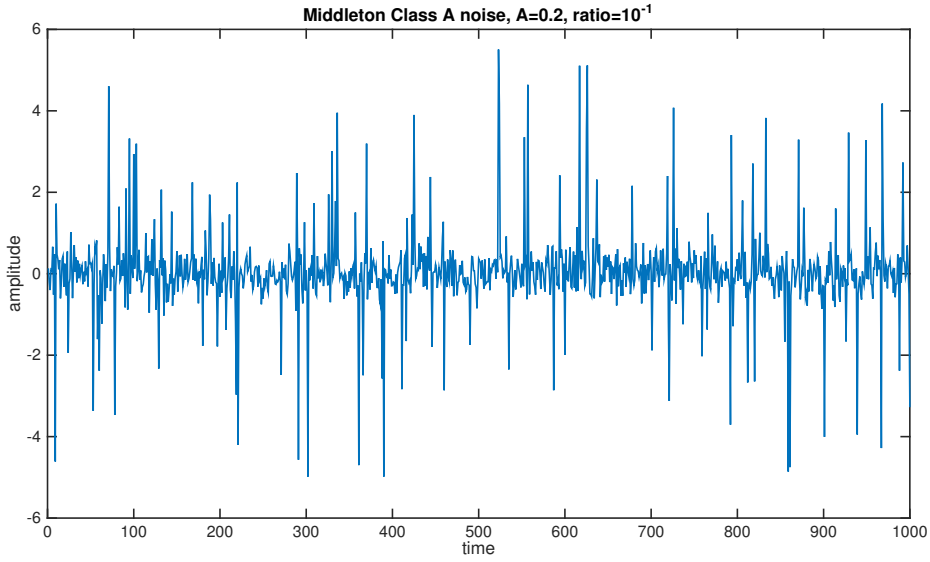


Figure 1.3: Gaussian noise A$= 0.2$, Ratio$= 10^{-1}$

Figure 1.3 and 1.4 shows the Middleton Class A noise when A$= 0.2$, Ratio$= 10^{-1}$ and

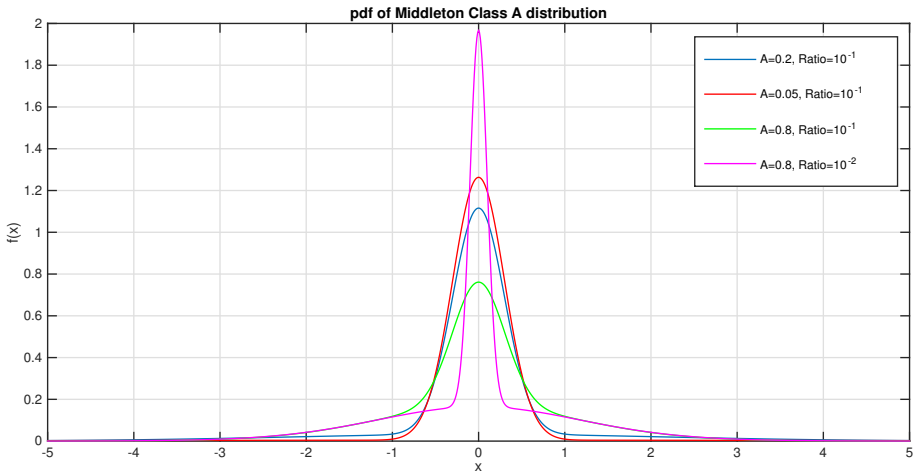


Figure 1.4: Middleton Class A distribution pdf with different parameter setting

its pdf curve with different parameter setting. From the pdf figure, we could see that under the ratio of the intensity of the independent Gaussian component to the intensity of the impulsive non-Gaussian component, the overlap index change the thickness of its pdf's tail. The bigger overlap index is, the heavier tail it has.

Class B model can usually be approximated by an $\alpha$-stable distribution [63].

Middleton models have been widely used in different contexts (MIMO [24], OFDM [52] or power line communications [4]). However, the infinite sums are difficult to handle in practice and several approximation models have been proposed that we briefly survey in the following. That will lead us to consider the empirical approach that will be introduced later.

### 1.3.3 $\alpha$-stable model

#### Concept

As already mentioned, the denser deployment of wireless networks results in an interference that exhibits an impulsive behaviour that makes the Gaussian assumption no longer appropriate. The $\alpha$-stable distribution could well capture this kind of impulsive behaviour. A proof can be given based on the $\log$-characteristic function of the interference that can be written in the form:

$$\phi(\omega) = \log \mathbb{E}[\exp j\omega Y] = -\gamma |\omega|^{\alpha}, \tag{1.15}$$

which is characteristic of an $\alpha$-stable random variable.

The $\alpha$-stable distribution is a direct generalization of Gaussian distribution. In probability theory, a random variable is said to be stable if it has the property that a linear combination of two independent copies of the variable has the same distribution, up to location and scale parameters.

In this manuscript we will usually refer to stable distribution for the distribution of impulsive interference, so that it will exclude the Gaussian distribution, although the Gaussian distribution belongs to the family of stable distributions. The main difference between the stable and the Gaussian distribution is that the tails of the stable density, decreasing as a power law, are heavier than those of the Gaussian density. However, this family is very attractive because it shares many of the properties that make the Gaussian distribution an accurate models in a large number of situations:

- the convolution stability property, which means that the convolution of two $\alpha$-stable PDF is still the PDF of an $\alpha$-stable random variable (with the same $\alpha$). In other words the sum of two independent stable random variables is also a stable one, which gives its name to this family;
- the Generalized Central Limit Theorem: it is well-known that in many applications, the Gaussian assumption is justified by the Central Limit Theorem. However there is another more general theorem that is called the Generalized Central Limit Theorem (GCLT). This theorem states that if the normalized sum of i.i.d. random variables with or without finite variance converges to a distribution by increasing the number of variable, the limit distribution must belong to the family of stable laws. The finite variance case gives the central limit theorem and the Gaussian limit distribution.

**Theorem 2 (Generalized Central Limit theorem).** *$X$ is the limit in distribution of normalized sums of the form*

$$S_n = (X_1 + \cdots + X_n)/a_n - b_n \tag{1.16}$$

*where $X_1, \cdots, X_n$ are i.i.d. and $n \to \infty$, if and only if the distribution of $X$ is stable. In particular, if the $X_i$'s are i.i.d. and have finite variance, then the limit distribution is Gaussian. This is of course the result of the ordinary Central Limit Theorem.*

Except for the Gaussian, Cauchy and Levy situations, no closed-form expressions exist for the general stable density and distribution functions. They can however be defined through their characteristic function which is given by:

$$\Phi(\theta) = \begin{cases} \exp\{-\gamma^\alpha |\theta|^\alpha (1 - i\beta \text{sign}(\theta) \tan\frac{\pi\alpha}{2} + i\mu\theta)\} & if \quad \alpha \neq 1 \\ \exp\{-\gamma|\theta|(1 + i\beta\frac{2}{\pi}\text{sign}(\theta)\ln|\theta| + i\mu\theta)\} & if \quad \alpha = 1 \end{cases} \tag{1.17}$$

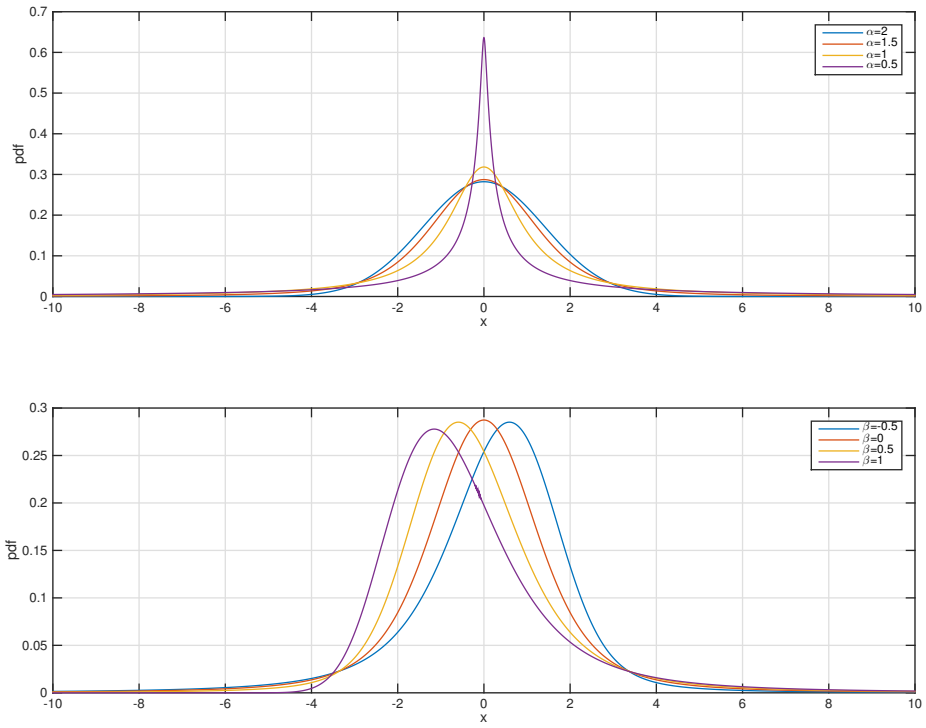


Figure 1.5: The probability density function of an $\alpha$-stable distribution with $\mu = 0$, $\gamma = 1$ and different values of $\alpha$ and $\beta$

where

$$\text{sign}(\theta) = \begin{cases} 1 & if \quad \theta > 0 \\ 0 & if \quad \theta = 0 \\ -1 & if \quad \theta < 0 \end{cases} \tag{1.18}$$

We can observe that an $\alpha$-stable characteristic function is completely determined by four parameters: $\alpha$, $\gamma$, $\beta$ and $\mu$.

- $\alpha$ is called characteristic exponent ($0 < \alpha < 2$). $\alpha$ controls the heaviness of the tail of the stable density. The small value of $\alpha$ means the variable or distribution is strongly impulsive. While when $\alpha$ approach to 2 means the variable has more Gaussian behaviour. For the extreme situation where $\alpha$ equals to 2 indicates the Gaussian situation.

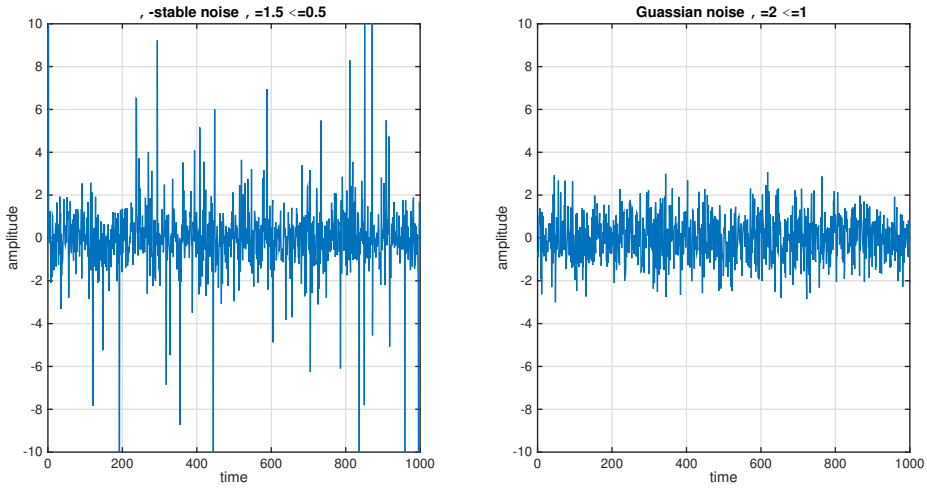


Figure 1.6: Comparison of noises for symmetric $\alpha$-stable distribution $(\alpha = 1.5)$ and Gaussian distribution $\alpha = 2$.

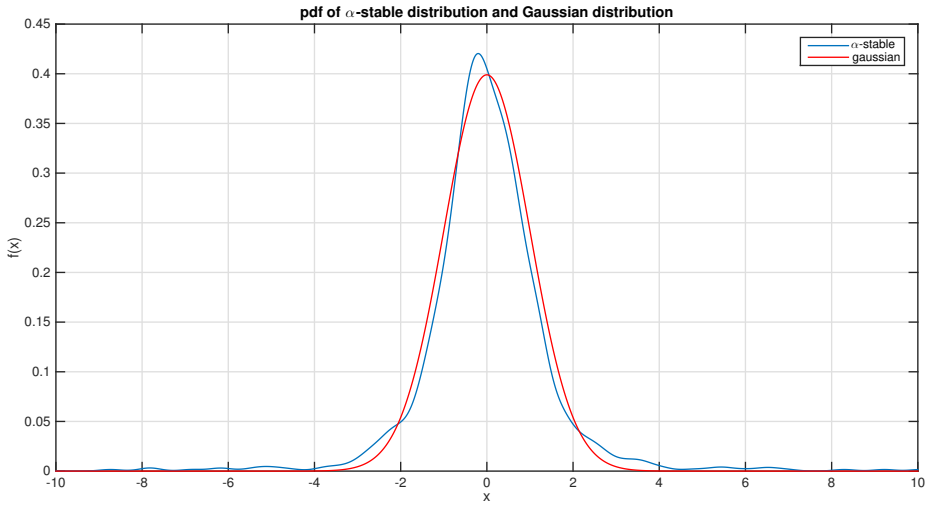


Figure 1.7: Comparison of probability density function for symmetric $\alpha$-stable distribution $(\alpha = 1.5)$ and Gaussian distribution $\alpha = 2$.

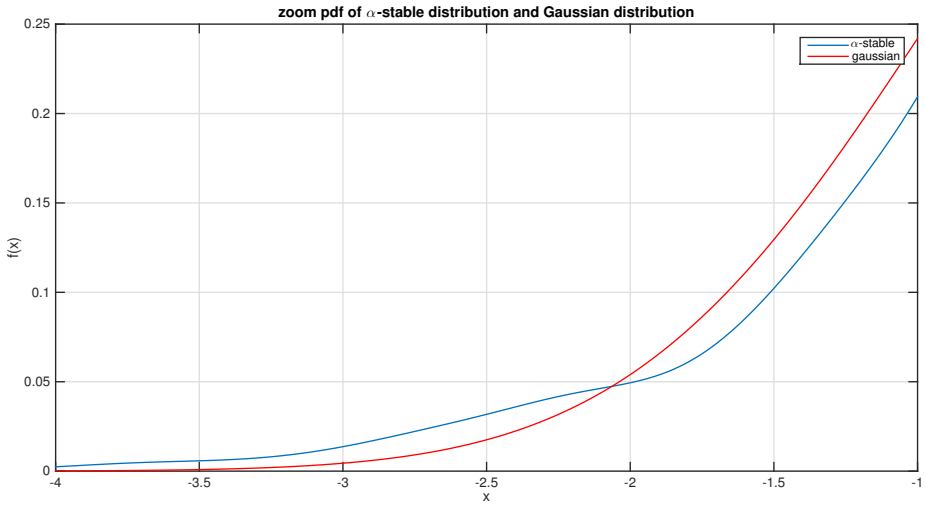


Figure 1.8: Zoom of probability density function for symmetric $\alpha$-stable distribution $(\alpha = 1.5)$ and Gaussian distribution $\alpha = 2$.

- $\gamma$ is the scale parameter ($\gamma > 0$). We also call it dispersion. It is like the variance of the Gaussian distribution. And in the Gaussian case, it equals to half of the variance.
- $\beta$ is the symmetry parameter ($-1 < \beta < 1$). It characterizes the symmetry of the density function around its central location. $\beta = 0$ means that the distribution is symmetric about $\mu$, that called symmetric $\alpha$-stable distribution ($S\alpha S$ distribution). The special cases, the Gaussian and the Cauchy cases, are all $S\alpha S$ distributions. When $\beta = 1$, the distribution is totally skewed to the right, and vice versa.
- $\mu$ is the location parameter ($-\infty < \mu < \infty$). Physically and visually, we could observe that most of the sample observed for a distribution are concentrated about this value. And for $S\alpha S$ distribution, it equals to the mean when $1 < \alpha \leq 2$ and to the median when $0 < \alpha < 1$.

This fact makes these distributions very attractive for modelling.

### Estimation of the parameters

If we will not explicitly use it in this manuscript, it is important to mention that the parameters can be estimated in different ways. Indeed, a receiver will have to estimate those parameters if we want to implement it. Several approaches exist but estimation on short sequences is difficult because the model is chosen for its ability to represent rare

events. In most cases, $\alpha$-stable distributions have no analytical expression. So it is hard to estimate its parameters by a simple estimator. But it is very important to estimate the parameters from an observed sample in practical cases, such as configure the receivers with the parameters estimated. In the case of $\alpha$-stable situation, the estimation of characteristic exponent $\alpha$ and scale parameter $\gamma$ is more important. Three methods are most known:

- **Maximum likelihood method**: This method is proposed in [28]. DuMouchel obtained a maximum likelihood (ML) estimation of $\alpha$ and $\gamma$ in the case where he assumed $\mu = 0$. By approximating the likelihood function by multinomial, DuMouchel showed that the estimates is consistent and asymptotically normal. Brorsen and Yang [18] proposed also a direct maximum likelihood estimation. The ML technique is efficient asymptotically, but its inconvenience is that computation is hard.

- **Quantiles method**: In [31], Fama and Roll estimated for symmetric parameters ($\beta = 0$,$\mu = 0$) and $1 < \alpha \leq 2$. They used the sample quantiles properties of the symmetric $\alpha$-stable variable to give an approximation of dispersion $\gamma$. And then, they estimated the parameter $\alpha$ by using the $\alpha$-stable distribution's tail property. This method is very simple but it is theoretically restricted by $\alpha$ and $\beta$. [61] improved this method. retaining the simplicity of computation, he gave a consistent estimator of all the four parameters in the condition of $0.6 \leq \alpha \leq 2$.

- **Regression-type method**: this method is presented by Koutrouvelis in [56] to estimate all the four parameters. From the characteristic function $\Phi(\theta)$, we could get that:

$$\log\left(\log|\Phi(t)|^2\right) = \log\left(2\gamma^\alpha\right) + \alpha\log\left(|t|\right) \tag{1.19}$$

this equation depends only on $\alpha$ and $\gamma$. We could then estimate the parameters by regressing $y_k = \log\left(\log|\Phi(t_k)|^2\right)$ on $w_k = \log\left(|t_k|\right)$ in the model:

$$y_k = m + \alpha w_k, \text{ and } k = 1, 2, ..., K \tag{1.20}$$

It is important to carefully choose $t_k$. A recommended choice is: $t_k = \frac{\pi k}{25}$. Knowing $\alpha$, the intersection with the $y$-axis gives $\gamma$ thanks to: $m = \log(2\gamma^\alpha)$. $K$ is an appropriate integer between 9 and 134.

From the characteristic function $\Phi(\theta)$, we could also get:

$$\arctan\left(\frac{Im(\Phi(\theta))}{Re(\Phi(\theta))}\right) = \mu t + \beta\gamma^\alpha \text{sign}(\theta)\tan\left(\frac{\pi\alpha}{2}\right)|t|^\alpha \tag{1.21}$$

The symmetry index $\beta$ and the location parameter $\mu$ are estimated by regressing $z_l = \arctan(\frac{Im(\Phi(u_l))}{Re(\Phi(u_l))})$ on $u_l$ and $\text{sign}(u_l)|u_l|^\alpha$ in:

$$z_l = \mu u_l + \beta\gamma^\alpha \text{sign}(u_l)\tan(\frac{\pi\alpha}{2})|u_l|^\alpha, \text{ and } l = 1, ..., L \tag{1.22}$$

where $u_l = \frac{\pi l}{50}$ and $L$ is an appropriate integer from 9 to 70.

A lot of works have evaluated the 3 estimation methods mentioned above. When the characteristic exponent $\alpha$ approaches 2, the regression-type method is better than the quantile methods, even using Mcculloch's method [61]. This is due to the fact that the distribution becomes a Gaussian with a very thin tail. If $0.6 \leq \alpha \leq 1.0$, the quantile methods are better. The problem is when $\alpha < 0.6$, we can not use these methods to estimate $\alpha$. It is easy to compute the characteristic function and consequently the regression type method. When no parameter is known *a priori*, it is more accurate and it does not require any restriction on the values of the parameters. However, when $\alpha < 1$, the estimation is less accurate which can be easily understood due to the very impulsive nature of the random variable.

### Generation

As already mentioned, in the general case, the $\alpha$-stable distributions have no exact expression for the probability density function. However, it is important to be able to generate $\alpha$-stable random variables. It will be of great importance for us to simulate interference. It could also be of importance in order to implement some Monte Carlo based receivers. Chambers, Mallows, and Stuck [53] introduced an accurate and inexpensive algorithm for generating stable random variables for any characteristic exponent $\alpha \quad (0 < \alpha \leq 2)$ and symmetry parameter $\beta \quad (-1 \leq \beta \leq 1)$. This algorithm is based on a non-linear transformation of two independent uniform random variables into one stable random variable. This stable random variable is a continuous function of each of the uniform random variables and of $\alpha$ and a modified symmetry parameter $\beta'$ throughout their respective permissible ranges. Consider that we want to generate a random sample $X$ from the standard $(\alpha, \beta)$ stable distribution, where $0 < \alpha \leq 2, -1 \leq \beta \leq 1$. If $\alpha = 1$, we define:

$$\beta_A = \beta, \quad \gamma_A = \pi/2 \tag{1.23}$$

and if $\alpha \neq 1$, we define:

$$k(\alpha) = 1 - |1 - \alpha| \tag{1.24}$$

$$\beta_A = 2\arctan(\beta/\cot(\pi\alpha/2))/(\pi k(\alpha)) \tag{1.25}$$

$$\gamma_B = \cos(\pi\beta_A k(\alpha)/2) \tag{1.26}$$

$$\Phi_0 = -0.5\pi\beta_A(k(\alpha)/\alpha) \tag{1.27}$$

Furthermore, define:

$$\beta' = \begin{cases} -\tan(0.5\pi(1-\alpha))\tan(\alpha\Phi_0), & \alpha \neq 1 \\ \beta_A, & \alpha = 1 \end{cases} \tag{1.28}$$

Then, $Y = X/\gamma_B^{\frac{1}{\alpha}}$ has the following characteristic function:

$$\phi_Y(t) = \begin{cases} \exp(-|t|^\alpha - jt(1-|t|^{\alpha-1})\beta'\tan(0.5\pi\alpha)), & \alpha \neq 1 \\ \exp(-|t|(1+\frac{2}{\pi}j\beta'\log|t|\text{sign}(t))), & \alpha = 1 \end{cases} \tag{1.29}$$

Now, we can generate the random variable $Y$ as follows: we first generate two independent samples $\Phi$ and $W$, where $\Phi$ is uniform on $(-\frac{\pi}{2}, \frac{\pi}{2})$ and $W$ is exponentially distributed with unit mean. We define the following quantities:

$$\epsilon = 1 - \alpha, \tag{1.30}$$

$$\tau = -\epsilon\tan(\alpha\Phi_0), \tag{1.31}$$

$$a = \tan(0.5\Phi), \tag{1.32}$$

$$B = \tan(0.5\epsilon\Phi)/(0.5\epsilon\Phi), \tag{1.33}$$

$$b = \tan(0.5\epsilon\Phi), \tag{1.34}$$

$$z = \frac{\cos(\epsilon\Phi) - \tan(\alpha\Phi_0)\sin(\epsilon\Phi)}{W\cos\Phi}, \tag{1.35}$$

$$d = \frac{z^{\epsilon/\alpha} - 1}{\epsilon}. \tag{1.36}$$

Then,

$$Y = \frac{2(a-b)(1+ab) - \Phi\tau B(b(1-a^2)-2a)}{((1-a^2)(1+b^2))}(1+\epsilon d) + \tau d. \tag{1.37}$$

is an $\alpha$-stable random variable with the characteristic function given in 1.29.

### 1.3.4 $\epsilon$-contaminated model

As we mentioned in the section 1.3.2, the infinite sums of Middleton models are difficult to handle in practice and several approximation models have been proposed to tackle the problem. The main approach is to consider only the most significant terms in (1.14). It is for instance claimed in [86] that, in many situations, two or three terms can be sufficient to obtain a good approximation of the noise. With two terms, a $\epsilon$-contaminated noise is obtained, see [5, 73].

The principal idea of the $\epsilon$-contaminated model is to combine two Gaussian models with the same mean value but with different weight and standard deviation. By adjusting the weight of the part with largest standard deviation, we can adjust the impulsiveness of the model. An $\epsilon$-contaminated mixture pdf is:

$$f_\epsilon(x) = (1-\epsilon) f_G\left(x; 0, \sigma^2\right) + \epsilon f_G\left(x; 0, \kappa\sigma^2\right), \tag{1.38}$$

where $\epsilon$ represents the level of contamination, that is to say that $\epsilon$ controls the proportion of the impulsive part, and $\kappa$ represents the impulsive strength. In the first term, $f_G\left(x; 0, \sigma^2\right)$ is the pdf of Gaussian distribution with mean $0$ and variance $\sigma^2$. The second term $\epsilon f_G\left(x; 0, \kappa\sigma^2\right)$ represents the impulsive part: the bigger $\epsilon$ is, the bigger proportion has the impulsive part, and the more often large values appear. As recommended in (reference), in practical applications we chose $0 \leq \epsilon \leq 0.1$ and $10 \leq \kappa \leq 100$.

Figure 1.9 shows the comparison of the probability density function of an $\epsilon$-contaminated distribution $(\epsilon = 0.1, \kappa = 10, \sigma^2 = 1)$ and a Gaussian distribution $\mu = 0, \sigma^2 = 1$. We notice that the $\epsilon$-contaminated distribution has a heavier tail than the Gaussian one. Figure 1.10 and 1.11 show the more impulsive behaviour of the $\epsilon$-contaminated than of the Gaussian noise. In fact, the second Gaussian introduces the rare events. The weight is usually small, meaning the probability of apparition is small. But the larger variance makes possible the apparition of significantly large values.

In [66, 32], the class A model is represented by a Markov process: the noise distribution depends on the state of the process. It reduces to the $\epsilon$-contaminated case when only two states (the two first term in (1.14) when $A << 1$) are present, but with an additional feature of time dependence structure, see [33].

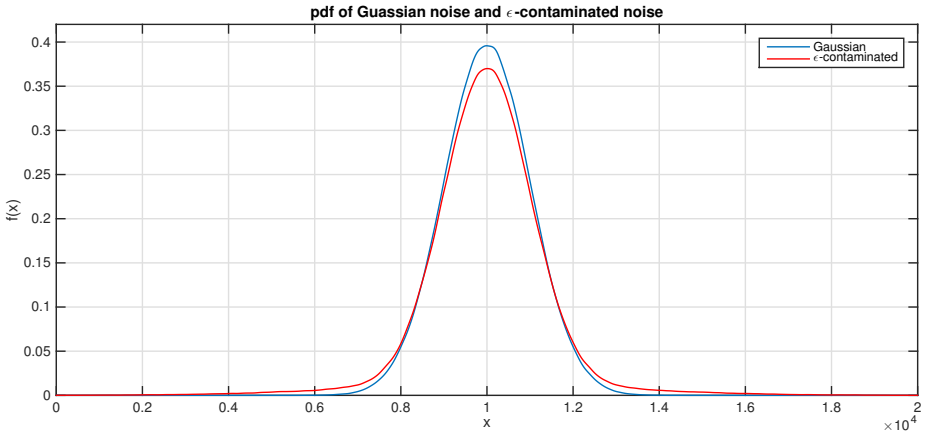


Figure 1.9: Comparison of probability density function for $\epsilon$-contaminated distribution $(\epsilon = 0.1, \kappa = 10, \sigma^2 = 1)$ and Gaussian distribution $\mu = 0, \sigma^2 = 1$.

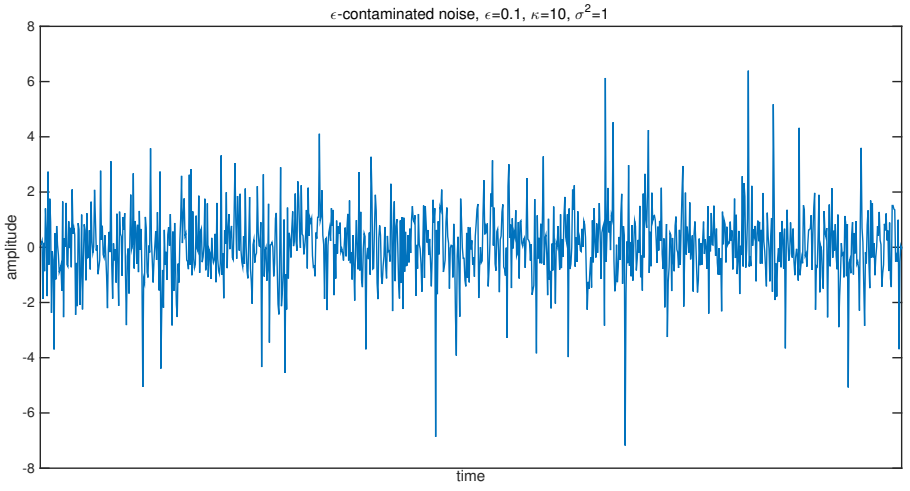


Figure 1.10: $\epsilon$-contaminated noise

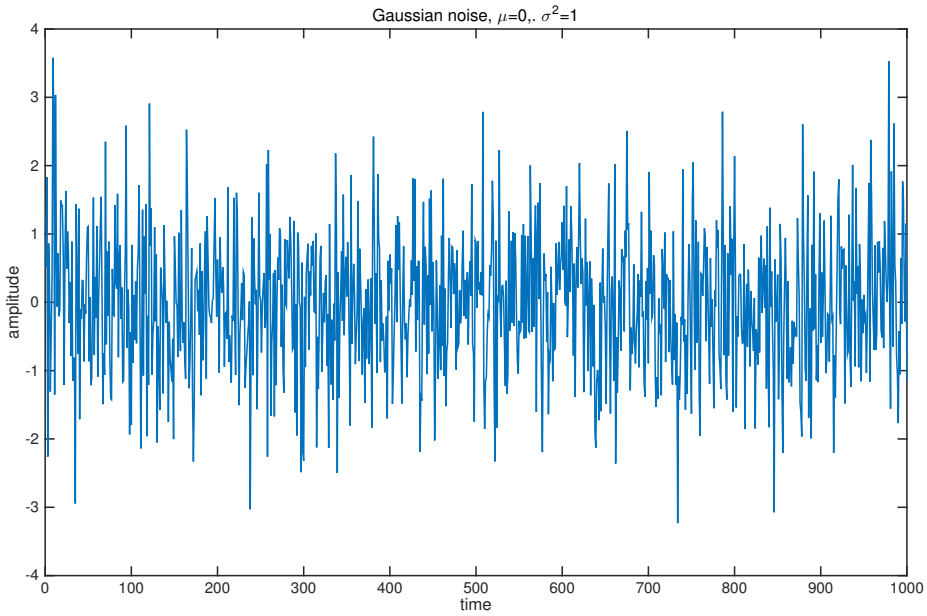


Figure 1.11: Guassian noise

### 1.3.5 Mixture of Gaussian model

Gaussian mixtures were proposed in [50]. The idea of this model is similar to the $\epsilon$-contaminated one. The difference is that more than two Gaussians are used and that the different components do not have the same mean value. The principal idea is to thicken the tail of the distribution by adding small components which are translated toward larger (absolute) values, meaning they have different means. A Mixture of Gaussian model's pdf is:

$$f_{GM}(x) = \sum_{k=1}^{K} \lambda_k \frac{1}{\sqrt{2\pi\sigma_k^2}} \exp\left(\frac{(x-\mu_k)^2}{2\sigma_k^2}\right), \tag{1.39}$$

where $\mu_k$ are the mean values of the summed Gaussian components, and $\sigma_k$ are the variances of each component. Their relative weights $\lambda_k$, which has the similar function as $\epsilon$ in $\epsilon$-contaminated model, satisfies $\sum_{k=1}^{K} \lambda_k = 1$.

The pdf of the Gaussian mixture noise is shown in Figure 1.12, and the noise comparison with the Gaussian case is shown in Figure 1.13 and Figure 1.14. The Gaussian mixture is a very flexible distribution. It can represent a lot of different situations, symmetric or not, and the tail can be very precisely controlled if we accept a large number

of components.

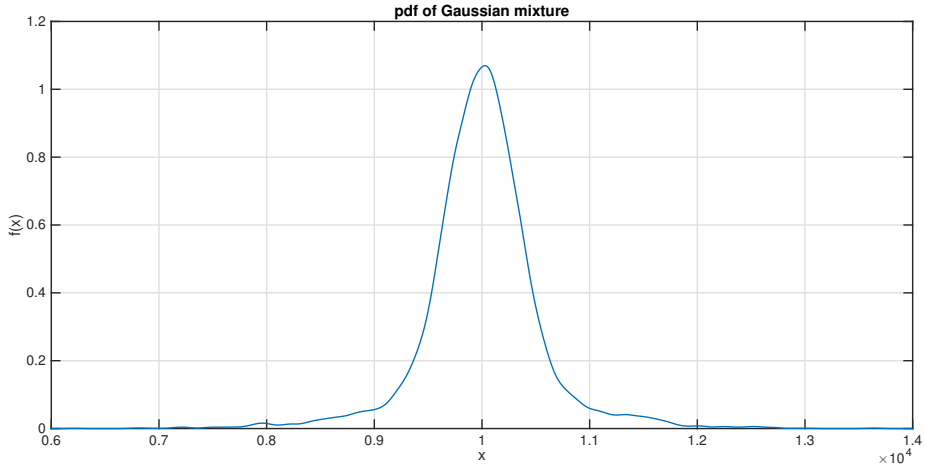


Figure 1.12: pdf of Gaussian mixture noise ($P = 3$, $\lambda_1 = 0.1$, $\mu_1 = -0.1$, $\sigma_1^2 = 1$, $\lambda_2 = 0.8$, $\mu_2 = 0$, $\sigma_2^2 = 0.1$, $\lambda_3 = 0.1$, $\mu_3 = 0.1$, $\sigma_3^2 = 1$)

### 1.3.6 Generalized Gaussian distribution model

Generalized Gaussian distributions (GGD)[35, 13, 55] have been proposed to model the multiple access interference in ultra-wide bandwidth systems. Several forms of generalized Gaussian distribution can be used. In this manuscript, we use the pdf of generalized Gaussian distribution parametrized as follows:

$$f_{GG}(x; S_m, \sigma, \beta) = \frac{1}{\Gamma(1+\frac{1}{\beta})A(\beta,\sigma)} \exp(-|-\frac{x-S_m}{A(\beta,\sigma)}|^{\beta}), \tag{1.40}$$

where $S_m$ is the mean, $A(\beta,\sigma) = [\frac{\sigma^2\Gamma(1/\beta)}{\Gamma(3/\beta)}]^{\frac{1}{2}}$ is a scaling factor to make $\mathrm{Var}(x) = \sigma^2$, $\Gamma(\cdot)$ is the Gamma function and $\beta$ is the shape parameter.

Generalized Gaussian distribution allows for tails that are either heavier (when $\beta < 2$) or lighter (when $\beta > 2$) than the Gaussian case. So they become a very useful and flexible way to model the impulsive noise which has heavier tail than Gaussian. However this approach remains empirical without any theoretical justifications of the model.

Figure 1.15 shows the Generalized Gaussian distribution noise when $\alpha = 1$ and $\beta = 0.2$. Figure 1.16 compare the pdf of Generalized Gaussian distribution with different $\beta$. We could observe that the bigger the shape parameter $\beta$ is, the heavier is its tail, that means beta increase the possibility of occur of large value event.

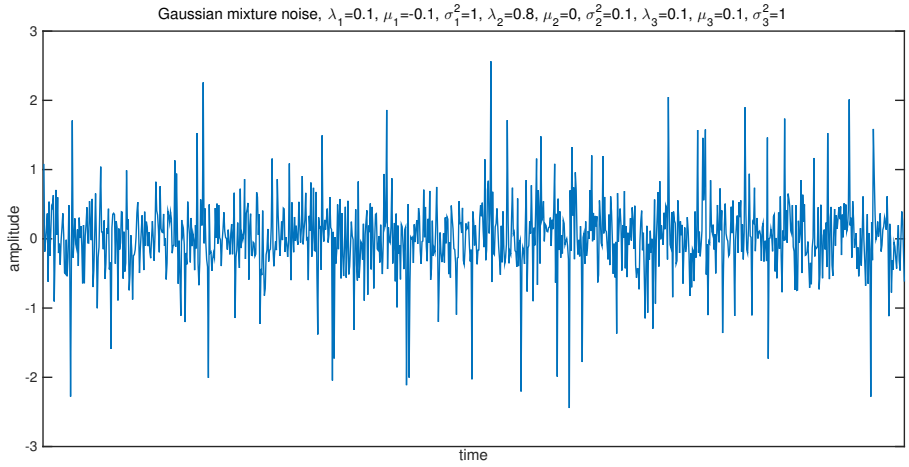


Figure 1.13: Gaussian mixture noise ($P = 3$, $\lambda_1 = 0.1$, $\mu_1 = -0.1$, $\sigma_1^2 = 1$, $\lambda_2 = 0.8$, $\mu_2 = 0$, $\sigma_2^2 = 0.1$, $\lambda_3 = 0.1$, $\mu_3 = 0.1$, $\sigma_3^2 = 1$)

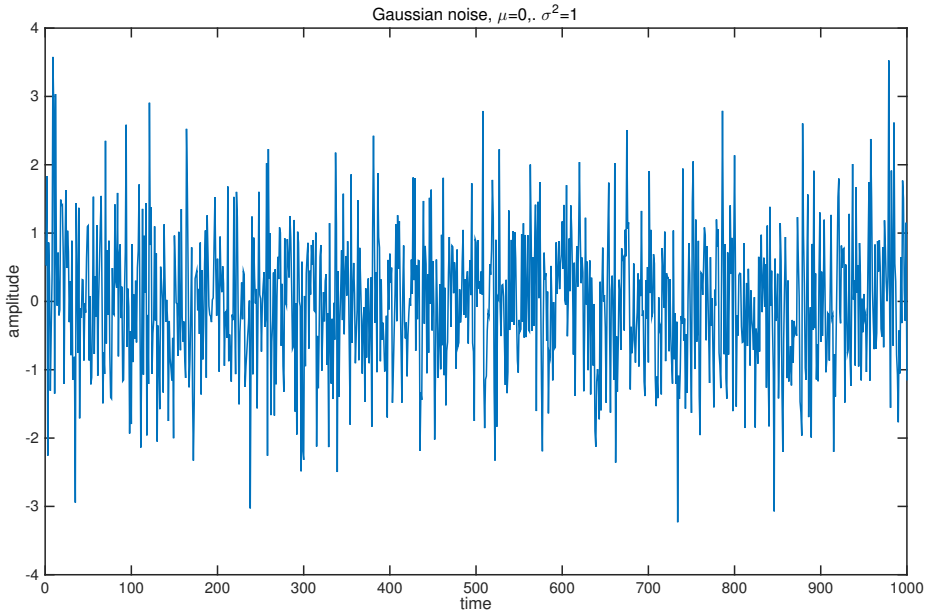


Figure 1.14: Gaussian noise

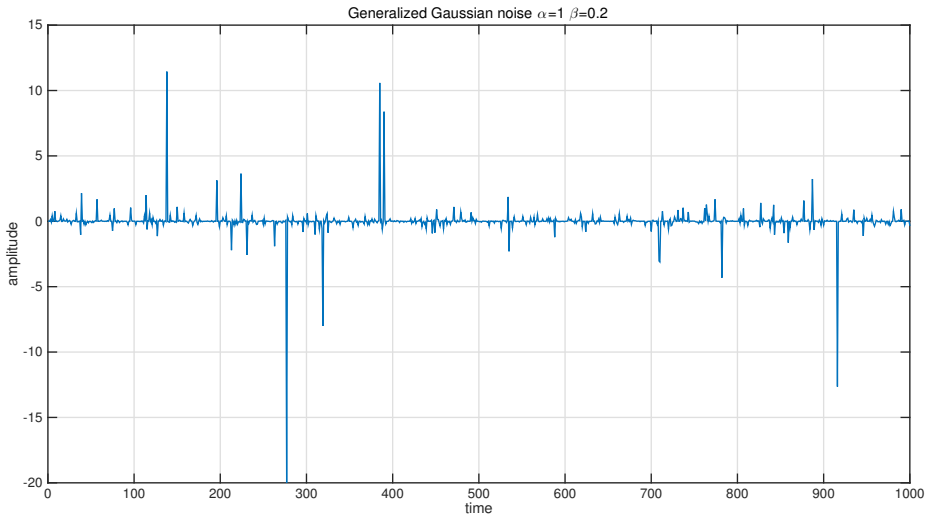


Figure 1.15: Generalized Gaussian distribution noise

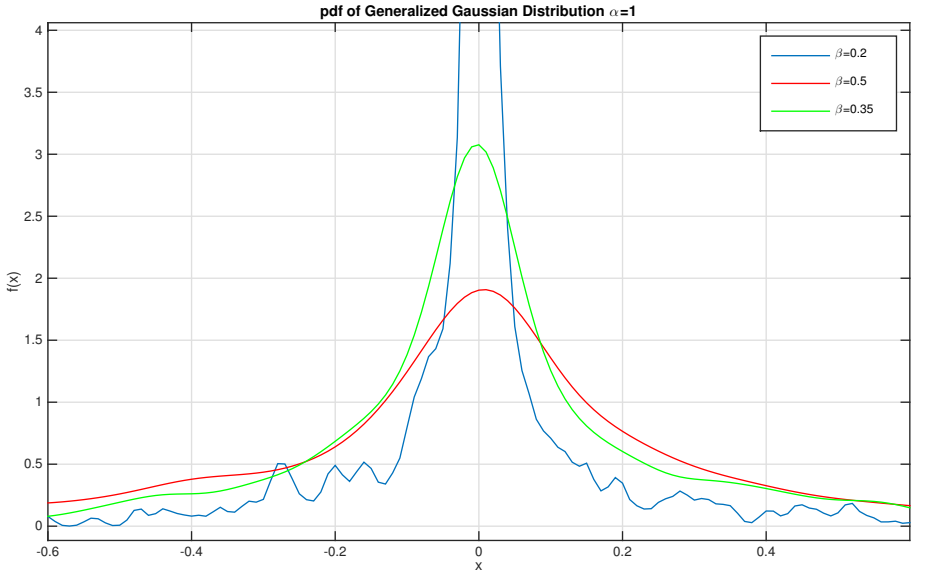


Figure 1.16: pdf of Generalized Gaussian distribution with different parameters

Chapter 2

# Receiver Design - the independent case

We have addressed in the previous chapter the interference modelling. One important fact is that in many situations the interference is not Gaussian. We have also presented several approaches for the modelling, without being exhaustive. Several approaches have proved to be well adapted to specific situations. We would now like to develop a receiver that would adapt to the different cases that can be encountered. Of course it can no longer be an optimal receiver (in the Bayesian sense, maximizing the likelihood) because to implement such a receiver would necessitate to know the exact model. Our approach is to consider that models are only models and that the communication situation can highly vary: wireless networks or power line, dense or point to point, Line of sight or obstructed situations... Many situations that will impact the characteristic of the interference. Because we do not want to design one specific receiver for each situation, we would like a receiver able to cope with a large set of different interference (impulsive or not, Generalized Gaussian, $\alpha$-stable, Middleton...).

This is the challenge we address in the following of the chapter. After defining the scenario, we will try to clarify the impact of the interference on the optimal receiver. We will the describe different approaches to design a robust receiver.

## 2.1 System scenario

We consider a block fading scenario where a frame consisting of $J$ data symbols is transmitted over wireless channels and $K$ versions of each symbol are received.

The general model of the system is as follows:

$$\mathbf{y} = \mathbf{h}x + \mathbf{i} + \mathbf{n}. \tag{2.1}$$

- The unknown transmitted symbol, denoted by $x$, is defined on a discrete support $\Omega$ with equally likely elements to be transmitted.
- $\mathbf{h} = (h_0, h_1, ..., h_{K-1})$. The block fading channel coefficients are a random vector denoted by $\mathbf{h} \in \mathbb{R}^K$. The distribution of the coefficients depends on the considered channel model (e.g. Rayleigh, Nakagami, Rician etc.). We assume perfect channel state information at the receiver.
- $\mathbf{i} = (i_0, i_1, ..., i_{K-1})$ is the interference component whose distribution model is discussed in Chapter 1.3. In this chapter we consider independent samples in interference. This assumption is strong questionable. we will keep this question for chapter 3.
- The thermal noise at the receiver is a random vector $\mathbf{n} = (n_0, n_1, ..., n_{K-1})$ in which all elements are assumed i.i.d. with a Gaussian distribution $N_k \overset{\text{i.i.d.}}{\sim} \mathcal{N}(0, \sigma^2)$.
- The impulsive interference random vector is independent of the thermal noise random vector, i.e., $\mathbf{I} \perp \mathbf{N}$.
- The received signal $\mathbf{y}$ is composed of the channel coefficient weighted signal component $\mathbf{h}x$, the interference component and the independent thermal noise component.

We assume that the block fading channels are perfectly known at the receiver.

This transmission structure can be motivated by many different practical wireless communication systems, for example transmission through different channel paths (rake receiver) [71], at different receive antennas under a single-input-multiple-output system [34], in a cooperative communication system involving multiple relays [22] or in impulse radio Ultra Wide Band systems where repetitions of the transmitted symbol occur [39].

This can be illustrated by the following examples:

- The $K$ replicas can, for instance, correspond to $K$ repeated pulses in an impulse radio Ultra Wide Band system transmission. The reception make decision according to the channel assumption and the reception setting.
- The $K$ replicas can also correspond to the different replicas received at multiple antennas configuration, like SIMO system (Single-Input Multi-Output), which is showed as the figure 2.1.

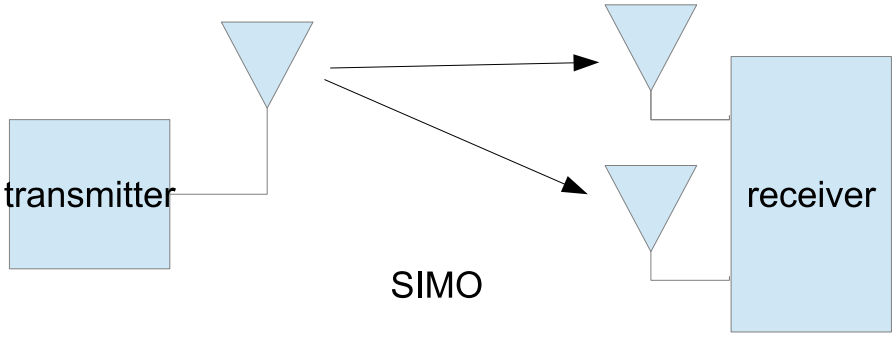


Figure 2.1: The system SIMO

- The $K$ replicas can correspond to the signal received from different relays in a cooperative scheme. We consider that communications are realized by a decode-and forward (DF) relaying scheme with the cooperation of multiple relays. Figure 2.2 shows a general decode-and forward relaying communications scheme. The system is consisting of one source, N possible relays and one destination. A set of $K$ relays, which has the strongest relay-to-destination channel coefficient $\mathbf{h}$, is selected among N possibilities. Figure 2.3 shows a simple relaying communication system. The blue points represent the senders, and the red points represent the receivers. The black arrows means the signal is from the senders or relays corresponding to the receiver, that is to say the signal is useful. On the contrary, the orange ones means the signal is from the senders corresponding to other receivers. So the signal received for this receiver is useless. We call it interference.

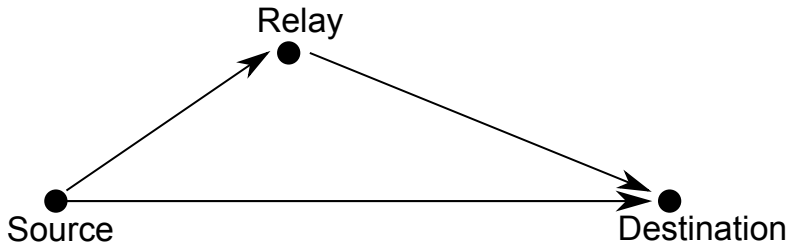


Figure 2.2: Decode-and forward (DF) relaying communications scheme

- The $K$ replicas could also represent the different fingers in a rake receiver shown in Figure 2.4.

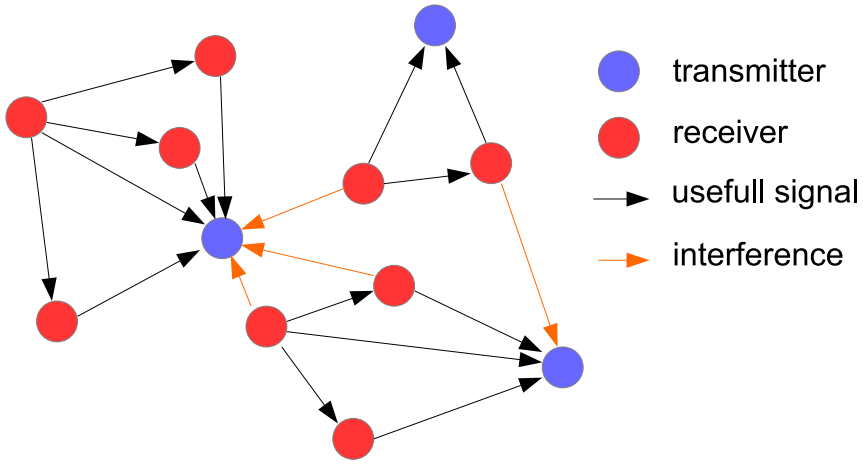


Figure 2.3: Relaying communications with interferences

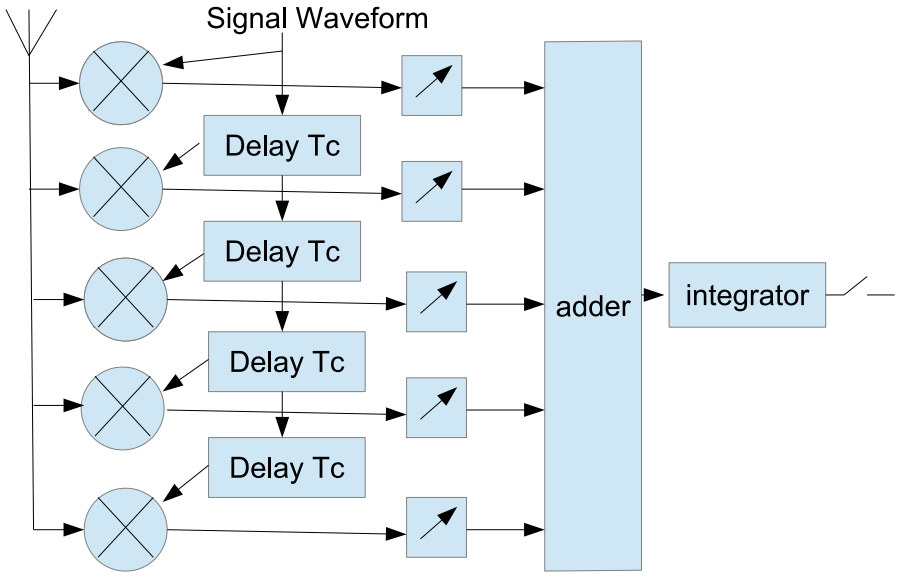


Figure 2.4: Rake receiver with 5 fingers

## 2.2 Impact of impulsive interference noise on optimal decision regions

The left and right tail of the interference distribution is important in optimal receiver design. One way to examine the impact of the noise on the optimal receiver design is to look at the decision regions. Let us consider two received samples $y_1$ and $y_2$. The value $v$ of a point in the plan giving $y_1$ in the $x$-axis and $y_2$ in the $y$-axis is given by the transmitted symbol that gives to the received point $(y_1, y_2)$ the highest value to be the transmitted one:

$$v = \underset{x \in \Omega}{argmax} \mathbb{P}(x|y_1, y_2). \tag{2.2}$$

The ensemble $v = x_i$ gives the region where a received point should lead to the decision $x_i$. When the received samples cover the whole space, we call the resulting plot a representation of the decision regions.

The tail behaviour of the impulsive noise distribution creates non-standard decision regions in the optimal receiver. The Gaussian interference whose tail is light gives simple linear decision region boundaries. The heavy-tailed impulsive interference induces the presence of non linearity in the decision boundaries. It is precisely the tail behaviour of the impulsive noise distribution who creates this characteristic. But this non linearity characteristic, if it explains the performance difference that we will see, also brings an increased complexity of the optimal receiver design.

The heavy-tailed interference noise dominates the light tailed Gaussian thermal noise in extremes and dictates the extent of the non linearity in the decision regions for the receiver.

We are interested in the influence that heavy-tailed impulsive noise may have on the optimal decision regions. It gives us a picture of how an optimal receiver should behave. In this regard we discuss practical examples of impulsive interference models that have been recently proposed in wireless communications. This provides a clear motivation for the importance of considering appropriate models for the total interference noise, impulsive noise and thermal noise, if one is to accurately design a receiver to make optimal detection decisions.

We generate the noise with different noise model as we have discussed above. The examples are shown in Figure 2.5.

In Figure 2.6, we show how the decision regions look like in different interference settings. We present the regions that maximize the probability of having transmitted s when Y is received under each model. This shows the linear operating range and the non linear operating range of the receiver created according to the impulsive noise. We assume there are 3 possible transmitted values $\Omega = \{-1, 0, 1\}$, and 2 repetitions

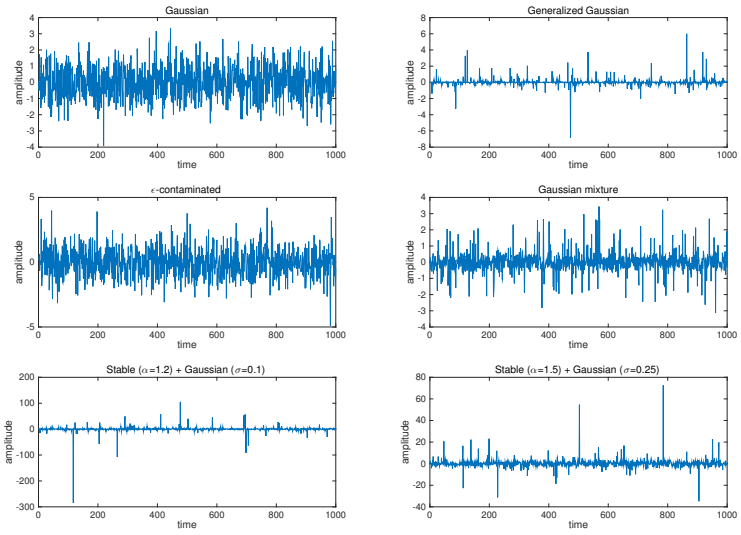


Figure 2.5: Example realisations for each different impulsive noise processes. The following parameters were used in each case: Gaussian case ($\mu = 0$ and $\sigma^2 = 1$); Generalized Gaussian case ($\alpha = 1$, $\beta = 0.2$); $\epsilon$-contaminated case ($\epsilon = 0.1$, $\kappa = 10$, $\sigma^2 = 1$); Gaussian mixture case ($P = 3$, $\lambda_1 = 0.1$, $\mu_1 = -0.1$, $\sigma_1^2 = 1$, $\lambda_2 = 0.8$, $\mu_2 = 0$, $\sigma_2^2 = 0.1$, $\lambda_3 = 0.1$, $\mu_3 = 0.1$, $\sigma_3^2 = 1$); Sum of Gaussian and $\alpha$-stable in a highly impulsive case ($\alpha = 1.2$, $\gamma = 1$ and $\sigma^2 = 0.1$); Sum of Gaussian and $\alpha$-stable in a moderate impulsive case ($\alpha = 1.5$, $\gamma = 1$ and $\sigma^2 = 0.25$).

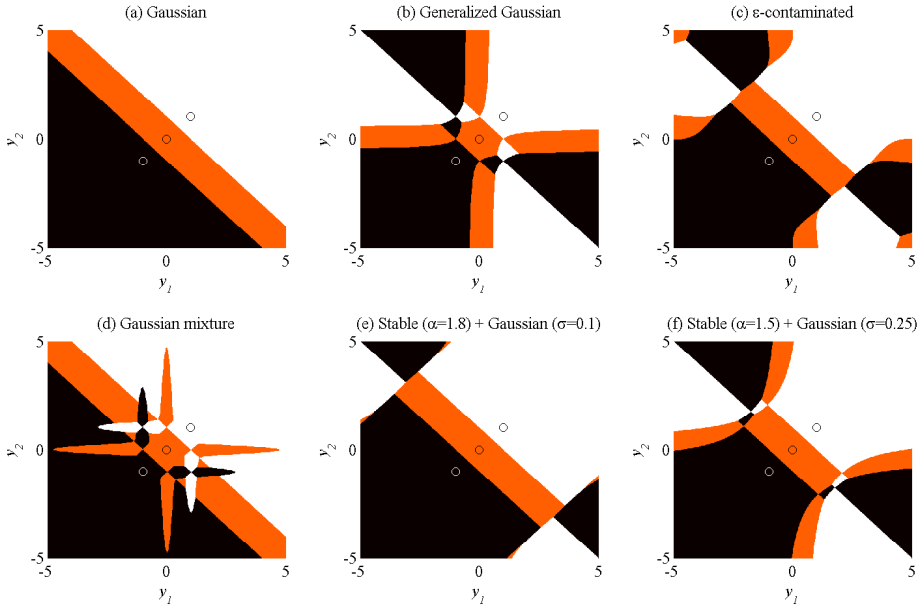


Figure 2.6: Optimal decision regions for the different noise processes. We use the same parameters defined in Fig. 2.5: the received vector $\mathbf{Y}$ is composed of two received samples (two dimensions, $\mathbf{Y} = [y_1\ y_2]$), the wireless channel is set to $\mathbf{h} = [1\ 1]$, and we consider three possible transmitted values (ie. $\Omega = \{-1, 0, 1\}$).

$\mathbf{Y} = (y_1, y_2)$ are received at the destination. We present the different decision regions in 3 different colors: the black region represents that symbol -1 is the decision we make; The orange region is for symbol 0; The white one is for symbol 1.

If we only consider 2 possible transmitted values $\Omega = \{-1, 1\}$, the decision regions will look like Figure 2.7.

Another way to think about this notion of impulsive interference is to consider how the heavy tailed features of such an interference will affect the decision regions when performing optimal detection. It is well known that the optimal decision regions are linearly separated regions under interference with exponential tail decay, such as the Gaussian case shown in Fig.2.6(a). However, as illustrated for other interference models in Fig.2.6 the optimal decision regions under examples of interference models with heavy tailed features, i.e. $\bar{F}_I = 1 - F_I$ is heavy eventually relative to a Gaussian, present complex non linearity and disjoint regions. We can identify two operating regions: for small received values $y_1, y_2$, frontiers are linear. However, when at least one value becomes larger, such linear boundaries (and euclidean distance) recover no longer the most likely transmitted symbol. The point at which this non linearity in the decision regions starts to appear is directly the point at which the tails of the impulsive or heavy-tailed interference distribution begins to dominate over the Gaussian thermal noise. As expected, the heavier the tails of the interference, the more rapidly the linear optimal decision regions is reduced in operating range.

Different noise distributions considerably modify the decision regions, so that decision rules need to be modified. However, as seen in Fig. 2.6, this modification results in non linear architectures and, consequently, computational complexity of the algorithm.

## 2.3 Robust reception

When it comes to receiver design, the first observation to make is the poor behaviour obtained by the simple linear receiver, which is optimal in a Gaussian noise but highly suboptimal in other interference settings. The second observation is the difficulty in developing an optimal receiver. One reason is the variety of proposed interference models: which model should I design my receiver for and how will it perform if my environment changes? Empirical models can then offer attractive solutions but their ability to adapt to different contexts is still to be proven. Another reason is that implementing a receiver can be complex for some specific interference distributions, for instance with the infinite series from Middleton's model or stochastic geometry or the absence of closed-form $\alpha$-stable PDF. In the following we propose to classify the different receiver design approaches into three categories, as shown in Table 2.1.

- Approach 1 includes the linear receivers. The well-known Maximum Ratio Combining (MRC) allows to maximize the SNR. However, when impulsive noise is

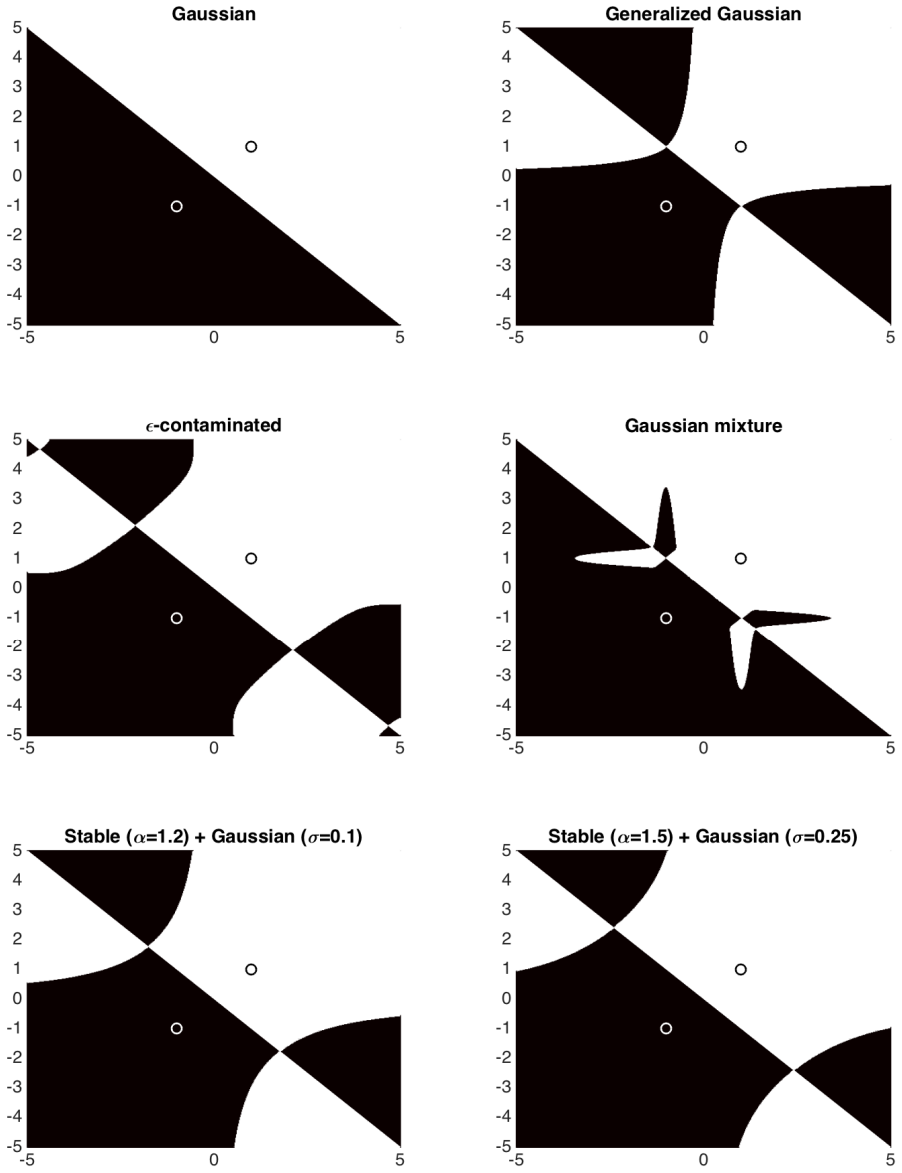


Figure 2.7: Optimal decision regions for the different noise processes. with two possible transmitted values

| Receiver Strategies | |
|---|---|
| Type of receiver | Method |
| Linear | Linear combiner |
| Noise distribution approximation | Cauchy<br>Myriad<br>NIG |
| LLR inspired | Soft limiter<br>Hole puncher<br>$p$-norm |

Table 2.1: Receiver strategies.

considered, large values should not be given the same weight so that the linear function to determine the log-likelihood is no longer adapted.

- Approach 2 selects a specific model. Such a design highly relies on the assumption that we make and is not necessarily robust when transmission conditions change. To gain this robustness, we need to choose a class of distributions that covers a wide range of conditions (Gaussian, skew, asymmetric tails and heavy tailed cases) and that can be simply adapted, meaning that the necessary parameters can be efficiently estimated online if required.

- Approach 3 directly approximates the LLR. We can think of detection as measuring a distance between the received and the possible transmitted vectors. The maximum LLR is given by the smallest distance. If Euclidean distance is selected, it may be suitable for Gaussian noises. However, in general, they will not be adapted to the geometry of impulsive noise settings. Alternative norm distances need therefore to be considered.

### 2.3.1 Optimal receiver

The optimal receiver is theoretically the the best receiver for a transmission system. A MAP (Maximum *a posteriori*) receiver could be made if the received signal $\mathbf{y}$ and the channel coefficient $\mathbf{h}$ are known. The aim is to find a signal $x$ which has the maximum likelihood probability at each time slot $t$:

$$\widehat{x}_t = \mathbf{argmax}\mathbb{P}_{\mathbf{Y}}(\mathbf{y}|s, \mathbf{h}) \tag{2.3}$$

The detection problem for a binary source, as the system model that we assumed in the presence of stable impulsive network interference and independent network equip-

ment thermal noise, can be written through a statement of a hypothesis test as:

$$\begin{cases} H_0 = \mathbf{h}s_0 + \mathbf{i} + \mathbf{n} \\ H_1 = \mathbf{h}s_1 + \mathbf{i} + \mathbf{n} \end{cases} \tag{2.4}$$

Here $s_0$ and $s_1$ is the transmitted binary symbols of the source ($x \in \{s_0, s_1\}$). We define $\mathbb{P}_{i+n}(y|s_1)$ and $\mathbb{P}_{i+n}(y|s_0)$. Here, $\mathbb{P}_{i+n}(\cdot)$ is the probability distribution function obtained from the combination of impulsive interference and independent thermal noise. So $\mathbb{P}_{i+n}(y|s_1)$ and $\mathbb{P}_{i+n}(y|s_0)$ represents the possibility of the reception of signal $\mathbf{y}$ in the condition of the emission of symbol $s_1$ or $s_0$. Furthermore, We define log-likelihood ration (LLR) as:

$$\begin{aligned} \Lambda &= \log \frac{\mathbb{P}_{i+n}(\mathbf{y}|s_1)}{\mathbb{P}_{i+n}(\mathbf{y}|s_0)} \\ &= \log \frac{\prod\limits_k f_{i+n}(y_k|s_1)}{\prod\limits_k f_{i+n}(y_k|s_0)} \\ &= \sum_k \log \frac{f_{i+n}(y_k|s_1)}{f_{i+n}(y_k|s_0)} \underset{H_0}{\overset{H_1}{\gtrless}} \eta \end{aligned} \tag{2.5}$$

Here, $f_{i+n}(\cdot)$ is the probability density function of the impulsive interference plus Gaussian thermal noise. The decision between two hypothesis is made through comparing the value of the log-likelihood ratio to a threshold $\eta$. Normally, under our assumption also, the two binary symbols of the source has the equal emission probability. In that case, $\eta$ equals to 0. If the channel coefficients are well known, we could have the $a$ $priori$ decision statistic as:

$$\Lambda = \sum_{k=1}^{K} \log \frac{f_{i+n}(y_k|h_k s_1)}{f_{i+n}(y_k|h_k s_0)} \underset{H_0}{\overset{H_1}{\gtrless}} 0 \tag{2.6}$$

The decision rule in (2.6) defines a decision region, which is equivalent to the critical region of a hypothesis testing inference problem if one recasts this optimal decision rule in the context of hypothesis testing. Calculating the expressions in (2.5-2.6) requires the evaluation of the measure $\mathbb{P}_{\mathbf{Y}}(\mathbf{y}|s)$. This involves the following steps which we explain below so that we can easily characterize which parts of this process are generally intractable in general heavy tailed interference settings:

1. Specify the representation of the impulsive noise $\mathbf{I}$, either by its characteristic function or distribution function (when it exists in closed form).

2. If the characteristic function of $I_k$ is known, according to $\varphi_{I_k}(\omega) = \mathbb{E}[e^{iI_k\omega}]$, find its density

$$f_{I_k}(\zeta) = \frac{1}{2\pi}\int_{-\infty}^{\infty} \varphi_{I_k}(t)\exp^{-i\zeta t}\mathrm{d}t, \quad \forall k \in \{1,\ldots,K\}. \tag{2.7}$$

3. Calculate the density of the total interference $I_k + N_k$, via the following convolution:

$$f_{I_k+N_k}(\zeta) = \frac{1}{2\pi}\int_{-\infty}^{\infty} f_N(\tau)\int_{-\infty}^{\infty} \varphi_{I_k}(t)\exp^{-i(\zeta-\tau)t}\mathrm{d}t\mathrm{d}\tau, \quad \forall k \in \{1,\ldots,K\}. \tag{2.8}$$

4. Conditional on the channel state information, find the likelihood function as a function of the unknown transmitted symbol values $s$ denoted by $\mathbb{P}_{\mathbf{Y}}(\mathbf{y}|s)$ via the linear transformation of the noise random variables according to

$$\mathbf{Y} = \mathbf{h}S + \mathbf{I} + \mathbf{N}. \tag{2.9}$$

   If the distribution of the noise has a density which is translation invariant then the distribution of the received signal used to characterise the likelihood, given by $f_{\mathbf{Y}}$ is in the same family as the solution to $f_{\mathbf{I}_k+\mathbf{N}_k}$ with modified parameters, for instance the location parameter.

From the above discussion it is clear that under the majority of cases encountered in practice there will be no closed form solution to the steps $2.-4.$. Sometimes we only know the characteristic function (CF). We have to use numerical integration methods to obtain the PDF, which can also be written as::

$$f(x) = \frac{1}{\pi}\int_0^{+\infty} \varphi(t)\cos(xt)\mathrm{d}t \tag{2.10}$$

where $\varphi(t)$ is the CF. However, the heavy computation cost of this integration should be considered. And also, for getting the expression of PDF, we have to know all the parameters of the CF. That may lead to a heavy estimation work too.

Hence, these challenges will influence how one approaches receiver design when it may be required in settings such as these which may involve intractable class of interference models, as encountered in most real world communication systems.

### 2.3.2 Gaussian receiver

The first strategy is to keep on using our Gaussian assumption because of its simplicity, though it may not be reliable any more. The Gaussian receiver is also called linear

receiver: it corresponds to the first approach in Table 2.1. Assuming that the PDF used in the decision statistic given in (2.6) is the Gaussian one,

$$f(x;\mu,\sigma) = \frac{1}{\sigma\sqrt{2\pi}} e^{-\frac{(x-\mu)^2}{2\sigma^2}} \tag{2.11}$$

where $\mu$ the mean value and $\sigma$ the standard deviation.

Obviously, the Gaussian receiver is the optimal receiver when the interference is Gaussian distributed. The decision statistic is then as:

$$\begin{aligned} \Lambda_{Gaussian} &= \sum_{k=1}^{K} \log \frac{f_{Gaussian}(y_k|h_k s_1)}{f_{Gaussian}(y_k|h_k s_2)} \\ &= \sum_{k=1}^{K} \log \frac{\exp[-(y_k-s_1)^2/2\sigma^2]}{\exp[-(y_k-s_0)^2/2\sigma^2]} \\ &= \frac{1}{\sigma^2} \sum_{k=1}^{K} y_k(s_1-s_0) \underset{H_0}{\overset{H_1}{\gtrless}} 0 \end{aligned} \tag{2.12}$$

where $\sigma$ is the standard deviation of the Gaussian distribution. Even though we preview that our interference environment will lead to an impulsive environment in which $\alpha < 2$, we still test this receiver because it has a simple implementation structure.

### 2.3.3 Conventional and optimal MRC receiver

The maximal ration combiner(MRC) receiver is another linear solution. The implementation is also simple, so it is widely used. The conventional MRC receiver use the decision statistic as:

$$\Lambda_{MRC} = \sum_{k=1}^{K} w_k y_k = \widehat{\mathbf{s}} + \widehat{\mathbf{n}} \tag{2.13}$$

where $\mathbf{w} = \{w_k\}_{k=1}^{K} \in \mathbb{R}^K$ is the weight of the combiner, $\widehat{\mathbf{s}}$ and $\widehat{\mathbf{n}}$ are the weighted signal part and noise part. Under the assumption of independent Gaussian channels, the conventional MRC receiver is optimal when $w_k = h_k^*$. The $*$ means complex conjugate. In the environment of impulsive interference, the conventional MRC receiver is no longer optimal. In [54, 70], an adapted MRC receiver is studied. It gives the weight strategy as:

$$\begin{cases} w_k^* = \text{sign}(s_k)|s_k|^{1/(\alpha-1)}, & 1 < \alpha \leq 2 \\ w_j^* = \text{sign}(s_j), w_k^* = 0 \forall k \neq j, & 0 < \alpha \leq 1 \end{cases} \tag{2.14}$$

for an arbitrary $j$ in $\mathbf{i} = \arg\{|s_i| = \max\{|s_1|, ..., |s_K|\}\}$.

This is further studied for a rake receiver in [71, 70] and for diversity combining schemes in a multi-antenna receiver in [23] in presence of symmetric $\alpha$-stable interference. However we found that the improvement over the standard linear approach is very limited in our studied examples and we have therefore omitted the corresponding BER curves in the following section.

### 2.3.4 Cauchy receiver

Another way to solve (2.5) is to find a distribution that would approximate well the true noise plus interference PDF $f_{I+N}(.)$ (whatever the dominant noise term), having an analytical expression and parameters that can be simply estimated. Erseghe *et al.* used this approach in [30] with a Gaussian mixture for UWB communications. In [65], the $\epsilon$-contaminated is used to study the impact of impulsive noise on Parity Check Codes. The importance to take the real noise model into account during the decoding is underlined. A review in the UWB case can be found in [14]. For instance Fiorina [35] proposed a receiver based on a generalized Gaussian distribution approximation. Beaulieu and Niranjayan [15] considered a mixture of Laplacian and Gaussian noise. The Cauchy model is proposed in [39]. Each solution is shown to significantly improve the performance in their specific context. We can wonder how robust they will be in case of a model mismatch.

We propose three receivers based on this approach: the Cauchy receiver [39], specifically designed for an impulsive noise; the Myriad receiver [41, 69], which is an improved version of the Cauchy receiver for a mixture of stable and Gaussian interference; as a complement to the work started in [43], we also propose the use of Normal Inverse Gaussian (NIG) distributions. It is a flexible family of distributions that contains as limiting cases both the Myriad filters and standard linear Gaussian receiver.

The first trial we can make is to use a receiver fully designed for impulsive noise. A natural choice in that case is to base the receiver on the assumption of interference with a Cauchy distribution. The Cauchy receiver is optimal for the signal detection under pure Cauchy noise. Estimation of the parameter is very important in this case. It has been shown in the [39] that this receiver is close to the optimal for $\alpha$-stable interference when $\alpha$ close to 1.

Cauchy distribution's PDF with dispersion $\gamma$ and median $\sigma$ is:

$$f_1(x) = \frac{\gamma}{\pi[\gamma^2 + (x-\sigma)^2]} \tag{2.15}$$

The corresponding decision statistic is given by:

$$\begin{aligned}\Lambda_{Cauchy} &= \sum_{k=1}^{K} \log \frac{f_1(y_k|h_k s_1)}{f_1(y_k|h_k s_0)} \\ &= \sum_{k=1}^{K} \log \left( \frac{\gamma^2+(y_k-h_k s_0)^2}{\gamma^2+(y_k-h_k s_1)^2} \right)\end{aligned} \tag{2.16}$$

We note that the Cauchy receiver remains rather difficult to implement because we need to determine the dispersion parameter $\gamma$ and this can be challenging from a statistical perspective given received interference observations: the estimation accuracy may be low for online adaptive impulsive environments, especially if interference is not Cauchy distributed. For simulation, we use the dispersion of the stable interference when a mixture of stable and Gaussian is considered and $\sigma^2/2$ when in pure Gaussian noise.

### 2.3.5 Myriad receiver

To improve the adaptability of the Cauchy receiver, the myriad filter has been discussed in [41, 69, 76]. It follows the Cauchy density with a modified dispersion parameter $\kappa$ replacing $\gamma$ in (2.15). The so called "linearity parameter" $\kappa$ was firstly used to adapt the receiver to interference with an $\alpha$-stable distribution for $\alpha \neq 1$.

We can propose an estimation procedure to estimate the $\kappa$. We assume that $\mu$=0, and the pdf of the distribution is:

$$f_X(x) = \frac{\kappa}{\pi\left(\kappa^2 + x^2\right)}. \tag{2.17}$$

We write the log-likelihood like:

$$\begin{aligned}\Lambda &= \ln f_X(x) \\ &= \ln \prod_{i=1}^{N} f_X(x_i) \\ &= \sum_{i=1}^{N} \ln(f_X(x_i)).\end{aligned} \tag{2.18}$$

where $x_i = (x_1, x_1, ..., x_N)$ which are samples of the interference. Here, the $\kappa$ is the only parameter to be estimated. The aim is to maximize the log-likelihood by choosing a $\kappa$ estimated.

To estimate $\kappa$, assuming that the log-likelihood is convex, we just need to find the zero point of its first-order derivative, and the corresponding $\kappa$ is what we try to find. So firstly, we write its first-order derivative as:

$$\frac{\partial \Lambda}{\partial \kappa} = \frac{N}{\kappa} - 2\kappa \cdot \sum \left(\frac{1}{x_i^2 + \kappa^2}\right). \tag{2.19}$$

we use Newton-Raphson method to find its zero point. In order to realize it, we also need to write its second-order derivative:

$$\frac{\partial^2 \Lambda}{\partial \kappa^2} = -N\kappa^{-2} - \sum_{i=1}^{N} \frac{2x_i^2 - 2\kappa^2}{(\kappa^2 + x_i^2)^2}. \tag{2.20}$$

As the principle of Newton-Raphson method, we begin with a first guess $\kappa_0$ for a root of the second-order derivative. And then a better approximation $\kappa_1$ is obtained by the following formula:

$$\kappa_1 = \kappa_0 - \frac{\frac{\partial \Lambda}{\partial \kappa}|_{x_0}}{\frac{\partial^2 \Lambda}{\partial \kappa^2}|_{x_0}}. \tag{2.21}$$

The process is repeated as:

$$\kappa_{n+1} = \kappa_n - \frac{\frac{\partial \Lambda}{\partial \kappa}|_{x_n}}{\frac{\partial^2 \Lambda}{\partial \kappa^2}|_{x_n}}. \tag{2.22}$$

until the difference between $\kappa_{n+1}$ and $\kappa_n$ is under $10^{-3}$, we stop the process and choose the current $\kappa$ as the value estimated.

The performance of the estimation results are illustrated in Table 2.2 under different impulsive noise settings. As expected, the value of $\kappa$ is close to $\gamma$ when the noise is highly impulsive and differs significantly when impulsiveness decreases. However it is quite difficult to interpret the parameter that depends both on the impulsiveness and on the signal strength.

| | Training sequence length | Mean | Standard deviation |
|---|---|---|---|
| Highly impulsive | 100 | 1.031 | 0.125 |
| | 500 | 1.027 | 0.0558 |
| | 1000 | 1.027 | 0.0392 |
| Moderately impulsive | 100 | 1.33 | 0.137 |
| | 500 | 1.33 | 0.0625 |
| | 1000 | 1.33 | 0.0431 |
| Slightly impulsive | 100 | 0.877 | 0.0826 |
| | 500 | 0.873 | 0.0391 |
| | 1000 | 0.873 | 0.0271 |
| Gaussian | 100 | 0.616 | 0.0613 |
| | 500 | 0.611 | 0.0258 |
| | 1000 | 0.612 | 0.0186 |
| $\epsilon$-contaminated | 100 | 0.477 | $4.41.10^{-4}$ |
| | 500 | 0.477 | $8.79.10^{-5}$ |
| | 1000 | 0.477 | $4.75.10^{-5}$ |

Table 2.2: Mean and variance for the estimated values of $\kappa$ in different situations and varying training sequence length. 1000 estimations were used.

### 2.3.6 Normal-Inverse-Gaussian receiver

We now develop a novel adaptive receiver based on an approximation of the noise distribution. This will be achieved through a flexible skew-kurtosis family of distributions known as the Normal-Inverse-Gaussian (NIG) model.

The NIG distribution was first motivated in the context of financial mathematics for stochastic volatility modeling in [9] and [10] and has since been utilized in a range of financial, signal processing and ecological applications, see for example [49] and [43]. We propose it as a useful model for the approximation of the optimal receiver in impulsive and time varying noise settings because of the fact that it has analytical expressions for the probability density and its first fours moments in terms of the model parameters. Also the normal inverse Gaussian distribution includes some common distributions, for example the Gaussian distributions and the Cauchy distribution, as special limiting cases. Thanks to these properties, there is a big interest to use it to approximate the noise and interference's intractable probability density function for using in our receivers.

The NIG model takes its name from the fact that it represents a Normal variance-mean mixture that occurs as the marginal distribution for a random variable $Y$ when cosidering a pair of random variable $(Y, Z)$ when $Z$ is distributed as an inverse Gaussian $Z \sim \mathcal{IG}(\delta, \sqrt{\alpha^2 - \beta^2})$, and $Y$ conditional on $Z$ is $(Y|Z = z) \sim \mathcal{N}(\mu + \beta z, z)$.

The NIG distributional family is characterized by four parameters $\alpha$, $\beta$, $\mu$ and $\delta$ (the same letters as the stable family which are used in a similar manner):

1. $\alpha$ is inversely related to the heaviness of the tails, where a small $\alpha$ corresponds to heavy tails that can accommodate outlying observations,
2. Skewness is directly controlled by the parameter $\beta$, where negative (positive) values of $\beta$ result in a left (right) skew, and $\beta = 0$ is the symmetric model,
3. Location (or translation) of the distribution is given by the parameter $\mu$,
4. Scale of the distribution is given by the parameter $\delta$.

The probability density function for the NIG model is given by:

$$f_{NIG}(y; \alpha, \beta, \mu, \delta) = \frac{\alpha\delta}{\pi} \frac{\exp[g\,(y)]}{h\,(y)} K_1[\alpha h\,(y)]. \tag{2.23}$$

where $g\,(y) = \delta\sqrt{\alpha^2 - \beta^2} + \beta\,(y - \mu)$ and $h\,(y) = [(y - \mu)^2 + \delta^2]^{1/2}$. $K_1()$ is a modified second kind Bessel function. Here the parameters should feed the condition :$\mu \in \Re$, $\delta > 0$, $0 \leq |\beta| \leq \alpha$.

The ease of estimation arises from the fact that the NIG distributional family has sufficient statistics given by the first four moments: mean, variance, skewness and kurtosis and the ability to explicitly solve for the parameters in terms of the cumulants of the distribution using Method of Moments.

Notably, when $\beta = 0$ and $\mu$ is arbitrary, the NIG model asymptotically approaches the Gaussian model $X \sim \mathcal{N}\left(\mu, \frac{\delta}{\alpha}\right)$ as $\alpha \to \infty$. Hence one could approximate the optimal linear Gaussian receiver if impulsive noise were not present at all time instants and only Gaussian thermal noise were incident on the received signal. In addition, when $\alpha = \beta = 0$ with $\mu$ and $\delta$ arbitrary, the NIG model approaches the Cauchy distribution. It can also approximate the skewness and kurtosis of the log-normal, Student's *t*, and gamma distributions, among others [49].

The NIG families flexibility can be captured by the shape triangle [12] of steepness and asymmetry:

$$\text{Steepness} = \left(1 + \delta\sqrt{\alpha^2 - \beta^2}\right)^{-1/2}, \quad \text{Asymmetry} = \frac{\beta}{\alpha} \times \text{Steepness}, \tag{2.24}$$

with $0 < \text{Steepness} < 1$ and $-1 < \text{Asymmetry} < 1$. Distributions with $\text{Asymmetry} = 0$ are symmetric, and the Gaussian and Cauchy distributions occur as limiting cases for $(\text{Asymmetry}, \text{Steepness})$ near (0,0) and (0,1), respectively. Fig. 2.8 provides a graphical representation of NIG probability example density functions.

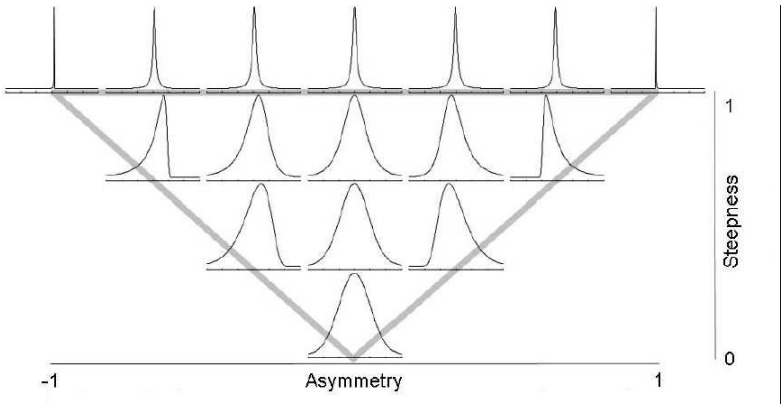


Figure 2.8: NIG triangle characterizing the flexibility of the skewness and kurtosis properties of the NIG family of models.

The sufficient statistics for the NIG model are given by the estimation of the moments

$$\begin{aligned}
\mathbb{E}[X] &= \mu + \frac{\delta\left(\frac{\beta}{\alpha}\right)}{\left(1 - \left(\frac{\beta}{\alpha}\right)^2\right)^{1/2}}, \quad \mathbb{V}\text{ar}[X] = \frac{\delta}{\alpha\left(1 - \left(\frac{\beta}{\alpha}\right)^2\right)^{3/2}}, \\
\mathbb{S}\text{kew}[X] &= \frac{3\left(\frac{\beta}{\alpha}\right)}{(\delta\alpha)^{1/2}\left(1 - \left(\frac{\beta}{\alpha}\right)^2\right)^{1/4}}, \quad \mathbb{K}\text{urt}[X] = 3\frac{4\left(\frac{\beta}{\alpha}\right)^2 + 1}{\delta\alpha\left(1 - \left(\frac{\beta}{\alpha}\right)^2\right)^{1/2}}.
\end{aligned} \tag{2.25}$$

which can be rearranged to solve for the model parameters in closed form as discussed below.

Its first four moments, mean, variance, skewness and kurtosis, which have closed-form expressions in our symmetric NIG model are:

$$\begin{aligned} \mathbb{E}[y_k] &= h_k x; && (2.26)\\ \mathbb{V}\mathbf{ar}[y_k] &= \frac{\delta}{\alpha}; && (2.27)\\ \mathbb{S}\mathbf{kew}[y_k] &= 0; && (2.28)\\ \mathbb{K}\mathbf{urt}[y_k] &= \frac{3}{\delta\alpha}. && (2.29) \end{aligned}$$

For the estimation, method of Moments is trivially achieved in general for NIG models if one restricts to a subfamily of the NIG distributions, through constraining on the existence of the first four cumulants, as detailed in [29], the expressions for the parameters of the NIG distribution in terms of its mean, variance, skewness and excess kurtosis under these constraints are then given in (2.30-2.31).

Given i.i.d. distributed NIG$(\alpha, \beta, \mu, \delta)$ random variables. The sample mean, sample variance, sample skewness and sample excess kurtosis, denoted by $\hat{\mathcal{M}}$, $\hat{\mathcal{V}}$, $\hat{\mathcal{S}}$ and $\hat{\mathcal{K}}$ respectively can be utilized to estimate the model parameters with a constraint imposed. Assume that the following constraint applies to the kurtosis $3\hat{\mathcal{K}} > 5$ and the skewness $\hat{\mathcal{S}}^2 > 0$, then the method of moments estimators for the parameters are given by

$$\begin{aligned} \hat{\alpha}_{\mathrm{MM}} &= 3\hat{\rho}^{1/2}(\hat{\rho}-1)^{-1}\hat{\mathcal{V}}^{-1/2}|\hat{\mathcal{S}}|^{-1},\\ \hat{\beta}_{\mathrm{MM}} &= 3(\hat{\rho}-1)^{-1}\hat{\mathcal{V}}^{-1/2}\hat{\mathcal{S}}^{-1},\\ \hat{\mu}_{\mathrm{MM}} &= \hat{\mathcal{M}} - 3\hat{\rho}^{-1}\hat{\mathcal{V}}^{1/2}\hat{\mathcal{S}}^{-1},\\ \hat{\delta}_{\mathrm{MM}} &= 3\hat{\rho}^{-1}(\hat{\rho}-1)^{1/2}\hat{\mathcal{V}}^{1/2}|\hat{\mathcal{S}}|^{-1}, \end{aligned} \qquad (2.30)$$

where $\hat{\rho} = 3\hat{\mathcal{K}}\hat{\mathcal{S}}^{-2} - 4 > 1$.

As we mentioned in the former chapter, we can further simplify these expressions since in this paper we consider the Symmetric NIG-Receiver where $f_{\mathrm{NIG}}(x; \alpha, \beta, \mu, \delta)$ is obtained according to (2.23) with parameter setting $\beta = \mu = 0$. This results in simpler parameter estimators given by:

$$\begin{aligned} \mathbb{E}[y_k] = 0;\ \mathbb{V}\mathrm{ar}[y_k] &= \frac{\delta}{\alpha};\\ \mathbb{S}\mathrm{kew}[y_k] = 0;\ \mathbb{K}\mathrm{urt}[y_k] &= \frac{3}{\delta\alpha}. \end{aligned} \qquad (2.31)$$

We note that special care has to be taken due to the high order moment calculation,

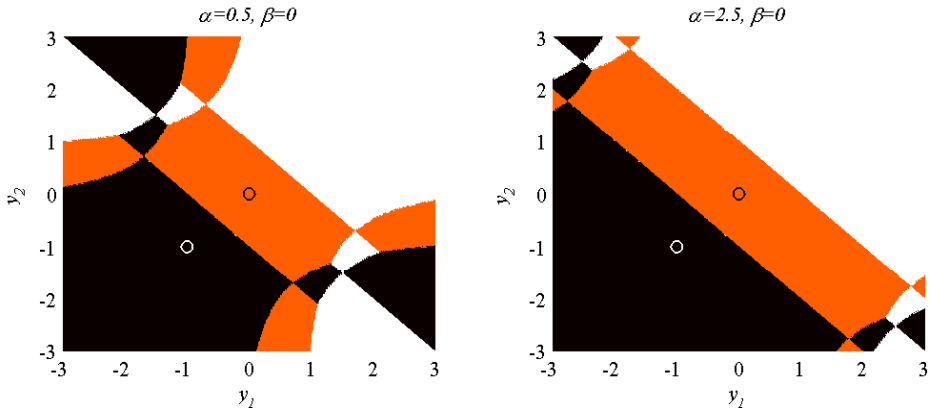


Figure 2.9: Decision regions for the NIG receiver when $\alpha = 0.3$ or $2.5$ ($\delta = 1$ and $\beta = \mu = 0$).

especially in the illustration we take involving stable distribution for the true impulsive interference distribution. To ensure the validity of the obtained parameters we need to reduce the impact of large samples in the training sequence. This is achieved by a soft thresholding method known widely in statistics as tempering the empirical distribution of the data before calculating the moments. This can also be known as exponential tilting and it ensures the approximate NIG receiver model is always well defined, see discussions in [51].

To illustrate how flexible the proposed NIG receiver is, we plot in Fig. 2.9 the decision regions as in Section 2.2, considering the maximisation problem in (2.3) with the density $f_{\mathrm{NIG}}(x; \alpha, 0, 0, \delta)$ given in (2.23).

We notice that the impact of impulsiveness is well taken into account and modifying the $\alpha$ will allow to adjust the "linear part" of the receiver. We can expect that this receiver will be able to adjust to different impulsiveness degrees approximating well a wide variety of sub-exponential impulsive noise models as well as the purely Gaussian noise.

In Fig. 2.10 and 2.11 we present two cases of fitting NIG and Myriad to the true interference data exhibiting high (Fig. 2.10) and low (Fig. 2.11) impulsive component for a training sequences of $100$ samples. A compact boxplot is used with the single thick black line for the truth and the estimated NIG or Myriad medians are dots with interquartile whiskers vertical black lines; outliers are denoted by "o" markers.

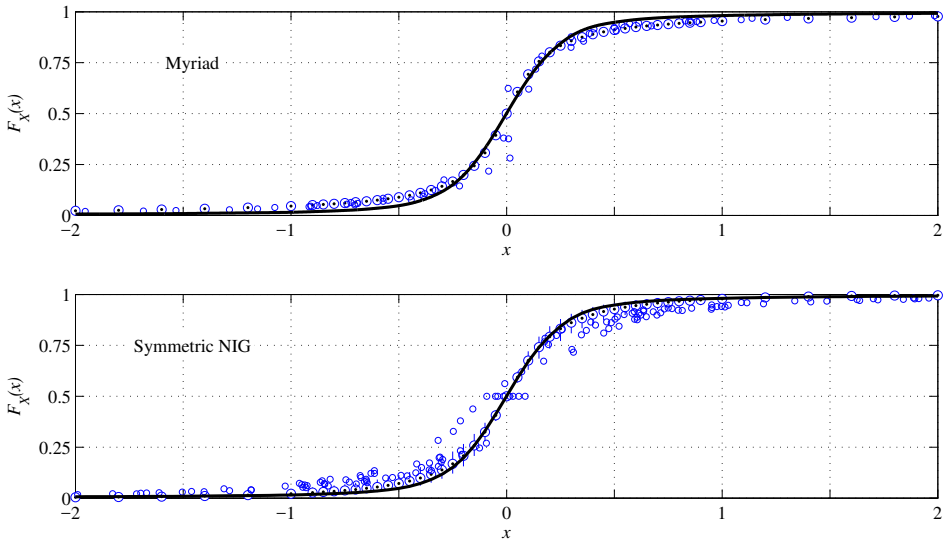


Figure 2.10: NIG and Myriad approximations of a mixture of stable ($\alpha = 1.2$ and $\gamma = 1$) and Gaussian ($\sigma^2 = 0.2$)(high impulsive case)

We see that the approximations are rather good and robust to estimation. The Myriad seems to be more accurate at the center of the curve and less for the tails, especially when impulsiveness decreases (Fig. 2.10). This is expected because the Myriad is inspired by the Cauchy distribution when the NIG covers a large range with Gaussian and Cauchy as limiting cases.

### 2.3.7 Hole-puncher and soft-limiter receiver

The three preceding examples were based on empirical choices of distribution families. At least the two last proposals (Cauchy, NIG) are supposed to cover a large range of situations. Consequently the designed receivers should be robust to a relatively large

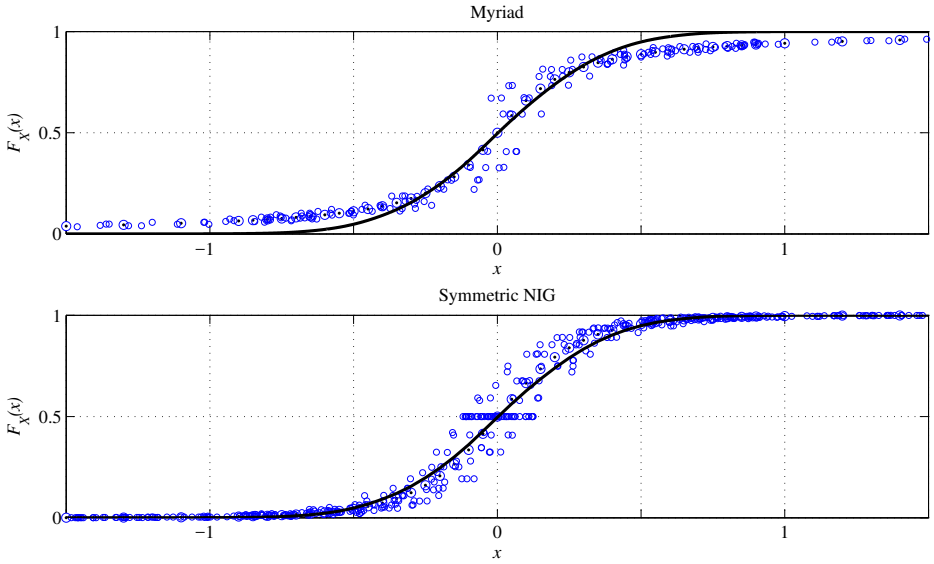


Figure 2.11: NIG and Myriad approximations of a mixture of stable ($\alpha = 1.2$ and $\gamma = 0.28$) and Gaussian ($\sigma^2 = 0.2$)(low impulsive case)

number of situations. We will now study another way to design the receiver. This approach is based on the log-likelihood ratio. When noise is impulsive, the optimal LLR tends to reduce the weight of large values in the decision. This means that we should not trust large absolute values, contrary to the decision weight that the linear receiver would attribute. This idea leads to a modification of the LLR function and classical examples are the soft limiter and the hole puncher [68, 3, 85, 76, 59]. For small received samples, a linear function is used and for large samples, respectively, a constant value or a zero are used as output of the LLR function.

The hole-puncher applies the following function before adding the different samples to take the decision:

$$g_{\text{hp}}(x) = \begin{cases} x, & |x| < \kappa \\ 0, & \text{otherwise} \end{cases} \tag{2.32}$$

For the soft-limiter receiver, it replaces $g_{\text{hp}}(x)$ by the following function:

$$g_{\text{sl}}(x) = \begin{cases} -\kappa, & x < -\kappa \\ x, & |x| < \kappa \\ \kappa, & x > \kappa \end{cases} \tag{2.33}$$

We tested several value of $\kappa$ and compare the optimal LLR with the real noise samples and we choose $\kappa = 1$ for Soft-limiter and $\kappa = 4$ for Hole-puncher for simulation.

Those functions have the advantage of simplicity. However, as will be seen in Fig. 2.12, they do not mimic very well the LLR and a performance degradation compared to the optimal case is to be expected.

### 2.3.8 $p$-norm receiver

Another way to analyse detection is to consider that the likelihood measures a distance between the received signal and the possible transmitted signals. Optimal in Gaussian noise, the Euclidean distance is not adapted to the impulsive case.

To improve the performance, a solution is then to modify this metric and to use the $p$-norm, which is recommended for GGD [13] and is a distance measurement in $\alpha$-stable situations with $p < \alpha$, see [42], as the $\alpha$-norm can be written

$$\|X - Y\|_\alpha = \begin{cases} [\mathbb{E}|X - Y|^p / C(\alpha, p)]^{1/p}, & 1 \leq \alpha \leq 2 \\ [\mathbb{E}|X - Y|^p / C(\alpha, p)]^{\alpha/p}, & 0 < \alpha < 1 \end{cases} \tag{2.34}$$

where $C(\alpha, p) = \frac{2^{p+1}\Gamma((p+1)/2)\Gamma(-p/\alpha)}{\alpha\sqrt{\pi}\Gamma(-p/2)}$. $\Gamma(\cdot)$ is the gamma function as:

$$\Gamma(t) = \int_0^\infty x^{t-1} e^{-x} dx \tag{2.35}$$

In [81], an interference suppression scheme for DS/CDMA systems in the presence of additive Symmetric $\alpha$-stable (S$\alpha$S) interference is proposed based on the $L_p$-norm instead of the standard Least Mean Square based on the $L_2$-norm.

It is interesting to see that we do not need any estimation of distribution parameters, and only a rough knowledge of $\alpha$ is enough. We give the $p$-norm metric in our decision statistic as:

$$\Lambda_p = \sum_{k=1}^{K} \left( |y_k - h_k s_0|^p - |y_k - h_k s_1|^p \right) \tag{2.36}$$

Even though we do not need to know any underlying interference distribution that would give us an optimal $p$, it is obvious that the estimation of the value of $p$ is important and will impact the quality of the receiver.

For the estimation, the question is to find the appropriate $p$ to have the best decision performance. Here we use the concept of generalized Gaussian distribution. We estimated the shape parameter $\beta$ which is used as the value $p$ for our $p$-norm. We adopt

an approximate maximum likelihood method. We again use Newton-Raphason method. First of all, we assume that the mean $\mu$ is equal to 0. We start from an initial guess of $\beta = \beta_0$, which is

$$\beta_0 = \frac{m_1}{\sqrt{m_2}}, \tag{2.37}$$

where

$$m_1 = \frac{1}{N}\sum_{i=1}^{N}|x_i|, \tag{2.38}$$

which is the first statistical moment of the absolute values and $m_2$ is the second statistical moment which is

$$m_2 = \frac{1}{N}\sum_{i=1}^{N}|x_i|^2. \tag{2.39}$$

We follow the iteration:

$$\beta_{i+1} = \beta_i - \frac{g(\beta_i)}{g'(\beta_i)}, \tag{2.40}$$

where

$$\begin{aligned} g(\beta) = 1 &+ \frac{\psi(1/\beta)}{\beta} - \frac{\sum_{i=1}^{N}|x_i|^\beta \log|x_i|}{\sum_{i=1}^{N}|x_i|^\beta} \\ &+ \frac{\log(\frac{\beta}{N}\sum_{i=1}^{N}|x_i|^\beta)}{\beta}, \end{aligned} \tag{2.41}$$

and

$$\begin{aligned} g'(\beta) = &- \frac{\psi(1/\beta)}{\beta^2} - \frac{\psi'(1/\beta)}{\beta^3} + \frac{1}{\beta^2} - \frac{\sum_{i=1}^{N}|x_i|^\beta(\log|x_i|)^2}{\sum_{i=1}^{N}|x_i|^\beta} \\ &+ \frac{(\sum_{i=1}^{N}|x_i|^\beta \log|x_i|)^2}{(\sum_{i=1}^{N}|x_i|^\beta)^2} + \frac{\sum_{i=1}^{N}|x_i|^\beta \log|x_i|}{\beta\sum_{i=1}^{N}|x_i|^\beta} \\ &- \frac{\log(\frac{\beta}{N}\sum_{i=1}^{N}|x_i|^\beta)}{\beta^2}, \end{aligned} \tag{2.42}$$

where $\psi(\cdot)$ is the digamma function as

$$\psi(x) = \frac{d}{dx}\mathbf{ln}\Gamma(x) \tag{2.43}$$

and $\psi'(\cdot)$ is the trigamma function as

$$\psi(x) = \frac{d^2}{dx^2}\mathbf{ln}\Gamma(x) \tag{2.44}$$

We repeat the integration until we get the estimated $\beta$.

The performance of the estimation is illustrated in Table 2.3. It shows that the estimator converges, with a slightly over estimated value when the training sequence is short (100 samples).

| | Training sequence length | Mean | Standard deviation |
|---|---|---|---|
| Highly impulsive | 100<br>500<br>1000 | 0.557<br>0.488<br>0.476 | 0.16<br>0.067<br>0.049 |
| Moderately impulsive | 100<br>500<br>1000 | 1.07<br>0.871<br>0.833 | 0.39<br>0.16<br>0.124 |
| Slightly impulsive | 100<br>500<br>1000 | 2.19<br>1.98<br>1.97 | 0.665<br>0.238<br>0.188 |
| Gaussian | 100<br>500<br>1000 | 3.72<br>2.02<br>2.01 | 48.2<br>0.204<br>0.148 |
| $\epsilon$-contaminated | 100<br><br>500<br>1000 | 1.64<br><br>1.2<br>1.14 | 0.105<br><br>0.0138<br>0.00465 |

Table 2.3: Mean and variance for the estimated values of $p$ in the same situations as Table 2.2 and varying training sequence length. 1000 estimations were used.

As expected, the $p$ value reduces when impulsiveness increases and is close to $2$ when the Gaussian thermal noise is dominant. We can also notice that for moderately and highly impulsive situations, the value of $p$ is less than $1$ which results in the *sharp* shape of the LLR.

We present in Figure 2.12 the optimal LLR (left plot) if the exact noise distribution was known in the case of $\epsilon$-contaminated, slightly and highly impulsive noises (left plot)

and the different approximations (right plot): the soft limiter, $p$-norm and hole puncher cases.

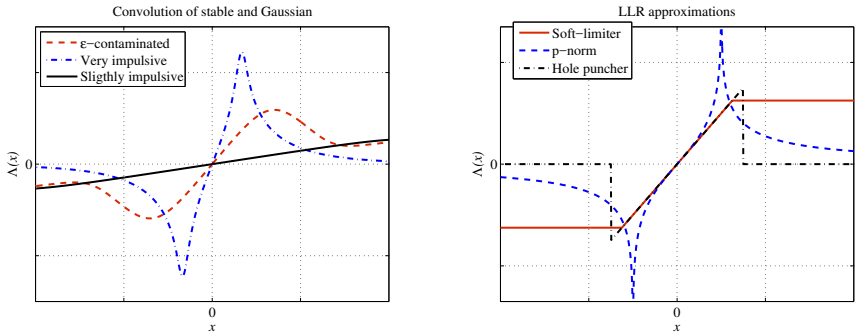


Figure 2.12: LLR for different noises. The very and slightly impulsive cases are defined as in Table 2.2 with $\gamma = 0.1$ in both case. The $\epsilon$-contaminated as the same parameters as in Fig. 1.10. The value of $p$ is $0.5$.

When noise is slightly impulsive the linear section of the LLR is larger while it is sharper when the level of impulsiveness increases. The approximated LLRs reduce the weight of large values in the decision but only the $p$-norm offers a shape that is capable to mimic the highly impulsive case. It is to be noted however that the shape will be significantly modified for different values of $p$ and takes the optimal form if $p = 2$ for the pure Gaussian noise. It is also worth mentioning that the $p$-norm could be viewed as an optimal receiver for a Generalized Gaussian interference and consequently considered as an approach that was attempting to approximate the noise distribution.

## 2.4 Simulation results

An analytical evaluation of our framework is difficult because we want to be flexible on the noise model. Some numerical integration could be adapted to any noise assumptions but they would be greedy to implement, especially when an $\alpha$-stable component is introduced. Consequently we have preferred to perform extensive simulations to compare the performance of the proposed detection solutions.

We chose the number of repetition of signal $K$ equal to 5. The channel is a Rayleigh fading channel independent and identically distributed for the 5 received samples.

Representing all interference situations is not possible but we propose to study five cases from highly impulsive to pure Gaussian:

1. pure Gaussian case; $\sigma^2 = 1$ for parameter estimation tests;

2. highly impulsive case: mixture of $\alpha$-stable and Gaussian noises with $\alpha = 1.2$ and the noise to interference ratio (NIR$= \sigma^2/(2\gamma)$) is set to $-10$ dB; $\gamma = 1$ for parameter estimation tests;
3. moderately impulsive case: mixture of $\alpha$-stable and Gaussian noises with $\alpha = 1.5$, NIR $= 0$ dB; $\gamma = 1$ for parameter estimation tests;
4. slightly impulsive case: mixture of $\alpha$-stable and Gaussian noises with $\alpha = 1.8$, NIR $= 10$ dB; $\gamma = 0.1$ for parameter estimation tests;
5. other impulsive noise model: $\epsilon$-contaminated model, Gaussian mixture, Generalized Gaussian distribution model and Middleton Class A model.

Figure 2.13 represent noise realisations for each example with 500 noise samples gen-

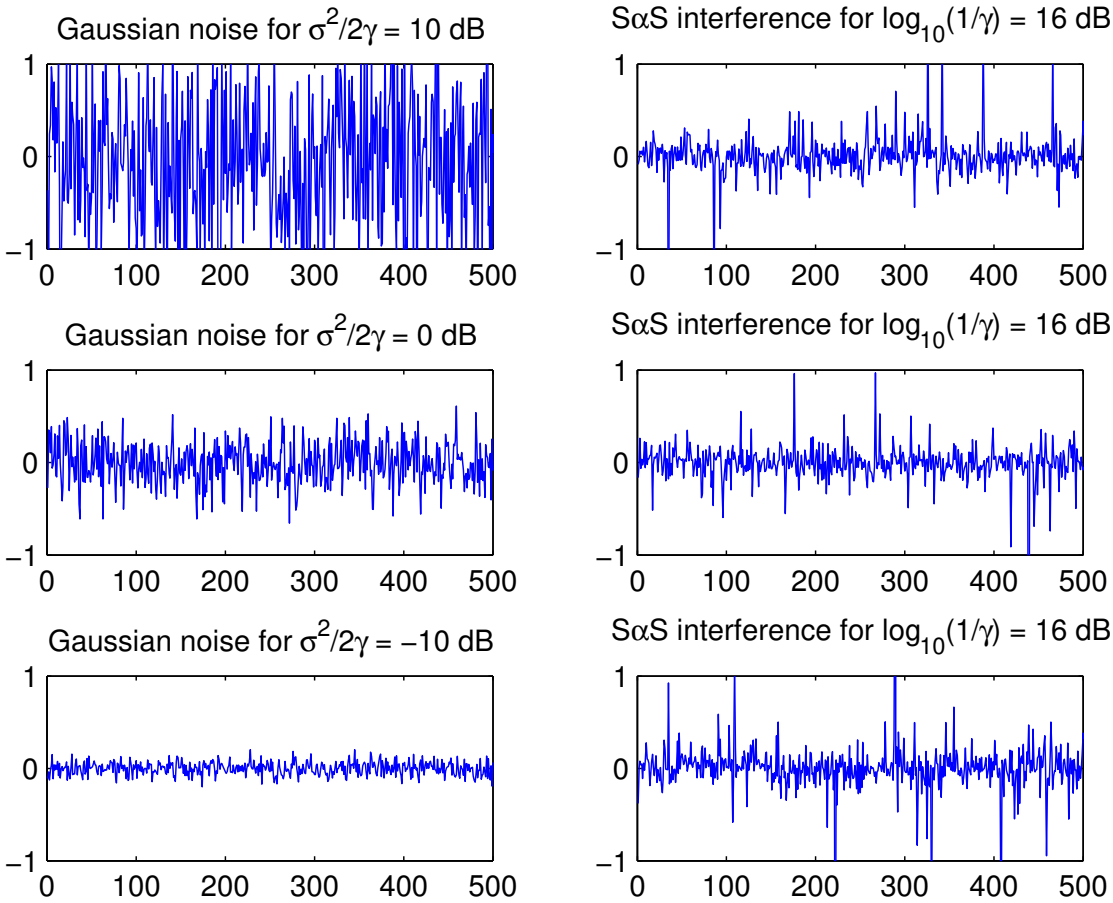


Figure 2.13: Comparison of different noise dominating environments

We compare in the following figures the BER performance of Gaussian, Cauchy, Myriad, symmetric NIG, soft-limiter and $p$-norm receivers. When the noise involves an

$\alpha$-stable impulsive interference, the BER is measured as a function of the inverse dispersion of the S$\alpha$S distributions $(1/\gamma)$ for network interference, since the increasing of inverse dispersion indicates the decreasing of the network interference strength, reflecting the conventional signal-to-noise ratios. When the noise is purely Gaussian or $\epsilon$-contaminated, the SNR at the receiver is used for the $x$-axis. The number of training samples for NIG, Myriad and $p$ estimations is set to 1000 bits.

### 2.4.1 Gaussian noise

Our first step is to observe the receivers' performance under a purely Gaussian noise.

In Fig. 2.14. the Gaussian receiver (MRC) used here is the conventional one.

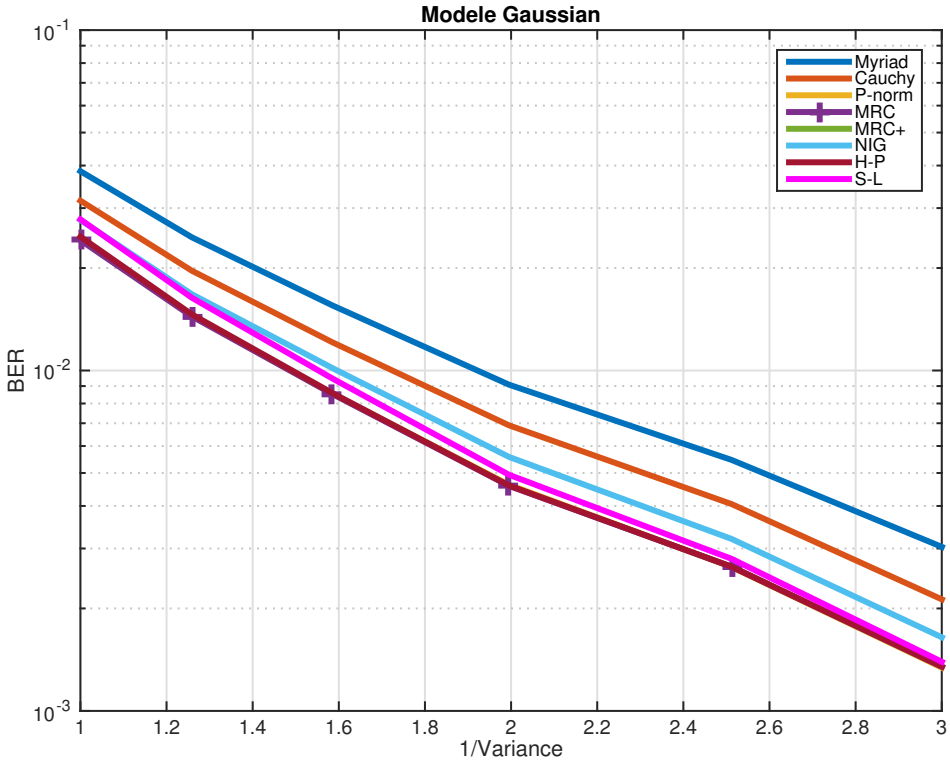


Figure 2.14: BER of different receivers under Gaussian noise

We observed that Myriad receiver gives us degraded BER compared to the MRC, which gives the best BER performance because it is the optimal receiver in the Gaussian case. Here we didn't use the adapted MRC which is designed for $\alpha$-stable case. NIG receiver performs close to the optimal one with a reasonable calculation precision gap.

Soft-limiter and Hole-puncher show also good performance, because in Gaussian noise case, the big value event occurs rarely. Their LLR function at small value is the same as the MRC receiver. $p$-norm receiver also gives a good performance because the estimated value is very close to 2 and it behaves as the linear receiver.(On the figure, it covered by the MRC, so we can't see it.) Cauchy receiver is expected to be optimal only in pure Cauchy noise, thus its performance is not good in this case. But in this case, Cauchy receiver gives a better performance than Myriad receiver, it seems that the estimation procedure of Myriad receiver doesn't work very well in the Gaussian case.

### 2.4.2 Slightly impulsive environment

In the convolution of an $\alpha$-stable interference and a Gaussian thermal noise, due to the infinite second moment of the $\alpha$-stable distribution, we use the dispersion $\gamma$ to denote the strength of the interference. The noise-to-interference ratio is defined as followed:

$$NIR = \frac{\sigma^2}{2\gamma}. \tag{2.45}$$

We launch our simulation with $NIR = 10$ dB $\alpha$=1.8, the dominant noise is Gaussian.

Figure 2.15 shows the BER of different receivers under slightly impulsive noise environment. The Cauchy receiver gives the poorest performance among all the receivers. We could notice that the Myriad is still less efficient. Inspired by the Cauchy distribution, the myriad performances should improve as impulsiveness increases. The dominant thermal noise makes the MRC receiver still efficient. The optimal MRC works even better than the conventional one. $p$-norm and NIG receiver behave also well. However Similarly the MRC looses a little at high SNR, when the significant part of the noise will be due to peaks from the impulsive interference and not from the Gaussian noise.

As this parameter configuration reflects a Gaussian noise dominated environment, any adapted methods tend to have good performance except for the more impulsive specific one.

### 2.4.3 Moderate impulsive environment

In Fig. 2.16, $\alpha$ is set to $1.5$ and NIR is $0$ dB.

In this case, the $\alpha$-stable modelled network interference and Gaussian modelled thermal noise are comparable. The interference environment is moderately impulsive.

As we previewed, the MRC receiver has difficulties in dealing with the impulsive interference. Even the optimal MRC receiver, which is adapted to the $\alpha$-stable case gives a bad performance compared to other receivers.

We can see that the Hole-puncher and Soft-limiter receivers allows an improvement

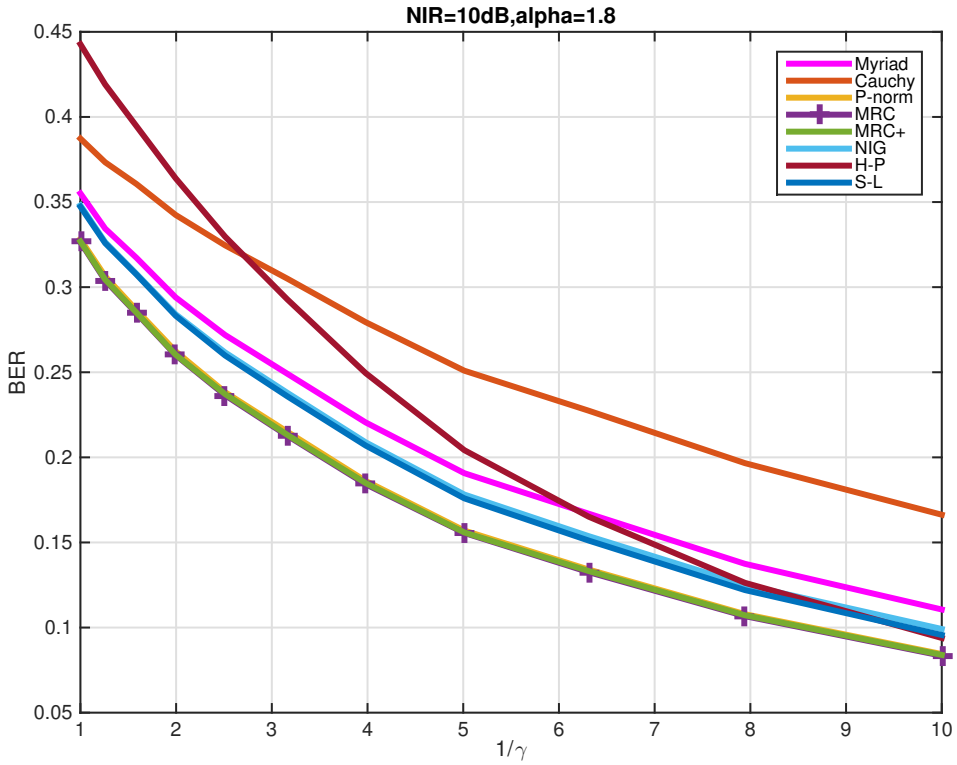


Figure 2.15: BER of different receivers under slightly impulsive noise environment

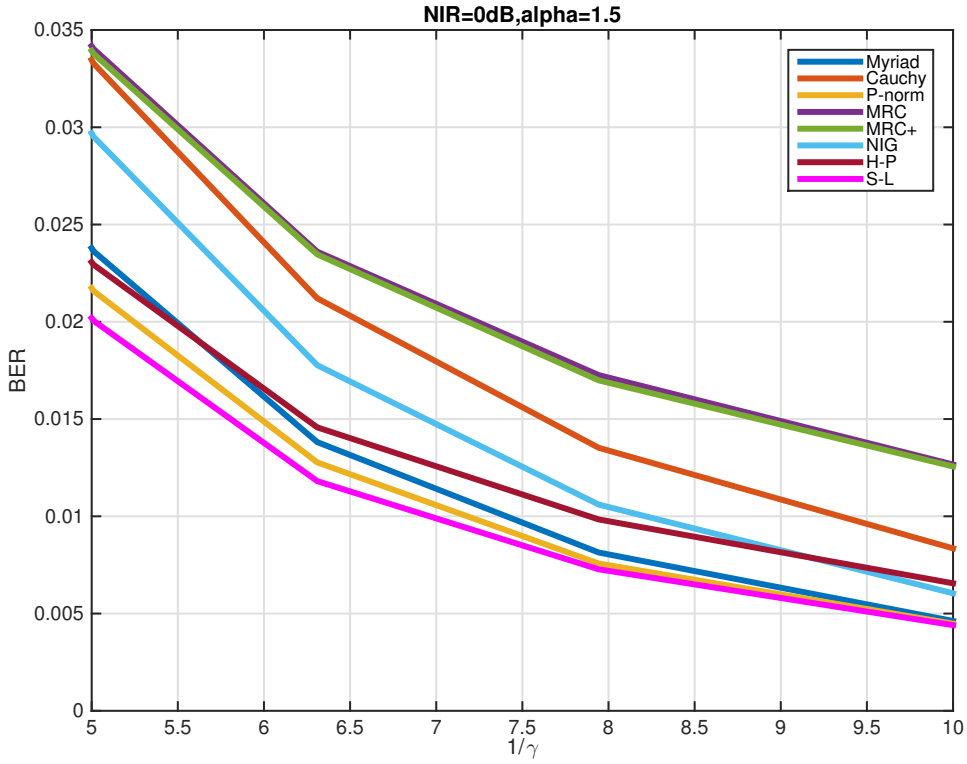


Figure 2.16: Moderate impulsive environment

compared to linear approaches. Especially, the Soft-limiter receiver gives the best performance among all.

The Cauchy receiver shows a little improvement compared to linear approaches due to the increased impact of the large samples. But it still gives the worst behaviour except for the MRC.

NIG receiver does not work perfectly at low $1/\gamma$, but it improves when $1/\gamma$ becomes bigger, when the performance becomes acceptable even for the best receivers. It remains so an interesting candidate.

The Myriad and $p$-norm receivers give good performances and are very close, even if the Myriad performs better and better when $1/\gamma$ gets higher, i.e. where the impulsive part of the noise is the limiting factor.

### 2.4.4 Highly impulsive environment

We consider in Fig. 2.17 the case where $\alpha = 1.2$ and NIR $= -10$ dB.

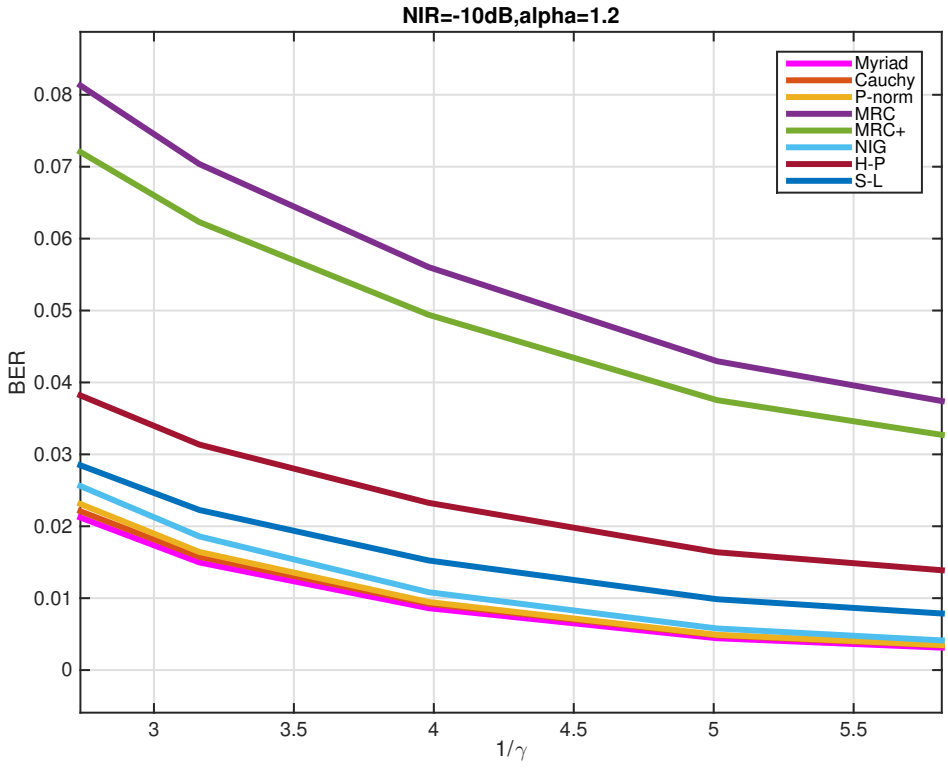


Figure 2.17: Highly impulsive environment

In this case, $\alpha$-stable modelled network interference dominates the whole noise.

The interference environment is strongly impulsive. The conventional MRC performs poorly in such an impulsive case. Even though the optimal MRC improves slightly the performance, it is not significant. On the other hand the Cauchy receiver becomes very efficient. Because in this case, the impulsive $\alpha$-stable interference dominates, and $\alpha$ is close to 1, which is the optimal case for Cauchy receiver. Other approaches give also good performance. NIG, Myriad and $p$-norm are well adapted in such a case. Finally, in this case Hole-puncher and Soft-limiter receivers begin to perform less well, but the result is still acceptable.

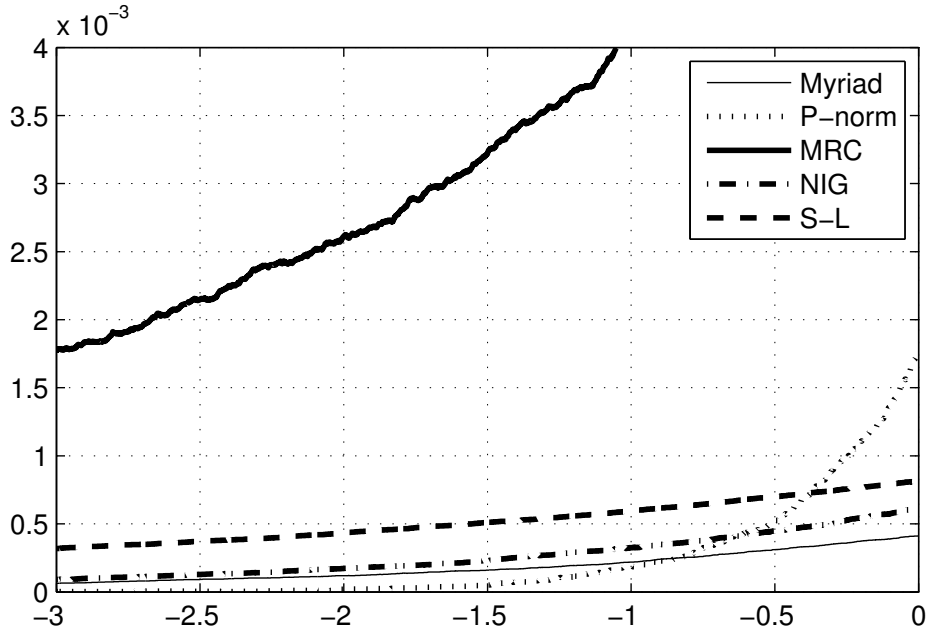


Figure 2.18: pdf of decision statistics in dominant $\alpha$-stable noise plus Gaussian noise.

Figure 2.18 shows pdf of the decision statistic for some of the receivers in dominant $\alpha$-stable noise plus Gaussian noise. For transmitted symbols with the same probability and symmetric noise plus interference, the BER is the area under the curves for the x-axis between minus infinity to 0. It gives a more straightforward way to explain the receivers' performance. In this case, we fix $\frac{1}{\gamma} = 10dB$. We did not present the result of the integration but it is clear that the tenancy is the same as in the BER plots. It is surprising however to note the different behaviour of the $p$-norm compare to the other approaches. Further investigation is needed about this aspect.

### 2.4.5 Other impulsive noise models

In the following we examine the reliability of our conclusions if the noise model is still impulsive but the $\alpha$-stable is not the right model.

#### $\epsilon$-contaminated case

We first use $\epsilon$-contaminated distribution as our noise case. Here, we fix the value of $\epsilon$ at $0.01$, which denotes the contamination of the impulsive part.

The factor of impulsive strength $\kappa$ is fixed at $100$. We change the value of $\sigma$ in the formula. The figure of result is functioned by the $1/$variance of the interference.

This situation represents a highly impulsive noise but without an heavy tail representation. MRC receiver gives the poorest performance. That confirms that the MRC receiver is not robust in the impulsive environment. Hole-puncher and Soft-limiter also do not work very well. We can however question the choice of the parameter for these two receivers. We can notice that the Myriad and the NIG are behaving well. The $p$-norm presents a slight loss and, probably, the estimated value for $p$ is too large in that case (see Table 2.3). However we can conclude that the proposed design strategies keep robust with different interference model.

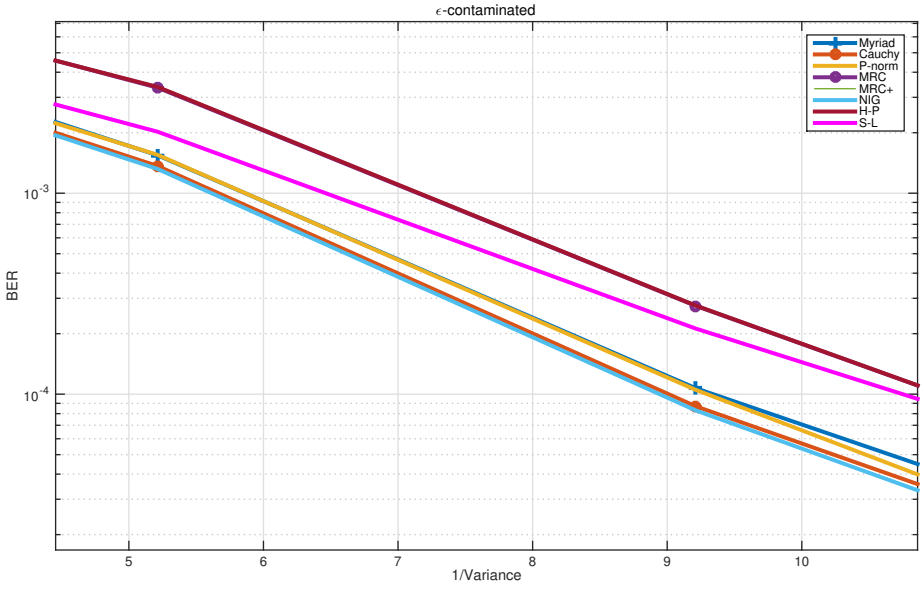


Figure 2.19: Performance in $\epsilon$-contaminated noise

Figure 2.20 shows pdf of the decision statistic for some of these receivers in $\epsilon$-contaminated noise.

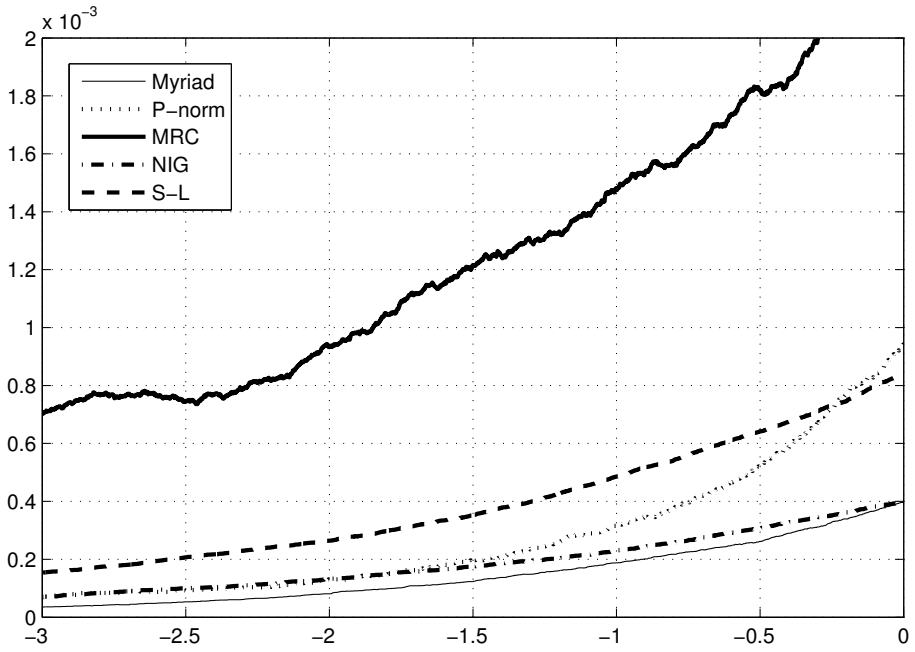


Figure 2.20: pdf of decision statistics in $\epsilon$-contaminated noise.

### Gaussian mixture case

In Gaussian mixture model case, to simplify our simulation, we take the symmetric case. We take only three terms, whose proportion is 95%, 2.5% and 2.5%. The one who has the biggest proportion is centred at 0, and the other two are centred at $+1$ and -1, both with the same variance. We fix the standard deviation for the centred one with the value of 0.2, and make the figure of BER in terms of the 1/variance while changing the standard deviation for the smaller two.

Figure 2.21 shows the BER of receivers in Gaussian mixture noise.

Myriad and the NIG are still behaving well as usual. It shows they are very robust in the impulsive environment no matter which model we choose. The $p$-norm performs a little less well than the former two, but it is still acceptable. Cauchy receiver give a medium performance. MRC, Hole-puncher and Soft-limiter receiver again work poorly.

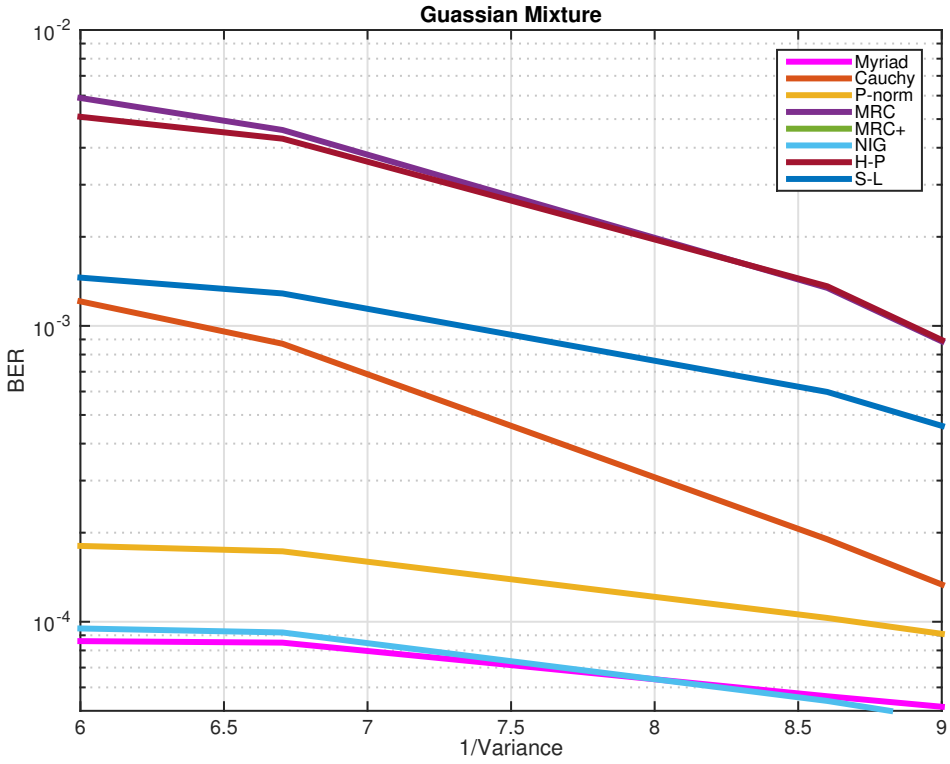


Figure 2.21: Performance in Gaussian mixture model noise.

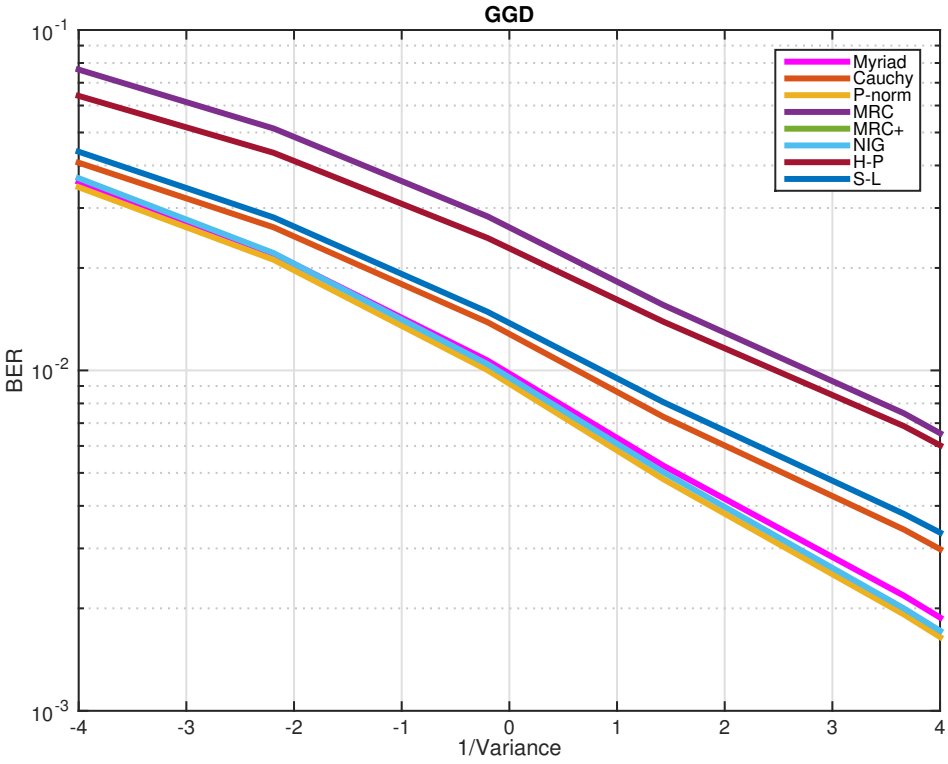


Figure 2.22: Performance in generalized Gaussian distribution model noise.

### Generalized Gaussian Distribution case

In generalized Gaussian distribution model case, we fix the shape parameter $\beta = 0.6$ and vary the variance. Figure 2.22 shows the BER of receivers in generalized Gaussian distribution noise.

The simulation result is similar to that of Gaussian mixture noise case. Myriad, NIG and $p$-norm receivers show a good robustness in the impulsive environment. Cauchy and Soft-limiter receiver give an acceptable BER result. And without surprise, Hole-puncher and MRC works poorly.

### Middleton Class A case

We try also the Middleton Class A noise. We fix the ratio of the intensity of the independent Gaussian component to the intensity of the impulsive non-Gaussian component and change the overlap index.

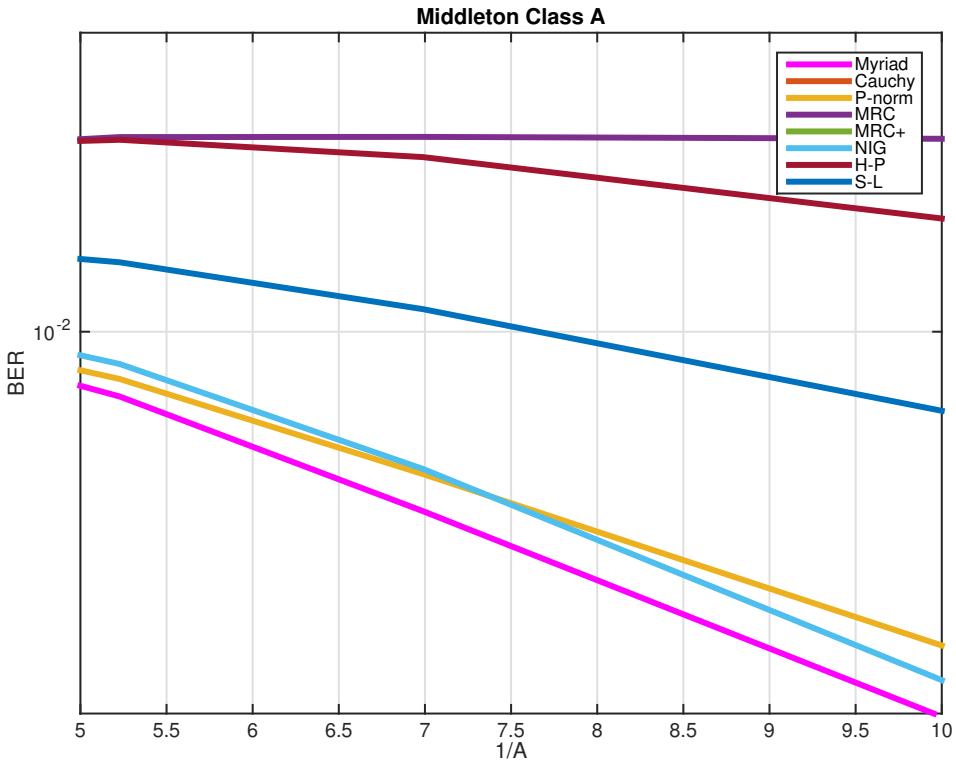


Figure 2.23: Performance in Middleton Class A noise.

Figure 2.23 shows the receivers' BER performance in Middleton Class A noise.

The result confirms the previous results in other impulsive situations. Myriad, NIG and $p$-norm receiver give almost the same and best BER value. Hole-puncher and MRC receiver have a great gap with the former three receivers. And Soft-limiter is between them.

### 2.4.6 Summary of results.

In Table 2.4, we compare the different receivers' performance in different noise. By comparing our simulation result, we can have some conclusions:

- The MRC receiver only give us good performance when the Gaussian noise is dominant. As soon as impulsive noise is not low, it performs poorly even if optimal linear receivers [54] are considered.

- Approaches trying to approximate the noise distribution give good performance. We evaluated two flexible families of distributions with parameters that can be easily and efficiently estimated: (*a*) the Myriad with a single parameter to be estimated with a quick and efficient root search. It gives the best performance and robustness among all the receivers. The use of Cauchy distribution limits however the flexibility of the model when impulsiveness decreases. We also proposed (*b*) the NIG distribution family: it presents both the required flexibility and an easy parameter estimation procedure based on moment estimation. Performance is good in all situations. Both approaches are robust and adaptive but the NIG outperforms the myriad when impulsiveness is low. Implementing the LLR based on the NIG however requires a more complex function, including a Bessel function, and the computational cost has to be evaluated.

- LLR approximation based approaches seem to have good potential. They have been less studied in the literature and more work has to be done in that direction. The intuitive approaches are the soft limiter and the hole puncher that limits the impact of the large values. They improve the performance of the linear approach when impulsive interference is present and have a limited impact when impulsiveness decreases. However they are significantly less efficient than other non linear solutions. Their performance is sensitive to the setting of parameters. The estimation of threshold should be improved to better approximate de real LLR.

- The $p$-norm allows either a "close to linear" or linear behaviour when the Gaussian noise is the main contribution to the noise and also approaches the *sharp* shape of the LLR when impulsiveness increases. A single parameter $p$ has to be estimated with a root search numerical procedure.

| | MRC | HP | SL | Cauchy | Myriad | p-norm | NIG |
|---|---|---|---|---|---|---|---|
| pure Gaussian | ++ | ++ | ++ | + | - | ++ | + |
| slightly impulsive | ++ | + | + | – | + | ++ | + |
| moderate impulsive | – | + | ++ | - | ++ | ++ | + |
| highly impulsive | – | - | + | ++ | ++ | ++ | ++ |
| $\epsilon$-contaminated | – | – | - | ++ | ++ | ++ | ++ |
| Gaussian-Mixer | – | – | - | + | ++ | + | ++ |
| GGD | – | – | + | + | ++ | + | ++ |
| Middleton Class A | – | – | - | | ++ | + | ++ |

Table 2.4: Comparison of different receivers' performance in different noise

- Other solutions could be developed based on a training sequence to obtain parameters directly on an estimated LLR. Other works have also proposed approximations of the LLR for weak signal detection [90] and could be extended to this type of detection strategy.

Analysing these environments, we can conclude that the analysis done on stable interference can be extended to other types of impulsive noises. The $p$-norm, Myriad and NIG receivers still show the best robustness. MRC and hole-puncher perform the worst. Hole-puncher and Soft-limiter receivers need a good choice of the parameter. The estimation of the parameters for the three best receivers adapts whatever the noise model. Our conclusion is that the assumptions needed to obtain the $\alpha$-stable characteristic function for the interference can be accepted. The model has a theoretical justification and is able to accurately represent different kinds of environments. Up to here, we stay under the i.i.d. assumption. In the following chapter, we will further study the spatial and temporal dependence generated by the space, time and frequency diversity. In result, we have to choose new models to well capture the dependence structure of the interference.

Chapter 3

# Dependence

In the previous chapters, we have discussed the case where there is not any dependency between the samples of the interference super-imposed to each replica of the information.

However, space, time or frequency diversity can result in vectors with dependent components. If in time hopping ultra wide band the combination of interferers changes at each pulse, a strong interferer can be present during a long period in comparison to the bit duration. It will increase the probability of strong interference simultaneously on different repetitions. In a multiple receive antenna system, a strong interferer will simultaneously be received on several antennas, giving a non zero probability of having several strong interference samples on the different replicas at the different receive antennas. Consequently, this independence assumption is, in many cases, not realistic.

Some papers have worked based on the assumption of signal or interference with correlation and dependence. Mahmood *et al*. in [60] use the symmetric $\alpha$-stable model for additive noise. When converted to its complex baseband form, the noise is generally not isotropic. It means that the real and imaginary components are dependent, which is different from the AWGN channel. Using the variable geometry offered by these distributions, they propose an efficient placement of the signal points on the constellation for a QPSK to improve the uncoded error performance of the system. In [57], outage and minimum duration outage probabilities have been evaluated for integrated CDMA systems and overall correlation between signal and interference was estimated. In [44], the joint temporal statistics of interference in the network is derived along with an assumption of a bounded path-loss function. Its closed-form statistics are asymptotically exact for low tail probabilities. In [38], a Taylor-series type expansion of functions of interference is provided, where in increasing the number of terms in the series provides a better approximation at the cost of increased complexity of computation. In [80], closed-form expressions and calculation rules for the correlation coefficient of the over-

all interference are derived. Three sources of correlation are considered: node locations, channel and traffic. In [23], a multiple antennas receiver is considered. Several cases are discussed, depending on the sets of interferers seen by each receiver antenna, either completely different, exactly the same, or partially identical. The dependence is then simulated with more or less similarities in the interferers' sets.

To our knowledge, however, no literature has yet addressed the impact of extremal tail dependence.

So we want to make an initial attempt to study the following features:

- we propose a way to model the dependence structure between interference random variables that may arise from spatial, temporal or spatio-temporal dependence structures;
- we study the impact of this dependence on the receivers' performance.

We observe that the dependence structure may arise from a number of different mechanisms. Therefore, we do not focus on such mechanisms and more works are needed to characterize them. Instead, we take a statistical signal processing perspective in which we argue that in the presence of dependent interference, it is essential to appropriately model it and study its impact of receiver design. Consequently, we propose a framework to model this dependence structure and show that its presence degrades the receiver performance. We are convinced that this general framework may adapt to most of the encountered scenarios and give solutions to define optimal receiver structures.

## 3.1 System model

First of all, we observe that the dependence structure may arise from a number of different mechanisms. To illustrate this dependence structure, we consider a generic multi-user wireless system model without power control.

The system model has been presented in chapter 1.1. Equation (1.9) gives the received interference. The multiplicity of random variables, whose real distributions are not necessarily known, makes difficult if not impossible an analytical study of the dependence structure. We will rely on two simulated scenarios to have a more precise idea about the existence, or not, of a dependence structure. The first studied case is n UWB communication; the seconde one is a SIMO link. We will then introduce general frameworks that can model the dependence in impulsive noises.

**Case 1** UWB

We first consider an UWB transmission with narrow band interferer. In that case two repetitions of a pulse will be impacted by different interferers due to the time-hopping code. On another hand, no down conversion is made, resulting in the fact

that the phase shift $\Psi_k^{(i)}$ can only take values in $\{0, \pi\}$. The channel amplitude follows a Rice distribution. Finally we consider that $c_k$ is Gaussian distributed. A large set of parameters give similar results as those we present in Fig. 3.1, so we do not give more details but only focus on the resulting plots. We represent on this figure two received interference samples on two replicas of a same information. The tail probability represents the probability that $x_1$ is larger than a given value $x$ knowing that $x_2$ is larger than $x$. It gives an idea if the existence of two large samples is possible or not. It would rapidly go to 0 in case of independent samples.

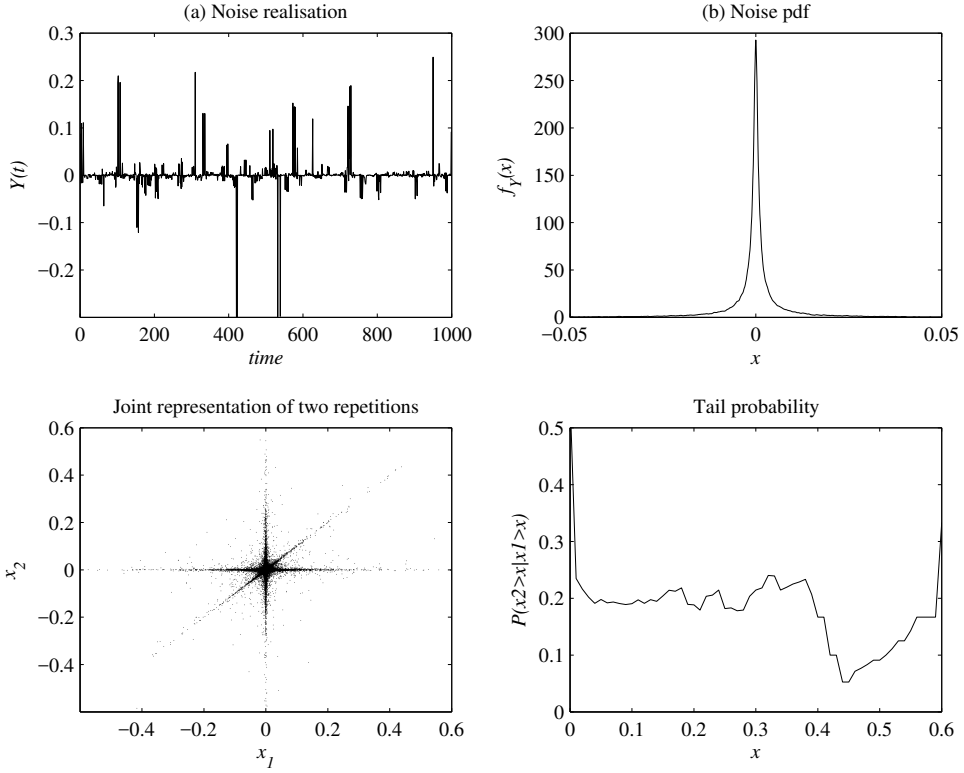


Figure 3.1: Case 1: example of interference samples on a TH-PPM-UWB system.

We notice especially on the joint representation that the probability of joint large events is significant. This shape is really different from what would result for an independent sample assumption.

**Case 2** SIMO

We consider a SIMO case with two receive antennas. In Fig. 3.2 the channels from interferers are drawn independently while in Fig. 3.3 they are correlated: phases are independent and uniformly distributed but only on $[-\pi/20, \pi/20]$ and the amplitude are

related by $A_1 = aA_2$ where $a$ is a Gaussian random variable with mean 1 and variance 0.01. This simple model allows to account for a strong correlation in the signals arriving at both antenna. The impact is clearly seen on the two dimensional representations

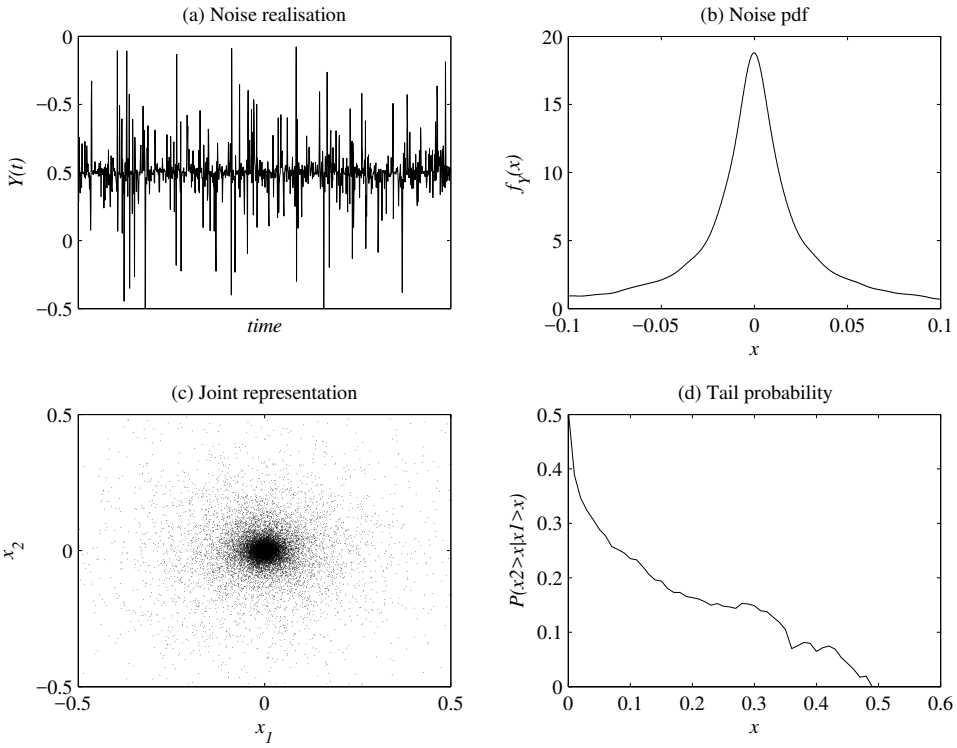


Figure 3.2: Case 2: example of interference samples on a SIMO system (independent).

in plots $c$ and the tail dependence in plots $d$. All the random factors let us think that at two different (but even close) points in space, the signals should be independent. However it is not fully acceptable, especially if you have some strong, line of sights, interferers. Then a dependency should be included, especially the probability of having simultaneous strong events appears to be an important parameter to model.

## 3.2 Sub-Gaussian Model

Modelling dependency in stable process is a difficult challenge because the usual correlation functions can not be used. We propose in a first step to consider a sub-Gaussian process, which is a special isotropic case of stable vectors that can be written as a Gaussian random vector with a random variance following a stable law.

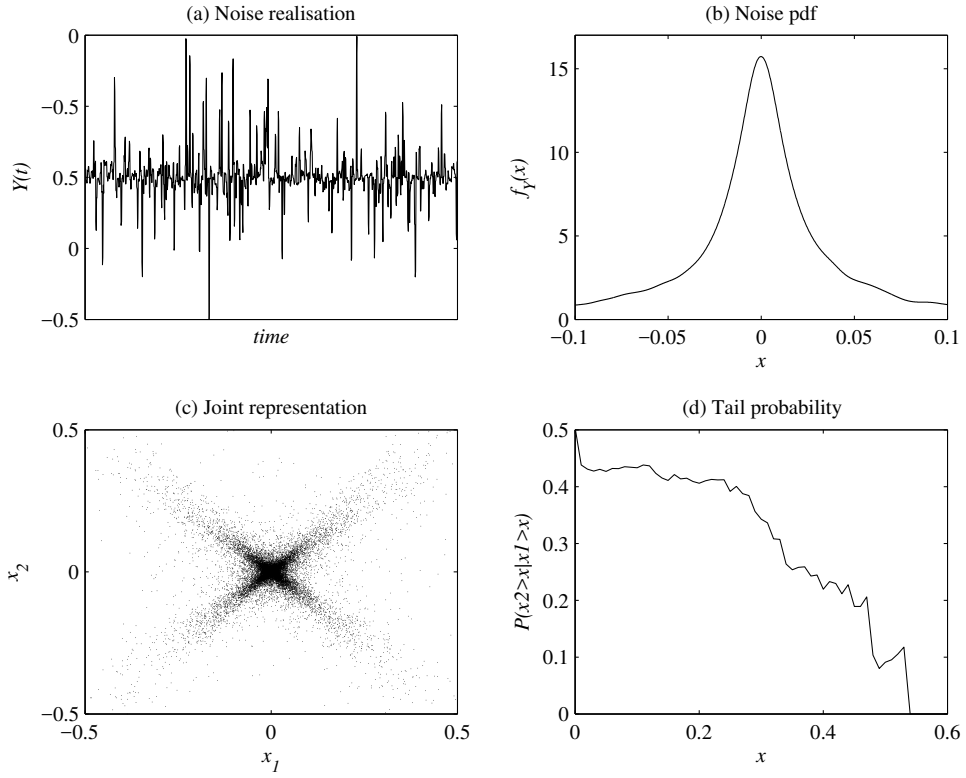


Figure 3.3: Case 2: example of interference samples on a SIMO system (dependent).

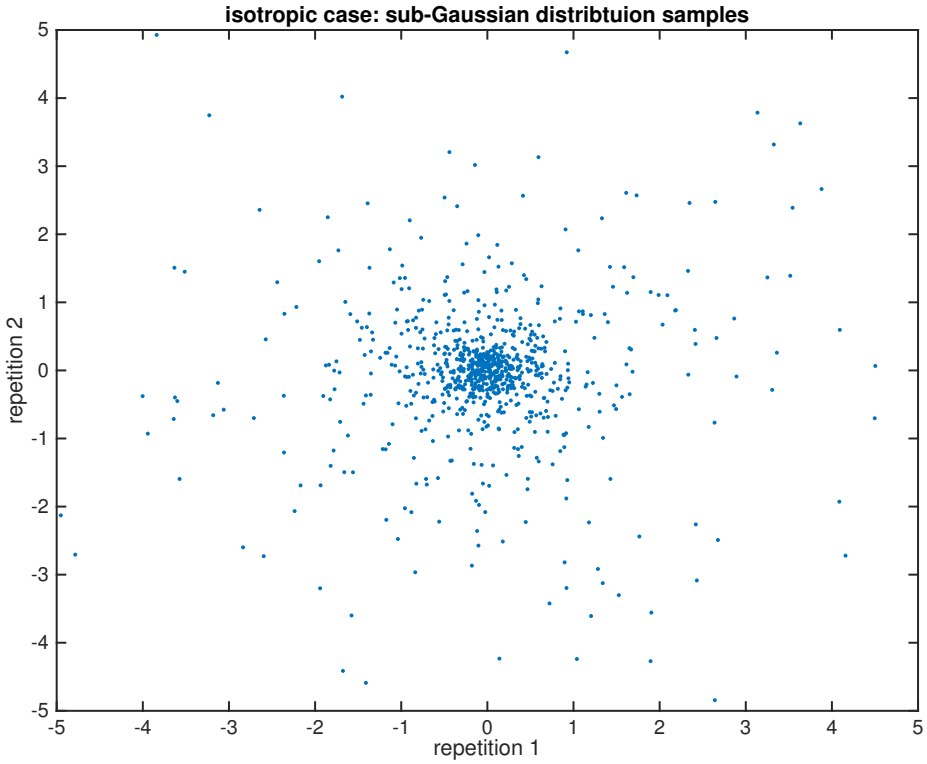


Figure 3.4: Isotropic Case: Sub-Gaussian samples

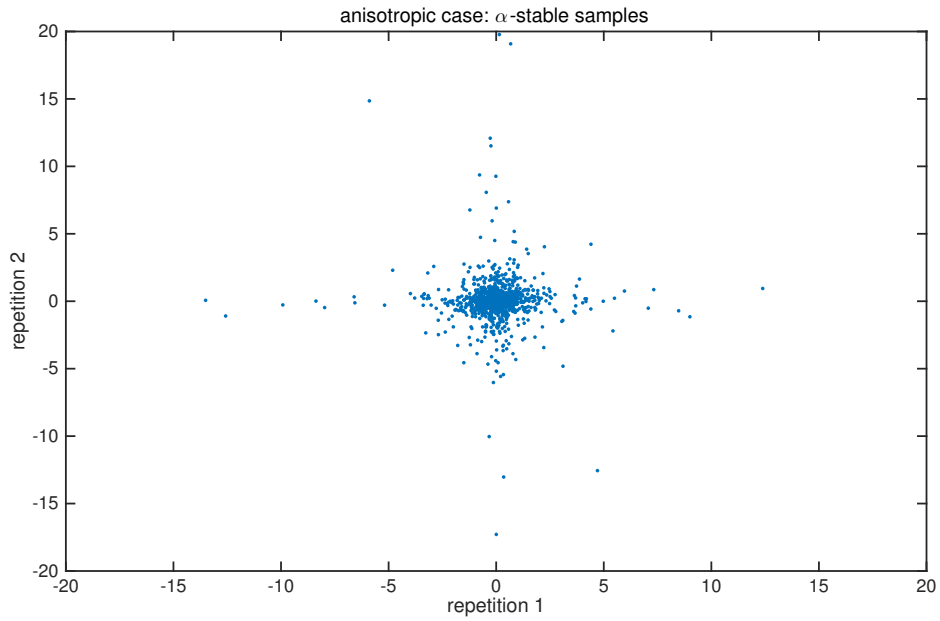


Figure 3.5: Anisotropic Case: $\alpha$-stable samples

Figure 3.4 and 3.5 show and compare of the isotropic case using Sub-Gaussian model and anisotropic case samples using $\alpha$-stable model.

In this case we can consider that during the transmission of a packet, the interference conditions do not change and the given temporal vector is of the sub-Gaussian form. To generate it, we generate a random Gaussian vector $\mathbf{G} = (G_1, G_2, ..., G_N) \sim \mathbf{N}(0, 2\delta^2)$, and a random variable $\mathbf{A}$ dependant of $\mathbf{G}$ which follows the distribution $\mathbf{S}\alpha\mathbf{S}(\alpha/2, 1, (cos\frac{\pi\alpha}{4})^{2/\alpha}, 0)$. Then we get the interference by multiplying $\mathbf{G}$ and $\mathbf{A}$ as follows:

$$\mathbf{X} = (\mathbf{A}^{1/2}\mathbf{G}_1, \mathbf{A}^{1/2}\mathbf{G}_2, ..., \mathbf{A}^{1/2}\mathbf{G}_N) \tag{3.1}$$

$X$ belongs to the sub-Gaussian family.

This approach is very similar to the one used by Win et al. [89] to calculate the capacity in an $\alpha$-stable interference. Considering a given block, they justify the use of the capacity formula in a Gaussian noise by the fact that the interfering environment does not change on this block so that the global noise is Gaussian with an added fixed interference. Then they integrate over the stable distribution of the interference. We have a similar model in our work: although interference is not constant it has a constant mean power given by the realisation of the random variable $A$. That brings the temporal correlation between the samples but we still keep the independence between the replicas by drawing a different $A$ for each of the $K$ received replicas of the single transmitted

symbol.

## 3.3 Copula

Copula is used to describe the dependence of random variables in statistical signal processing. It is a multivariate probability distribution for which the marginal probability distribution of each variable is uniform.

According to different dependence expressions, copulas have different categories. There are many parametric copula families available. Typically, a specific family of copula has several parameters which are used to express the strength and the form of dependence. Copula is very popular in high-dimensional statistical applications, because it allows to model and estimate the distribution of random vectors easily by estimating marginals and copula separately. Copulas are widely used in financial and economical areas to estimate the probability distribution of losses on pools of loans or bonds. Also, the use of copula functions to model asset returns has increased dramatically in recent years, because it has proven to be a valuable addition to the econometrician's toolbox. Multivariate distributions that were extremely difficult and time consuming to fit can now be estimated rapidly. Our objective in this chapter is to apply this concept of copulas in the telecommunication area in order to model the dependencies encountered in interference in wireless sensor networks.

As we will see, the key point of copulas that makes them very attractive is the Sklar's Theorem that says that any multivariate joint distribution can be written in terms of univariate marginal distribution functions and a copula. This allows to separate the dependence structure and the marginal distributions, generally impulsive in our case.

### 3.3.1 Definition

Consider that $(X_1, X_2, ..., X_d)$ is a random vector. Supposing its margins are continuous, then we write the marginal CDF as $F_i(x) = \mathbb{P}[X_i \leq x]$. By doing the probability integral transform to each component, we get a random vector

$$(U_1, U_2, ..., U_d) = (F_1(X_1), F_2(X_2), ..., F_d(X_d)) \tag{3.2}$$

which has uniformly distributed marginals.

So we define:

$$C(u_1, u_2, ..., u_d) = \mathbb{P}[U_1 \leq u_1, U_2 \leq u_2, ..., U_d \leq u_d] \tag{3.3}$$

as the copula of $(X_1, X_2, ..., X_d)$, which is the joint cumulative distribution function of

$(U_1, U_2, ..., U_d)$.

We can see that the copula $C$ has all the informations on the dependence structure of $(X_1, X_2, ..., X_d)$ whereas $F_i$ the marginal cumulative distribution function has all the informations on the marginal distributions. The most important part of it is the fact that the reverse of the step can be used to generate the pseudo-random samples from a multivariate probability distributions.

If we have a sample $(U_1, U_2, ..., U_d)$ generated from a copula distribution, we can generate a sample specified as:

$$(X_1, X_2, ..., X_d) = (F_1^{-1}(U_1), F_2^{-1}(U_2), ..., F_d^{-1}(U_d)) \tag{3.4}$$

where $F_i^{-1}$ is unproblematic as the $F_i$ is assumed to be continuous.

The copula function can also be rewritten to correspond to $F_i^{-1}$ as:

$$C(u_1, u_2, ..., u_d) = \mathbb{P}[X_1 \leq F_1^{-1}(u_1), X_2 \leq F_2^{-1}(u_2), ..., X_d \leq F_d^{-1}(u_d)] \tag{3.5}$$

### 3.3.2 Sklar's Theorem

Sklar's theorem, [82] named after Abe Sklar, provides the theoretical foundation for the application of copulas. It proves that any multivariate distribution with continuous margins has a unique copula representation.

**Theorem 3 (Sklar's Theorem).** *Consider a d-dimensional multivariate cumulative distribution function $H(x_1, ..., x_d) = \mathbb{P}[X_1 \leq x_1, ..., X_d \leq x_d]$ of a random vector $(X_1, X_2, ..., X_d)$ with the marginals $F_i(x) = \mathbb{P}[X_i \leq x]$. there exists a copula $C$, Such that:*

$$H(x_1, ..., x_d) = C(F_1(x_1), ..., F_d(x_d)) \tag{3.6}$$

*If the multivariate distributions has a density $f$ and the marginal density distribution is $f_i(x)$, we have:*

$$f(x_1, ..., x_d) = c(F_1(x_1), ..., F_d(x_d)) \cdot f_1(x_1) \cdot ... \cdot f_d(x_d) \tag{3.7}$$

*where $c$ is the density of the copula $C$.*

*The theorem also states that, given the multivariate cumulative distribution function $H$, if the marginals $F_i$ are continuous, then the copula $C$ is unique; otherwise, $C$ is uniquely determined on $Ran(F_1) \times ... \times Ran(F_d)$, the Cartesian product of the ranges of the marginal cumulative distributions.*

*Conversely, if the copula $C$ is given, and $F_i$ are distribution functions, then the function $H$ defined by* (3.6) *is a joint distribution function with margins $F_i$.*

### 3.3.3 Concordance measurement

In our work, we no longer assume i.i.d. impulsive interference noise samples. Typically in wireless communications, the second order moments are assumed finite, so that all dependence structures are adequately captured by the familiar notion of a correlation coefficient, a type of concordance measure, used to represent the dependence structure of the noise in a linear sense. For instance, the Pearson correlation coefficient $\rho_{X,Y}$ between random variables $X$ and $Y$ with expectation $\mu_X$ and $\mu_Y$ and standard deviation $\sigma_X$ and $\sigma_Y$ is:

$$\rho_{X,Y} = \frac{\operatorname{cov}(X,Y)}{\sigma_X \sigma_Y} = \frac{\mathbb{E}[(X-\mu_X)(Y-\mu_Y)]}{\sigma_X \sigma_Y} \tag{3.8}$$

where $\mathbb{E}[\cdot]$ means expectation, and $\operatorname{cov}(\cdot)$ means covariance.

This approach presents two drawbacks

1. it is not adapted to impulsive interference and especially to the $\alpha$-stable distributions, for which it is not defined.

2. it will not allow to model some extremal tail dependence features, representing the probability to have several strong interference samples in the same vector.

Consequently, we are interested in other models for dependence that offers more flexible concordance measures that may easily arise in impulsive multivariate interference settings.

Informally, a pair of random variables are concordant if 'large' values of one tend to be associated with 'large' values of the other and 'small' values of one with 'small' values of the other. Analogous definitions of discordance are available in reverse directions.

There are numerous ways of mathematically trying to quantify this statement, and, consequently, many measures of concordance are available. In [79] a set of axioms for general concordance measures is proposed (normalization,monotonicity, duality...). A popular concordance measures of dependence that is widely used in practice is:

**Tail dependence**: it quantifies the dependence in extremes of a multivariate distribution [21]. The notion of bivariate tail dependence coefficient is defined as the conditional probability that a random variable exceeds a certain threshold given that the other random variable has exceeded this threshold. Consider two random variables $X_1$ and $X_2$ with distributions $F_i, i = 1, 2$. The coefficient of upper tail dependence is:

$$\lambda_u := \lim_{u \uparrow 1} \mathbb{P}\left[X_2 > F_2^{-1}(u) \,|\, X_1 > F_1^{-1}(u)\right] \tag{3.9}$$

and similarly we define the coefficient of lower tail dependence by:

$$\lambda_l := \lim_{u \downarrow 0} \mathbb{P}\left[X_2 \leq F_2^{-1}(u) \,|X_1 \leq F_1^{-1}(u)\right] \tag{3.10}$$

NOTE: Similar to rank correlations, the tail dependence coefficient is a simple scalar measure of dependence. We will not detail it here but it depends on the copula of two random variables but not on their marginal distributions.

Tail dependence can be extended to arbitrary $d$-variate cases for $d > 2$, see for instance [26, 58].

## 3.4 Skew-$t$ copula

As we have seen, if we consider a random vector of interference given by $(X_1, ..., X_d)$, with each $X_i$ admitting a continuous marginal CDFs $F_i(x) = \mathbb{P}(X_i \leq x)$, then one may write:

$$(U_1, ..., U_d) = (F_1(X_1), ..., F_d(X_d)) \tag{3.11}$$

where the random vector $(U_1, ..., U_d)$ has marginals distributed on $[0, 1]^d$. We may then consider the model for the copula

$$C(u_1, ..., u_d) = \mathbb{P}[U_1 \leq u_1, ..., U_d \leq u_d] \tag{3.12}$$

to produce the joint cumulative distribution function of $(U_1, ..., U_d)$. The copula $C$ has all the informations on the dependence structure of $(X_1, ..., X_d)$ whereas the functions $F_i$ give the informations on the marginal distributions. The most important part of it is the fact that the reverse of the step can be used to generate the pseudo-random samples from a multivariate probability distributions.

In our work, we chose skewed student's $t$ distribution, which is denoted by $X \in t_n(\nu, \mu, \Sigma, \gamma)$. The skew-$t$ copula is the implicitly defined copula that produces the multivariate dependence in the generalized multivariate Hyperbolic family of distributions when the marginals are also in this family.

There are a lot of variants of the skewed-t distribution such as [48, 16, 6, 72]. It is a very flexible family which exhibits several interesting properties [27, 2]:

- **Upper and lower tail dependence** ($\lambda_{ij,u} \neq 0$ for all $i$ and $j$ and the same for the lower tail dependence coefficient): the copula allows for asymptotic dependence (unlike the Gaussian copula for instance)
- **Asymmetric dependence**: upper and lower tail dependence can differ.

- **Heterogeneous dependence**: dependence between different pairs can be different, which is difficult to obtain with other copulas families like the Archimedean.
- **Scalability in high dimension** so that it can be applied to some high dimension problems.

In this work, we follow the skewed-t distribution of DeMarta and McNeil [27] that derives from the Generalised Hyperbolic distribution.

**Definition 1** (**Normal Mean-Variance Mixture**). *The random variable $X$ is said to have a multivariate normal mean-variance mixture distribution if*

$$X \overset{d}{=} \mu + W\gamma + \sqrt{W}AZ \tag{3.13}$$

*where $Z \sim \mathcal{N}(0, I_k)$. $W \geq 0$ is a positive, scalar-valued r.v. which is independent of $Z$. $A \in \mathbb{R}^{d\times k}$ is a matrix. $\mu$ and $\gamma$ are parameter vector in $\mathbb{R}^d$.*

We can see that

$$X|W \quad \sim \quad \mathcal{N}_d(\mu + W\gamma, W\Sigma) \tag{3.14}$$

where $\Sigma = AA'$. If the mixture variable $W$ is generalized inverse Gaussian distributed, then $X$ is said to have a generalized hyperbolic distribution.

**Definition 2** (**Generalised Inverse Gaussian Distribution (GIG)**). *The random variable X is said to have a generalized inverse gaussian (GIG) distribution if its probability density function is*

$$h(x;\lambda,\chi,\psi) = \frac{\chi^{-\lambda}(\sqrt{\chi\psi})^{\lambda}}{2K_{\lambda}(\sqrt{\chi\psi})} x^{\lambda-1} exp(-\frac{1}{2}(\chi x^{-1} + \psi x)), \quad x > 0 \tag{3.15}$$

*where $K_\lambda$ denotes a modified Bessel function of the third kind with index $\lambda$, and the parameters satisfy*

$$\begin{aligned} &\chi > 0, \quad \psi \geq 0 \quad if \lambda < 0 \\ &\chi > 0, \quad \psi > 0 \quad if \lambda = 0 \\ &\chi \geq 0, \quad \psi > 0 \quad if \lambda > 0 \end{aligned} \tag{3.16}$$

*In short, we write $X \sim \quad N^-(\lambda,\chi,\psi)$ if $X$ is GIG distributed.*

**Definition 3** (**Generalised Multivariate Hyperbolic Distribution**). *The Generalised Multivariate Hyperbolic distribution where $\mu$ is a vector, $\Sigma$ is a matrix, $\gamma$ is a vector, and $\chi$ and*

*$\psi$ are constant is given by*

$$f(x) = c\frac{K_{\lambda-d/2}\sqrt{(\chi+(x-\mu)'\Sigma^{-1}(x-\mu))(\chi+\gamma'\Sigma^{-1}\gamma)}e^{(x-\mu)'\Sigma^{-1}\gamma}}{(\sqrt{(\chi+(x-\mu)'\Sigma^{-1}(x-\mu))(\chi+\gamma'\Sigma^{-1}\gamma)})^{d/2-\lambda}} \tag{3.17}$$

*where the normalising constant is*

$$c = \frac{(\sqrt{\chi\psi})^{-\lambda}(\psi+\gamma'\Sigma^{-1}\gamma)^{d/2-\lambda}\psi^{\lambda}}{(2\pi)^{d/2}|\Sigma|^{1/2}K_{\lambda}(\sqrt{\chi\psi})} \tag{3.18}$$

*$K_\lambda$ denotes a modified Bessel function of the third kind with index $\lambda$.*

**Definition 4** (**Modified Bessel Function of the Third Kind with Index** $\lambda$)**.** *The integral presentation of the modified bessel function of the third kind with index $\lambda$ can be found in [11].*

$$K_{\lambda}(x) = \frac{1}{2}\int_0^{\infty} y^{\lambda-1}e^{-\frac{x}{2}(y+y^{-1})}dy, \quad x>0 \tag{3.19}$$

The Generalised Hyperbolic family includes several important distributions. If $\lambda = (d+1)/2$, we have the hyperbolic distribution; if $\lambda = -1/2$, we will get the normal-inverse Gaussian distribution; if $\lambda = -\nu/2$, we will get the Generalised Hyperbolic skewed-t distribution following McNeil, Frey and Embrechts [62].

**Definition 5** (**Multivariate Skewed-t Distribution**)**.** *The Multivariate Skewed-t distribution is given by*

$$f(x) = \frac{cK_{(\nu+d)/2}\sqrt{(\nu+Q(x))\gamma'\Sigma^{-1}\gamma}e^{(x-\mu)'\Sigma^{-1}\gamma)}}{(\sqrt{(\nu+Q(x))\gamma'\Sigma^{-1}\gamma})^{-(\nu+d)/2}(1+Q(x)/\nu)^{(\nu+d)/2}} \tag{3.20}$$

*where $Q(x) = (x-\mu)'\Sigma^{-1}(x-\mu)$. The normalising constant is*

$$c = \frac{2^{1-(\nu+d)/2}}{\Gamma(\nu/2)(\pi\nu)^{d/2}|\Sigma|^{1/2}} \tag{3.21}$$

The mean and variance of skewed-t distributed random vector $\mathbf{X}$ are

$$\mathbb{E}(\mathbf{X}) = \mu + \gamma\frac{\nu}{\nu-2} \tag{3.22}$$

$$\text{cov}(\mathbf{X}) = \frac{\nu}{\nu-2}\Sigma + \gamma\gamma'\frac{2\nu^2}{(\nu-2)^2(\nu-4)} \tag{3.23}$$

The covariance matrix is defined only when $\nu > 4$.

One can obtain the following location-scale mixture representation for a skew-$t$ distributed $d$-dimensional random vector.

**Definition 6 (Normal Mean-Variance Mixture Representation of Skewed-t Distribution).** *The d dimensional skewed-t distributed random vector $\mathbb{X}$ denoted by*

$$\mathbb{X} \sim SkewedT_d(\nu, \mu, \Sigma, \gamma) \tag{3.24}$$

*is a multivariate normal mean-variance mixture variable with distribution given by*

$$\mathbf{X} \overset{d}{=} \mu + \gamma W + \sqrt{W}\mathbf{Z} \tag{3.25}$$

*where $W$ is an inverse Gamma random variable ($W \sim IG(\nu/2, \nu/2)$) an independent from random vector $\mathbf{Z}$ which has normal distribution $\mathbf{Z} \sim \mathcal{N}(\mathbf{0}, \Sigma)$.*

### 3.4.1 Skewed-t Copula Simulation

Having given the main definitions for a skew-t copula, we can now develop the framework for the generation of dependent random variables. Let us consider the random vector $(X_1, ..., X_d)$ with continuous marginal cumulative distributions $F_i(x) = \mathbb{P}(X_i \leq x)$ and a dependence structure defined by the skewed-$t$ copula $C$ is. Its generation can be done through the following steps:

- Draw $N$ independent $n$-dimensional vectors from the multivariate normal distribution $\mathcal{N}(0, \Sigma)$.
- Draw $N$ independent random numbers from the inverse gamma distribution with parameters $IG(\nu/2, \nu/2)$.
- Calculate *simulations* by $S = \mu + \gamma W + Z\sqrt{W}$
- Transform *simulations* $S$ to *uniform simulations* $U$ using the sample cumulative distribution function of the marginals: $\hat{G}_k(x) = \frac{1}{N} \sum_{j=1}^{N} I\{S_{jk} \leq x\}$ where $I(A) = 1$ if $x \in A$ and $0$ if $x \notin A$ and $U_{jk} = \hat{G}_k(S_{jk})$.
- Transform $U = \{U_{jk}\}$ by the inverse of the one-dimensional marginal distribution functions $R_{jk} = F_k^{-1}(U_{jk})$

### 3.4.2 Estimation of Skew-t Distribution

To estimate the parameters of Skew-t distribution, we use an EM (expectation-maximization) algorithm. The EM algorithm is a two-step iterative process in which (E-step) an expected log likelihood function is calculated using current parameter values, and then (M-step) this function is maximized to produce updated parameter values. The EM algorithm can be easily applied to the mean-variance representation of generalized hyperbolic distributions that is a great advantage. We first follow the EM algorithm framework of [62] for generalized hyperbolic distributions. And then we give the special case of skewed-t distribution as an example of generalized hyperbolic distribution.

Given $X_1, \ldots, X_n$, where $X_i \in \mathbb{R}^d$. We want to fit these data to a multivariate generalized hyperbolic distribution. The parameters are denoted by $\zeta = (\lambda, \chi, \psi, \Sigma, \mu, \gamma)$. So to implement the EM algorithm, we need first to write its log-likelihood function:

$$\log L(\zeta; X_1, \cdots, X_n) = \sum_{i=1}^{n} \log f_{X_i}(X_i; \zeta) \tag{3.26}$$

The goal is to maximize this log-likelihood function to find the right parameters. But it is almost impossible to maximize this function directly if the dimension is more than 3. So we introduce the latent mixing variables $W_1, \ldots, W_n$ and we suppose that they are observable at the beginning.

So our log-likelihhod function becomes:

$$\log \widetilde{L}(\zeta; X_1, \cdots, X_n, W_1, \ldots, W_n) = \sum_{i=1}^{n} \log f_{X_i, W_i}(X_i, W_i; \zeta) \tag{3.27}$$

The log-likelihood function of the mean-variance mixture representation of generalized hyperbolic distribution can be written as:

$$\begin{aligned} \log \widetilde{L}(\zeta; X_1, \cdots, X_n, W_1, \ldots, W_n) &= \sum_{i=1}^{n} \log f_{X_i|W_i}(X_i|W_i; \mu, \Sigma, \gamma) + \\ &\quad \sum_{i=1}^{n} \log h_{W_i}(W_i; \lambda, \chi, \psi) \\ &= L_1(\mu, \Sigma, \gamma; X_1, \cdots, X_n|W_1, \ldots, W_n) + \\ &\quad L_2(\lambda, \chi, \psi; W_1, \ldots, W_n) \end{aligned} \tag{3.28}$$

where $X|W \sim \mathcal{N}(\mu + w\gamma, w\Sigma)$. $f_{X|W}(x|w)$ is the density of conditional normal distribution. $h(w)$ is the density function generalized inverse Gaussian distributed mixing random variable.

The equation above shows that the estimation of $\Sigma$,$\mu$, $\gamma$ and $\lambda$, $\chi$, $\psi$ can be separated.

We can write the density of conditional normal distribution as

$$f_{X|W}(x|w) = \frac{1}{(2\pi)^{\frac{d}{2}}|\Sigma|^{\frac{1}{2}}w^{\frac{d}{2}}} e^{(x-\mu)'\Sigma^{-1}\gamma} e^{\frac{-\rho}{2w}} e^{-\frac{w}{2}\gamma'\Sigma^{-1}\gamma} \tag{3.29}$$

where

$$\rho = (x-\mu)'\Sigma^{-1}(x-\mu) \tag{3.30}$$

So the log-likelihood function $L_1$ is as:

$$\begin{aligned} L_1(\mu,\Sigma,\gamma; X_1,\cdots,X_n|W_1,\cdots,W_n) &= -\tfrac{n}{2}\log|\Sigma| - \tfrac{d}{2}\sum_{i=1}^{n}\log W_i + \sum_{i=1}^{n}(X_i-\mu)'\Sigma^{-1}\gamma \\ &\quad -\tfrac{1}{2}\sum_{i=1}^{n}\tfrac{1}{W_i}\rho_i - \tfrac{1}{2}\gamma'\Sigma^{-1}\gamma\sum_{i=1}^{n}W_i \end{aligned} \tag{3.31}$$

The log-likelihood function $L_2$ can be got from the GIG distribution:

$$\begin{aligned} L_2(\lambda,\chi,\psi; W_1,\cdots,W_n) &= (\lambda-1)\sum_{i=1}^{n}\log W_i - \tfrac{\chi}{2}\sum_{i=1}^{n}W_i^{-1} - \tfrac{\psi}{2}\sum_{i=1}^{n}W_i - \tfrac{n\lambda}{2}\log\chi \\ &\quad +\tfrac{n\lambda}{2}\log\psi - n\log(2K_\lambda(\sqrt{\chi\psi})) \end{aligned} \tag{3.32}$$

So for now, we separate the estimation of $\Sigma$,$\mu$, $\gamma$ and $\lambda$, $\chi$, $\psi$. The estimation of $\Sigma$,$\mu$, $\gamma$ can be done by maximizing $L_1$. Supposing that $W_1,\cdots,W_n$ are observable, we take the partial derivative of $L_i$ with respect to $\Sigma$, $\mu$ and $\gamma$:

$$\frac{\partial L_1}{\partial \mu} = 0 \tag{3.33}$$

$$\frac{\partial L_1}{\partial \gamma} = 0 \tag{3.34}$$

$$\frac{\partial L_1}{\partial \Sigma} = 0 \tag{3.35}$$

We can get from the equations (3.33),(3.34) and (3.35)

$$\gamma = \frac{n^{-1}\sum_{i=1}^{n} W_i^{-1}(\bar{X} - X_i)}{n^{-2}(\sum_{i=1}^{n} W_i)(\sum_{i=1}^{n} W_i^{-1}) - 1} \tag{3.36}$$

$$\mu = \frac{n^{-1}\sum_{i=1}^{n} W_i^{-1} X_i - \gamma}{n^{-1}\sum_{i=1}^{n} W_i^{-1}} \tag{3.37}$$

$$\Sigma = \frac{1}{n}\sum_{i=1}^{n} W_i^{-1}(X_i - \mu)(X_i - \mu)' - \frac{1}{n}\sum_{i=1}^{n} W_i \gamma\gamma' \tag{3.38}$$

Estimation of $\lambda$, $\chi$, $\psi$ is done by maximizing $L_2$. In general, we assume $\lambda$ to be a constant. To maximize $L_2$, we take the partial derivative with respect to $\chi$ and $\psi$ and solve the following equations:

$$\frac{\partial L_2}{\partial \chi} = 0 \tag{3.39}$$

$$\frac{\partial L_2}{\partial \psi} = 0 \tag{3.40}$$

Solving the above equations leads us to solve $\theta = \sqrt{\chi\psi}$ from the following equation first,

$$n^{-2}\sum_{i=1}^{n} W_i \sum_{j=1}^{n} W_j^{-1} K_\lambda^2(\theta)\theta + 2\lambda K_{\lambda+1}(\theta)K_\lambda(\theta) - \theta K_\lambda^2(\theta) = 0 \tag{3.41}$$

Once $\theta$ is solved, we can get parameters $\chi$ and $\psi$.

$$\chi = \frac{n^{-1}\theta\sum_{i=1}^{n} W_i K_\lambda(\theta)}{K_{\lambda+1}(\theta)} \tag{3.42}$$

$$\psi = \frac{\theta^2}{\chi} \tag{3.43}$$

Especially for skew-t distribution with degree of freedom $\nu$, we set $\psi = 0$; $\lambda = -\nu/2$;

$\chi = \nu$. So we can solve the only parameter $\nu$ from the following equation:

$$-\phi(\frac{\nu}{2}) + \log\frac{\nu}{2} + 1 - n^{-1}\sum_{i=1}^{n} W_i^{-1} - n^{-1}\sum_{i=1}^{n}\log(W_i) = 0 \tag{3.44}$$

where $\phi(\cdot)$ is the di-gamma function. However, the mixing variable $W_1, \cdots, W_n$ are not observable. So we take a EM algorithm.

In E-step, the conditional expectation of the log-likelihood function with current parameter is estimated and sample data is calculated. At the $k$-th step, we calculate the conditional expectation as followed:

$$Q(\zeta; \zeta^{[k]}) = E(\log\widetilde{L}(\zeta; X_1, \cdots, X_n, W_1, \cdots, W_n)|X_1, \cdots, X_n; \zeta^{[k]}) \tag{3.45}$$

in M-step, we maximize the above function to estimate new $\zeta^{[k]}$. It is equivalent to updating all the $W_i$, $W_i^{-1}$, and $\log(W_i)$ in the log-likelihood function by their conditional estimates $E(W_i|X_i; \zeta^{[k]})$, $E(W_i^{-1}|X_i; \zeta^{[k]})$, and $E(\log(W_i)|X_i; \zeta^{[k]})$. To calculate those conditional expectations, we write the conditional density function:

$$f_{W|X}(W|X; \zeta) = \frac{f(X|W; \zeta)h(W; \zeta)}{f(X; \zeta)} \tag{3.46}$$

By some algebra work, we have:

$$W_i|X_i \quad \sim \quad N^-(\lambda - \frac{d}{2}, \rho_i + \chi, \psi + \gamma'\Sigma^{-1}\gamma) \tag{3.47}$$

where $N^-(\lambda, \chi, \psi)$ stands for GIG distribution.

We denote:

$$\delta^{[\cdot]} = \mathbb{E}(W_i^{-1}|X_i; \zeta^{[\cdot]}), \quad \eta^{[\cdot]} = \mathbb{E}(W_i|X_i; \zeta^{[\cdot]}), \quad \xi^{[\cdot]} = \mathbb{E}(\log(W_i)|X_i; \zeta^{[\cdot]}) \tag{3.48}$$

and

$$\bar{\delta} = \frac{1}{n}\sum_{1}^{n}\delta_i, \quad \bar{\eta} = \frac{1}{n}\sum_{1}^{n}\eta_i, \quad \bar{\xi} = \frac{1}{n}\sum_{1}^{n}\xi_i \tag{3.49}$$

for the multivariate skewed-t distribution, we have:

$$W_i|X_i \quad \sim \quad N^-(-\frac{d+\nu}{2}, \rho_i + \nu, \gamma'\Sigma^{-1}\gamma) \tag{3.50}$$

and

$$\delta_i^{[k]} = (\frac{\rho_i^{[k]} + \nu^{[k]}}{\gamma^{[k]\prime}\Sigma^{[k]-1}\gamma^{[k]}})^{-\frac{1}{2}} \frac{K_{\frac{\nu+d+2}{2}}\sqrt{(\rho_i^{[k]} + \nu^{[k]})(\gamma^{[k]\prime}\Sigma^{[k]-1}\gamma^{[k]})}}{K_{\frac{\nu+d}{2}}\sqrt{(\rho_i^{[k]} + \nu^{[k]})(\gamma^{[k]\prime}\Sigma^{[k]-1}\gamma^{[k]})}} \tag{3.51}$$

$$\eta_i^{[k]} = (\frac{\rho_i^{[k]} + \nu^{[k]}}{\gamma^{[k]\prime}\Sigma^{[k]-1}\gamma^{[k]}})^{\frac{1}{2}} \frac{K_{\frac{\nu+d-2}{2}}\sqrt{(\rho_i^{[k]} + \nu^{[k]})(\gamma^{[k]\prime}\Sigma^{[k]-1}\gamma^{[k]})}}{K_{\frac{\nu+d}{2}}\sqrt{(\rho_i^{[k]} + \nu^{[k]})(\gamma^{[k]\prime}\Sigma^{[k]-1}\gamma^{[k]})}} \tag{3.52}$$

$$\begin{aligned} \xi_i^{[k]} &= \tfrac{1}{2}\log\tfrac{\rho_i^{[k]}+\nu^{[k]}}{\gamma^{[k]\prime}\Sigma^{[k]-1}\gamma^{[k]}} \\ &+ \frac{\frac{\partial K_{-\frac{\nu+d}{2}+\alpha}(\sqrt{(\rho_i^{[k]}+\nu^{[k]})(\gamma^{[k]\prime}\Sigma^{[k]-1}\gamma^{[k]})})}{\partial\alpha}|_{\alpha=0}}{K_{\frac{\nu+d}{2}}\sqrt{(\rho_i^{[k]}+\nu^{[k]})(\gamma^{[k]\prime}\Sigma^{[k]-1}\gamma^{[k]})}} \end{aligned} \tag{3.53}$$

In M-step, we replace the latent variables $W_i^{-1}$ by $\delta^{[k]}$, $W_i$ by $\eta^{[k]}$, $\log(W_i)$ by $\xi^{[k]}$ in the maximization.

We renew $\Sigma^{[1]}$, $\mu^{[1]}$ and $\gamma^{[1]}$ by:

$$\gamma^{[k+1]} = \frac{n^{-1}\Sigma_{i=1}^n\theta_i^{[k]}(\bar{x} - x_i)}{\bar{\theta}^{[k]}\bar{\eta}^{[k]} - 1} \tag{3.54}$$

$$\mu^{[k+1]} = \frac{n^{-1}\Sigma_{i=1}^n\theta_i^{[k]}x_i - \gamma^{[k+1]}}{\bar{\theta}^{[k]}} \tag{3.55}$$

$$\Sigma^{[k+1]} = \frac{1}{n}\Sigma_{i=1}^n\theta^{[k]}(x_i - \mu^{[k+1]})(x_i - \mu^{[k+1]})' - \bar{\eta}^{[k]}\gamma^{[k+1]}\gamma^{[k+1]\prime} \tag{3.56}$$

We renew $\nu^{[k+1]}$ by solving:

$$-\phi(\frac{\nu}{2}) + \log\frac{\nu}{2} + 1 - \bar{\xi}^{[k]} - \bar{\theta}^{[k]} = 0 \tag{3.57}$$

we redo these steps until the relative increment of log likelihood is small.

### 3.4.3 Dependence structure

We first observe the effect when we change the three main parameters of skewed student's $t$ distribution ($\Sigma$, $\nu$ and $\gamma$). Table 3.1 shows the different parameter settings and the Pearson correlation coefficients for the studied cases. For simplicity and readability of the figures, the comparison, the marginals we use are Gaussians and we consider

2-dimensional vectors.

Figures 3.6 to 3.9 show the difference of the dependence structure that we can obtain when modifying the parameters. The two axes represent the amplitude of 2 repeated sample. Fig. 3.6 represents the independent case. In Fig. 3.7 we illustrate the impact the parameter $\nu$, the degrees of freedom. It increases the probability of having simultaneously two large events (tail dependence).

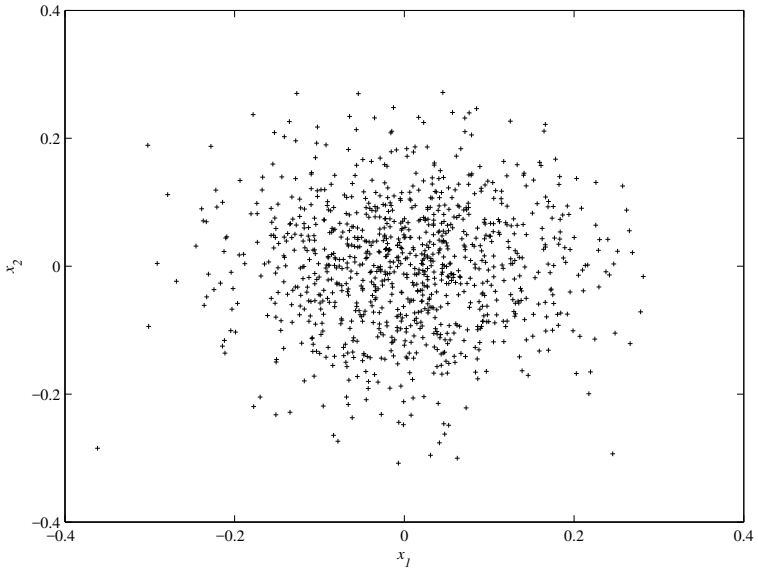


Figure 3.6: Case 1: independent samples. ($\nu = 5$, $\sigma = 0$, $\beta = 0$)

The parameter $\Sigma$ has the effect of correlation between the signals. $\Sigma = [\sigma_{ij}]_{1 \leq i,j \leq d}$ is the covariance matrix of the normal random vector $Z$.

$$\Sigma = \begin{pmatrix} \sigma_{11} & \sigma_{12} & \cdots & \sigma_{1n} \\ \sigma_{21} & \sigma_{22} & \cdots & \sigma_{2n} \\ \vdots & \vdots & \ddots & \vdots \\ \sigma_{n1} & \sigma_{n2} & \cdots & \sigma_{nn} \end{pmatrix} \tag{3.58}$$

We take all $\sigma_{ii} = 1$ and $\sigma_{ij}, i \neq j$ with the same value. When increasing $\sigma_{ij}$, the correlation between the two dimensions is larger, which is illustrated in Fig. 3.8 (linear dependence). The shape of the cloud becomes thinner indicating the stronger dependence.

Finally, parameter $\beta = (\beta_1, ..., \beta_n)$ is a $n$-dimensional vector accounting for the skewness. We choose the same value $\beta$ in all the dimensions. We can see from Fig. 3.9 that $\beta$

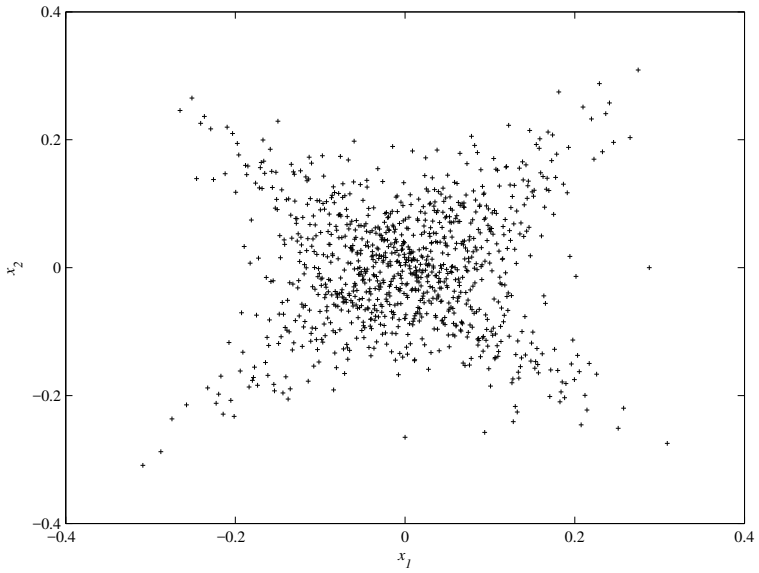


Figure 3.7: Case 2: tail dependence ($\nu = 1$, $\sigma = 0$ $\beta = 0$)

modifies the symmetry of the dependence structure. In the chosen example, dependence is stronger when large positive values occur.

Figure 3.10 shows the MRC receiver's performance in these 6 cases. We could see that the dependence has the negative effect impact. Different parameter change differently on the performance of dependence. The degrees of freedom $\nu$ increases the probability of having simultaneously two large events (tail dependence).The parameter $\Sigma$ has the effect of correlation between the signals. When increasing the value, the correlation between the two dimensions is larger. Finally, parameter $\beta = (\beta_1, ..., \beta_n)$ is a $n$-dimensional vector accounting for the skewness. It modifies the symmetry of the dependence structure.

| Case | $\nu$ | $\sigma$ | $\beta$ | $\rho$ (Gaussian marginals) |
|---|---|---|---|---|
| 1 | 1 | 0 | 0 | 0.05 |
| 2 | 5 | 0 | 0 | 0.005 |
| 3 | 3 | 0.5 | 0 | 0.38 |
| 4 | 3 | 0.9 | 0 | 0.76 |
| 5 | 3 | 0 | 2 | 0.55 |
| 6 | 3 | 0 | 5 | 0.65 |

Table 3.1: Different setting of parameter and their dependence

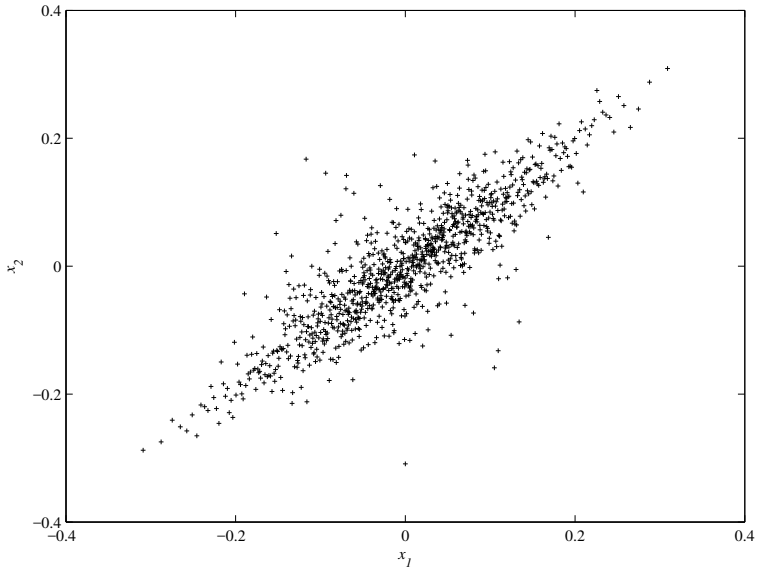


Figure 3.8: Case 3: linear dependence ($\nu = 3$ $\sigma = 0.9$ $\beta = 0$)

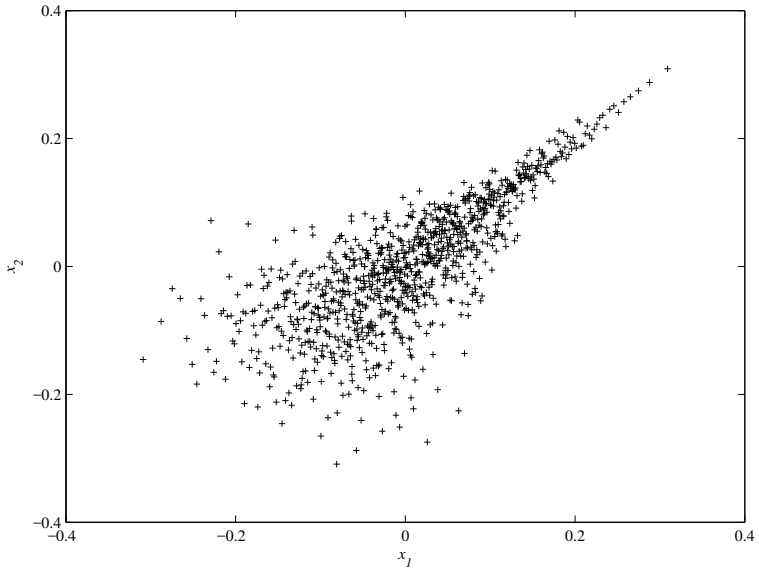


Figure 3.9: Case 4: asymetric dependence ($\nu = 3$ $\sigma = 0$ $\beta = 2$)

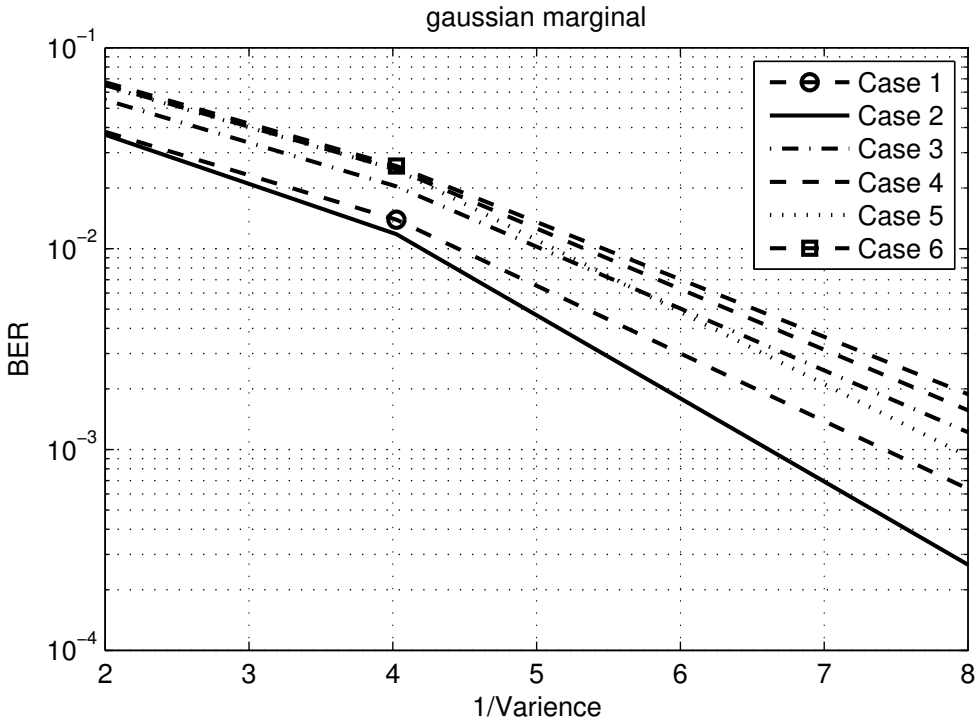


Figure 3.10: Effect of the parameters of copula

### 3.4.4 Estimation Simulation

To simulate the estimation process of skew-t copula, we take the algorithm as the following scheme. It is not as easy as the estimation of skew-t distribution, because in the copula case, we need to transform the uniform marginal value of the samples to the skew-t distribution samples without knowing the parameters. Because of the lack of an analytical likelihood function with which we could make EM algorithm directly form uniform value, we design the following steps to do the estimation:

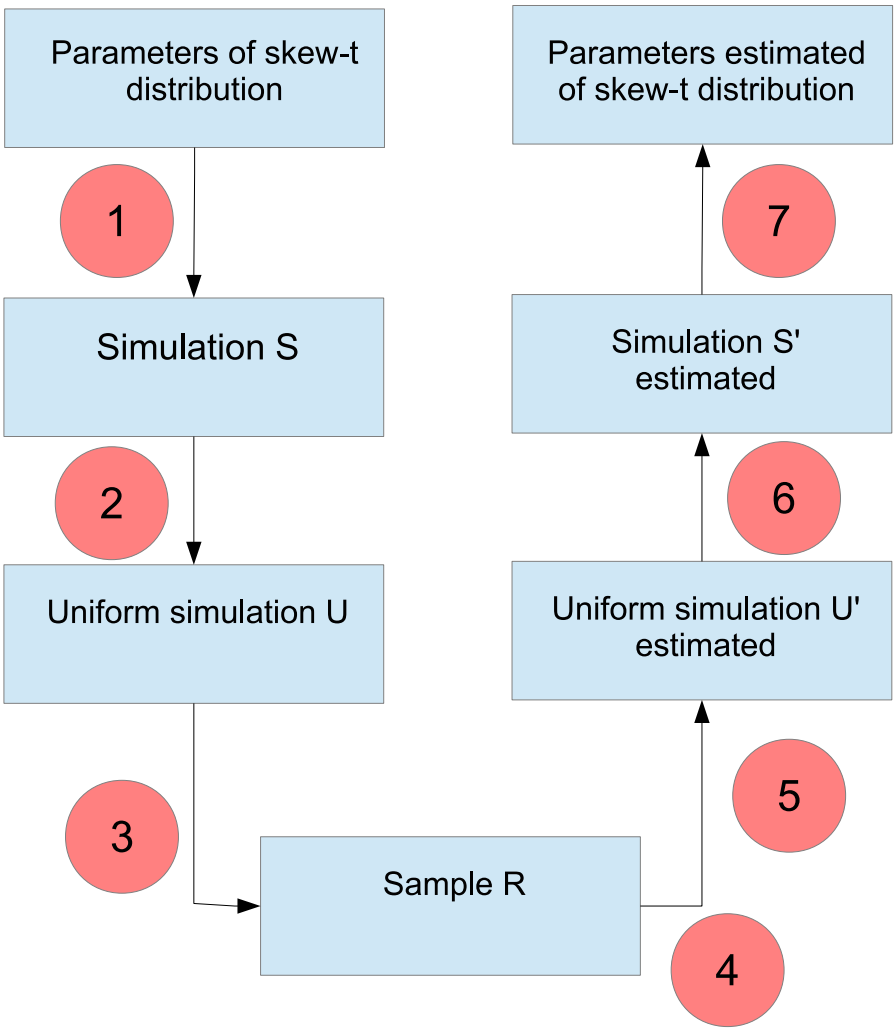


Figure 3.11: Estimation process of skew-t copula

- Step 1: We draw N independent n-dimensional vectors from the multivariate skewed-t distribution using the mean-variance representation with 4 parameters

($\Sigma$, $\gamma$, $\mu$ and $\nu$). The result we call it simulation S that is following skew-t distribution.

- Step 2: We estimate the sample CDF of the skew-t distributed sample. We transform the simulations S to uniform simulations U that belongs to $[0, 1]$.

- Step 3: We chose a fitted one-dimensional distribution functions, which is an inverse of CDF, to transform the uniform simulation U. Here we try two cases: Gaussian distribution and $\alpha$-stable distribution. The result we call it as samples R. We could also skip the steps above and use directly the samples from real signal, such as SIMO transmission system or Ultra Wide Band transmission system as samples R.

- Step 4: From the samples R, we estimate the parameters of the fitted one-dimensional distribution function. That depends on which marginals we want to choose to model the interference.

- Step 5: After having estimated the parameters in step 4, we generate the uniform marginal simulation U' by a CDF of fitted distribution function.

- Step 6: Because of the lack of an analytical likelihood function, we have to set an initial setting of the parameters. We use this initial setting to estimate the CDF of the skew-t distribution and generate an initial simulation S'.

- Step 7: From the simulation S', with the estimation program that we discussed in the subsection 3.4.2, we estimate the skew-t distribution's parameters. Here to simplify the estimation algorithm, we fixed the value of $\nu$ and estimate the other three parameters with different value of $\nu$. In the end we choose the setting of parameters which gives the best log-likelihood function value.

Table 3.2 shows some parameters estimation results of skew-t copula. In these examples, we use $\alpha$-stable distribution as the fitted distribution function where $\alpha = 1.8$, $\gamma = 0.1$, $\mu = \beta = 0$. As we previewed, the estimation of freedom parameter $\nu$ is difficult due to the fact that we fix it during the estimation and make different estimations when we change its value, choosing after hand the value that gives the highest likelihood. The other three parameters' estimation result seems more accurate but still need to be improved. In future work, we should find a analytical way to maximize the log-likelihood function directly from the marginal samples. That will lead to a more accurate estimation result.

| $\sigma$ | $\sigma'$ | $\gamma$ | $\gamma'$ | $\mu$ | $\mu'$ | $\nu$ | $\nu'$ |
|---|---|---|---|---|---|---|---|
| 0.8 | 0.8863 | 0.4 | 0.4336 | 0 | 0.1105 | 3 | 5 |
| 0.5 | 0.5478 | 0.4 | 0.4706 | 0 | 0.0251 | 3 | 5 |
| 0.5 | 0.5006 | 0.4 | 0.4017 | 0 | 0.1087 | 7 | 5 |
| 0.8 | 0.9292 | 0.7 | 0.5716 | 0 | -0.03 | 3 | 6 |
| 0.5 | 0.4308 | 0 | -0.3633 | 0 | -0.1366 | 7 | 4 |

Table 3.2: Estimation result of Skew-t copula

### 3.4.5 Receiver performance

We now illustrate the effect of the dependence structure on the receiver performance. These receivers are designed under the i.i.d assumption. So if the dependence structure has a negative effect on them, it underlines the importance to take it into account during the receiver design.

#### Receivers' performance with sub-Gaussian noise

We first observe the performance of the receivers under a sub-Gaussian noise. Similar as the case of $\alpha$-stable system interference plus Gaussian thermal noise case in the former chapter, We also test three environment which are lightly impulsive $NIR = 10dB$, moderately impulsive $NIR = 0dB$ and highly impulsive $NIR = -10dB$.

We first observe the sub-Gaussian noise with temporal dependence's effect on the receivers' performance. In this case, we maintain the independence between different repetitions. For instance this can represent a SIMO situation where the interferences on the different antennas are not correlated whereas the environment varies slowly so that consecutive interference samples are correlated. This case can be analysed as a slow-varying situation (non-ergodic case). Besides, due to the sub Gaussian assumption, the interference marginals will be Gaussian (the variance varying only at the next packet).

Figure 3.12 shows the receivers performance in sub-Gaussian noise under a slightly impulsive environment with temporal dependence.

NIG and $p$-norm receiver performs the best among all the receivers. Hole-puncher and Soft-limiter give a good performance at low $1/\gamma$ value, and get worse at high $1/\gamma$ value where the impulsive part of the noise is the limiting factor. MRC receiver degrades its performance at high $1/\gamma$ value with the same reason. Myriad is not very efficient in this case, but still it gives an acceptable performance. Cauchy works poorly because it is optimal for more impulsive case.

Figure 3.13 shows the receivers performance in sub-Gaussian noise under a moderately impulsive environment with temporal dependence.

Without surprise, the conventional and optimal MRC does not work well at all in the impulsive case. NIG in this case gives the best performance. $p$-norm and Myriad

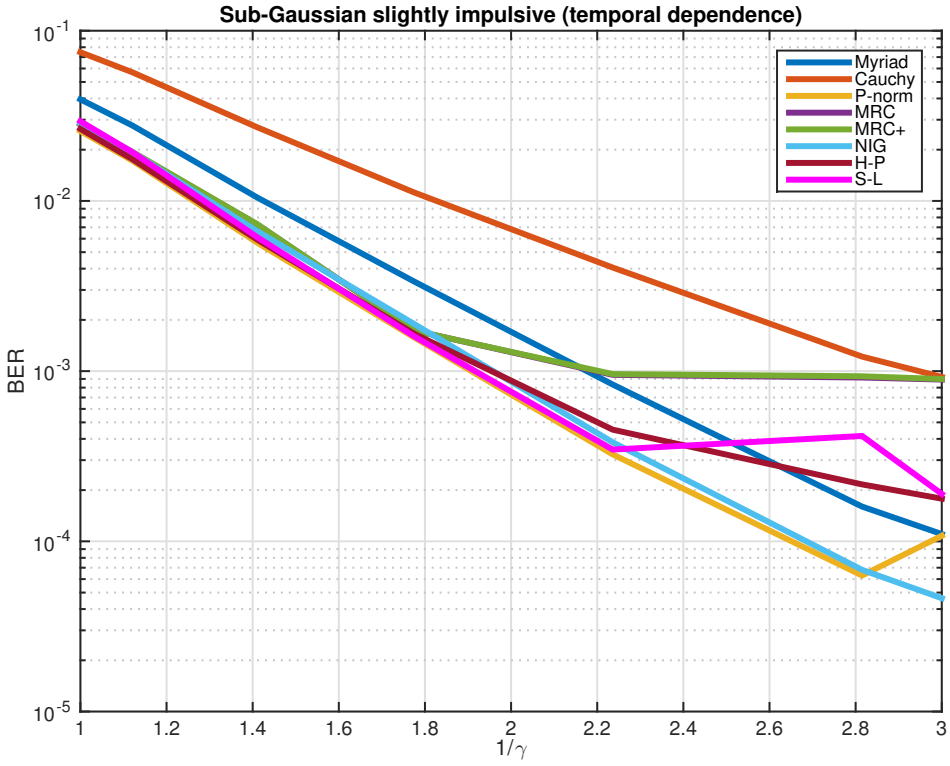


Figure 3.12: Receivers performance in sub-Gaussian noise under a slightly impulsive environment with temporal dependence $NIR = 10dB$

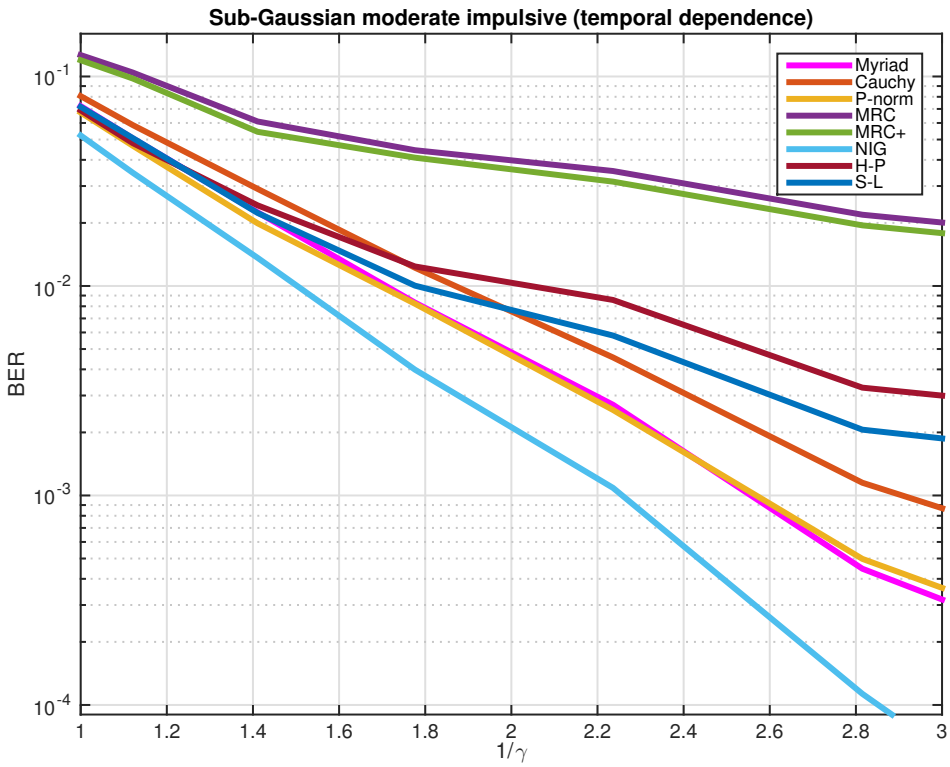


Figure 3.13: Receivers performance in sub-Gaussian noise under a moderate impulsive environment with temporal dependence $NIR = 0dB$

seems also to have a good robustness in the case with dependence. And the Cauchy, Hole-puncher and Soft-limiter works less good at high $1/\gamma$ value.

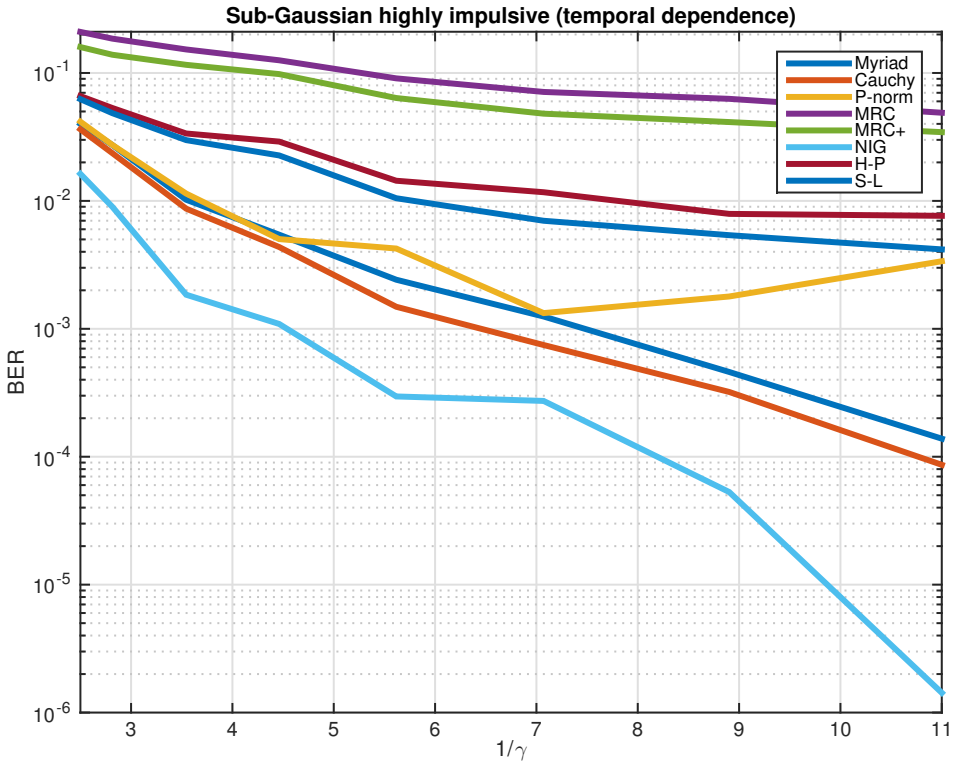


Figure 3.14: Receivers performance in sub-Gaussian noise under a highly impulsive environment with temporal dependence $NIR = -10dB$

Figure 3.14 shows the receivers performance in sub-Gaussian noise under a highly impulsive environment with temporal dependence.

NIG, $p$-norm and Myriad are still robust in this case. The Cauchy receiver improves a lot its performance because the environment is very impulsive and close to Cauchy distribution case. Hole-puncher and Soft-limiter do not work as well as them in the less impulsive case. That means the threshold should be well estimated. MRC is not adapted in the impulsive, so consequently it does not work well.

We now test the spatial dependence, which means that between two receive antennas a dependence exists. On the time line, signals are independent between them which means that the received interference vectors on two consecutive information bits are independent.

Figure 3.15, 3.16 and 3.17 shows the receivers performance in sub-Gaussian noise with spatial dependence under a slightly, moderate and highly impulsive environment.

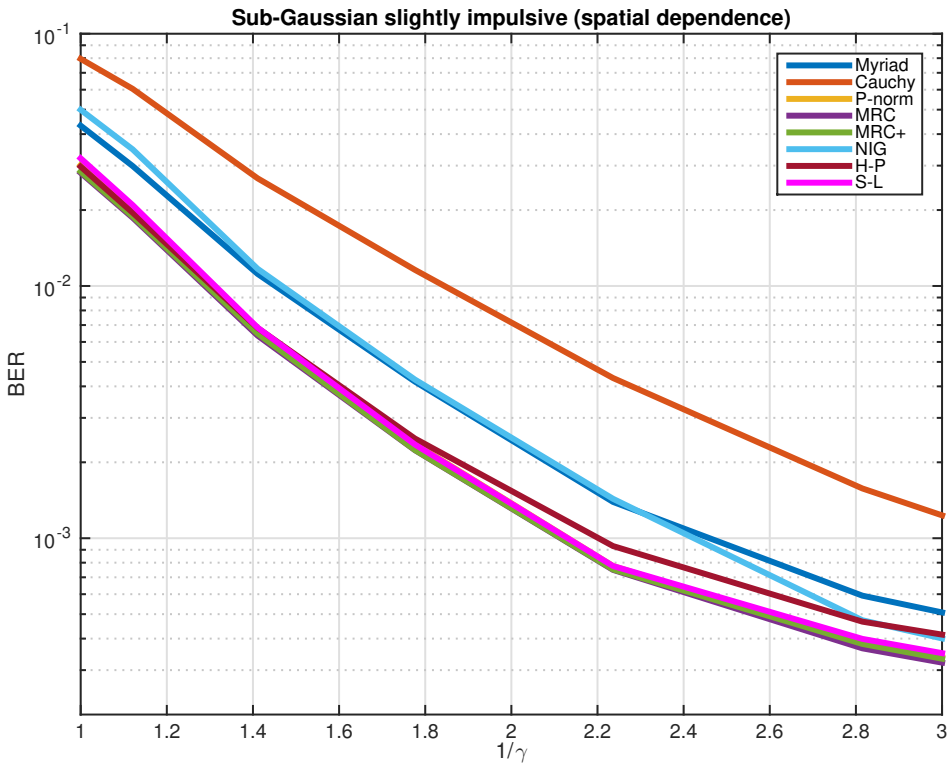


Figure 3.15: Receivers performance in sub-Gaussian noise under a slightly impulsive environment with spatial dependence$SNR = 10dB$

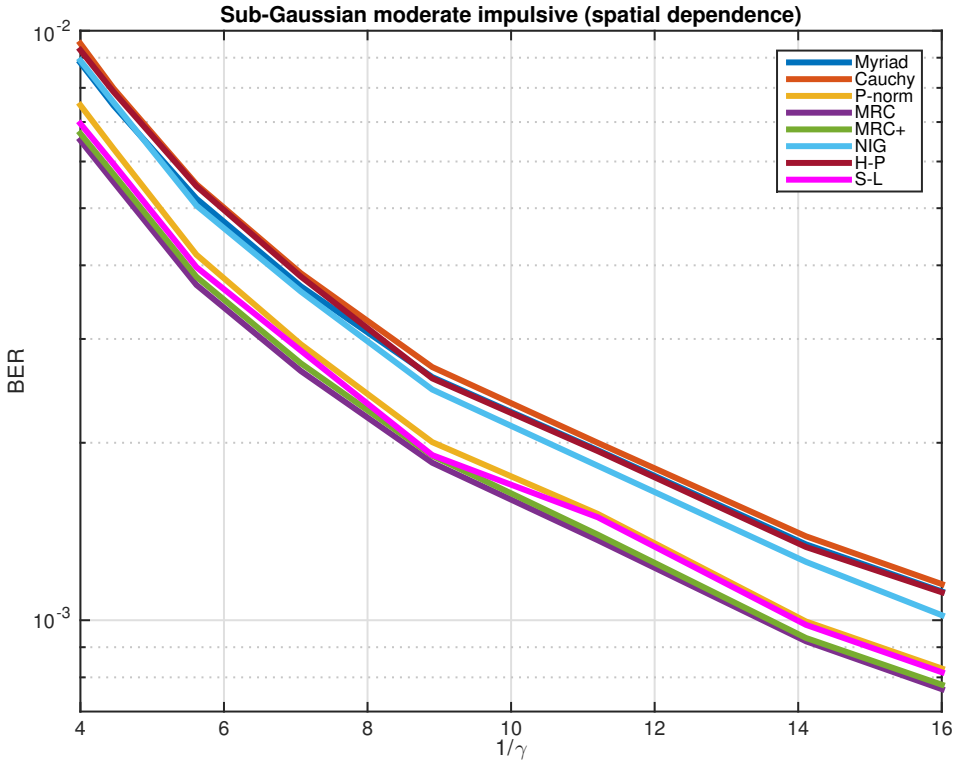


Figure 3.16: Receivers performance in sub-Gaussian noise under a moderate impulsive environment with spatial dependence$SNR = 0dB$

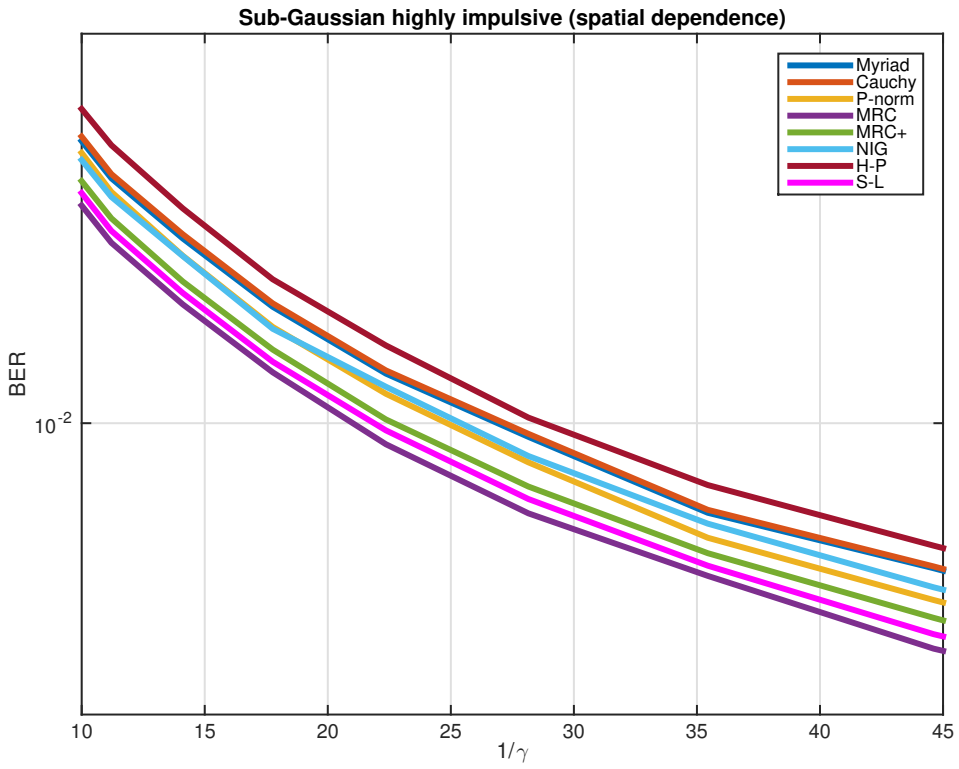


Figure 3.17: Receivers performance in sub-Gaussian noise under a highly impulsive environment with spatial dependence$SNR = -10dB$

The thing interesting is that the MRC receiver seems robust in this case, because MRC is the combiner between the receivers. And in this case, the signal between the receivers keeps Gaussian. Consequently, the Gaussian based approach remains efficient.

We compare also the result with the dependence and that without the dependence in chapter 2. We can note that the temporal dependence does not have a great impact on the robustness of the receivers. However, the spatial dependence have an important impact. For example, the MRC can give a great performance in the impulsive noise with spatial dependence which is totally different from the case without dependence. Hole-puncher can't deal with the spatial dependence well but give an acceptable performance in the independent case. Cauchy does also badly in the spatial dependence case.

### Receivers' performance with copula model

In this part, we use the skew-t copula to generate our interference.

In Fig. 3.18 we use a traditional linear receiver and Gaussian marginals. The four case that we want to test is: independence case ($\nu = 5$, $\sigma = 0$, $\beta = 0$), tail dependence case ($\nu = 1$, $\sigma = 0$, $\beta = 0$), linear dependence ($\nu = 3$, $\sigma = 0.9$, $\beta = 0$) and asymmetric dependence case ($\nu = 3$, $\sigma = 0$, $\beta = 2$). The linear and asymmetric case have a strong effect of the dependence on the MRC receiver's. It degrades its performance. In the tail dependence case, the impact is slight. This is rather expected, because the tails have a very low impact in Gaussian noise.

Fig. 3.19 shows the $p$-norm receiver BER performance in copula model with Gaussian marginals. The result confirms what we got using the MRC recevier case, which is that linear and asymmetric dependence has more impact than tail dependence on the receiver's performance.

Fig. 3.20 shows the $p$-norm receiver BER performance in $\alpha$-stable interference ($\alpha = 1.2$) with skew-t copula model. To avoid effect of estimation process, we used the value of $p$ to $0.5$ which is a good choice for this value of $\alpha$.

Again, it is seen that dependence affects the receiver's performance. The Linear dependence has the most impact and make the receiver's performance degrades. The tail dependence and asymmetric dependence has also a gap with the independence case in the BER performance. At the large $1/\gamma$ value, the gap is bigger, where the impulsive interference dominates the noise.

Fig. 3.21 shows the MRC receiver's performance in $\alpha$-stable interference with copula structure.

It seems for MRC receiver, the dependence's impact is less important than that for p-norm receiver.

To conclude the results above, we could see that, especially in impulsive noise, the tail dependence has a strong effect on the performance. This means tail dependence is a factor which can not be ignored when we tend to model an interference and design a

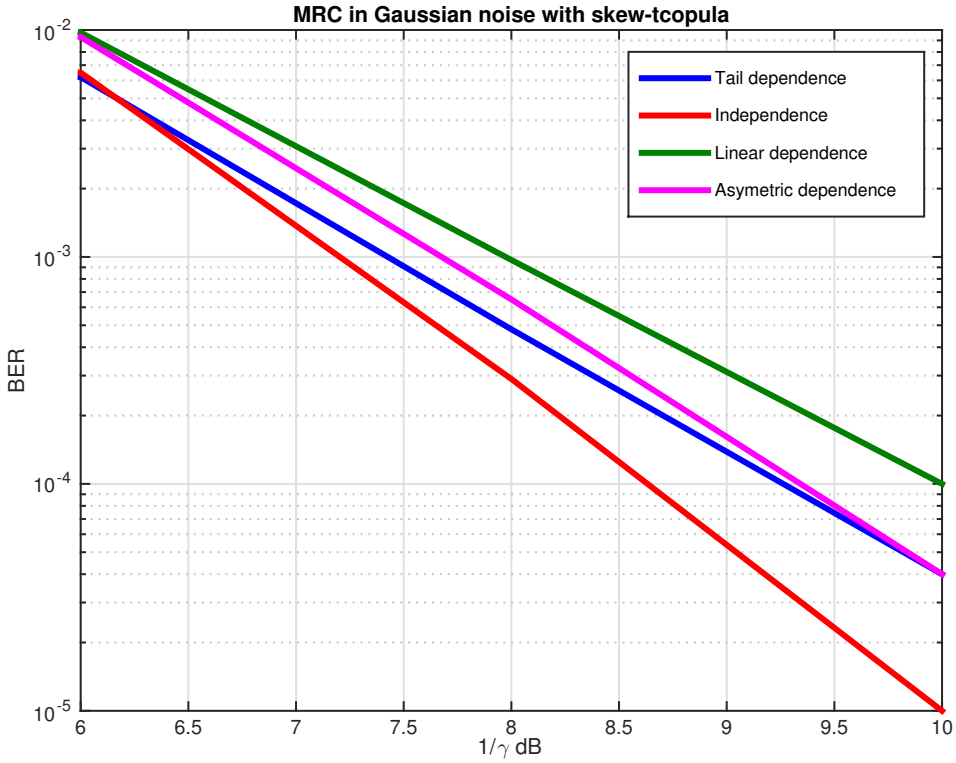


Figure 3.18: MRC in Gaussian noise with copula structure

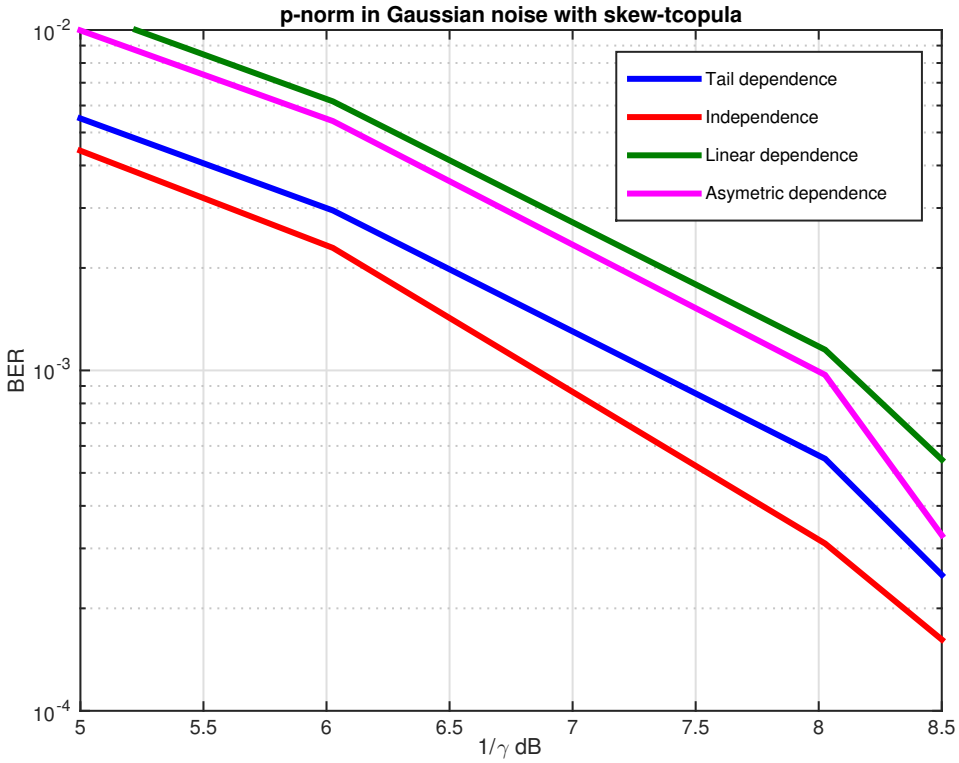


Figure 3.19: $p$-norm receiver in Gaussian noise with copula structure

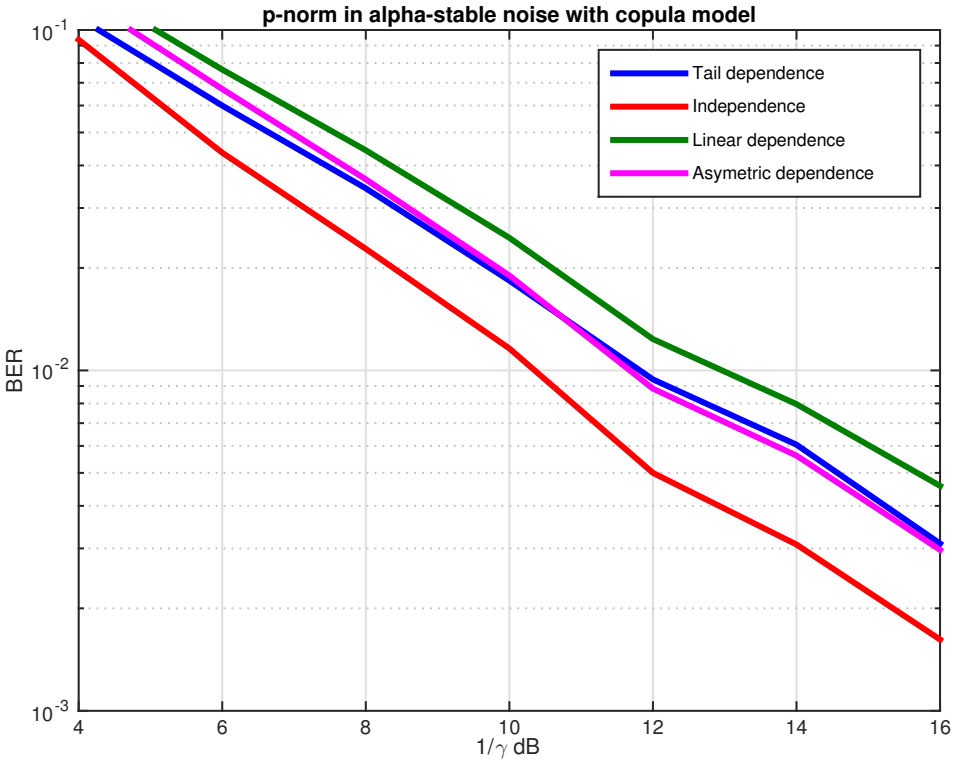


Figure 3.20: $p$-norm receiver in $\alpha$-stable noise copula structure

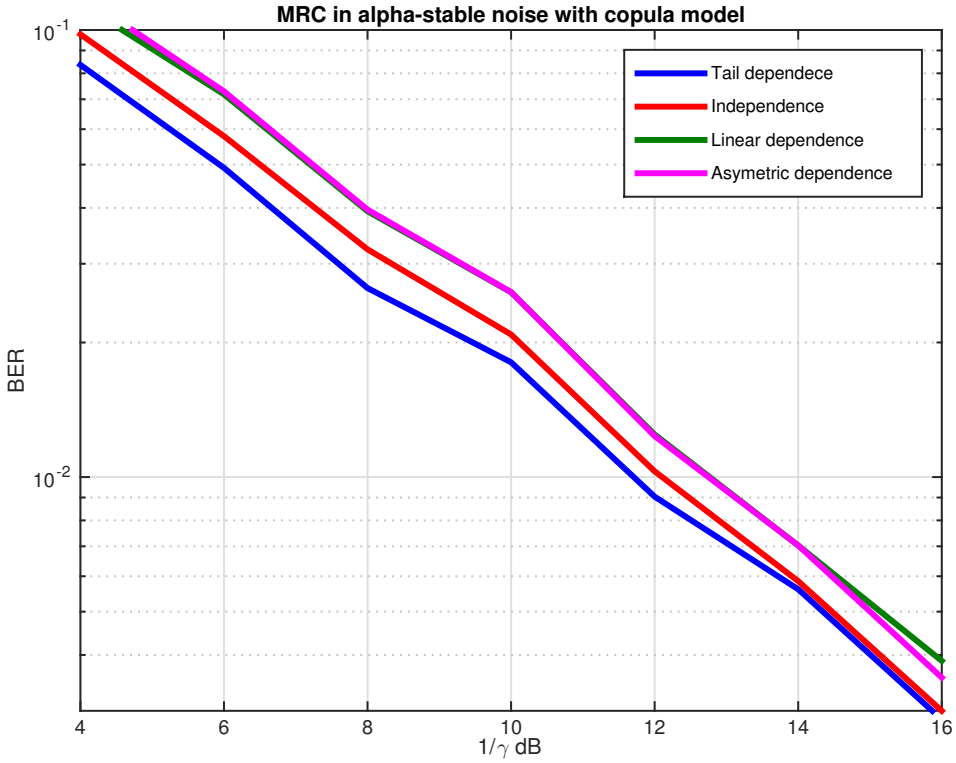


Figure 3.21: MRC receiver in $\alpha$-stable noise with copula structure

receiver. It should to be taken into account if it exists. It underlines the need of efficient and accurate dependence structure modelling.

## 3.5 Result analysis

We have shown in this chapter how we can model the dependence structure of interference in wireless networks using sub-Gaussian distribution and copula model. This is an important feature in many systems like MIMO, cognitive radio or time hopping ultra wide band where dependence is certainly present. We propose to use the copula framework to separate the one dimensional distribution of each received sample and the dependence structure. The skew-t copula we propose is an efficient solution that allows to represent different concordance measures like the tail dependence and the intermediate directional dependence. We show that the dependence structure, in time or in the *repetition* dimension has an important impact, but not necessarily the same. The slow changing case, where the interference environment keeps the same on one packet brings us back to the Gaussian case. Solutions adapted to Gaussian noises with different variances on each branch should be employed. In a second phase we analyse the impact of the *repetition* dimension. If it does not necessarily modify the relative performance of the different strategies, the different dependence structures that can be represented by the skew-$t$ copula have a significant impact on the performance. We only studied the case with two repetitions but we can expect an even more significant impact if more repetitions are done.

In future works we should improve the copula's parameters estimation method. A receiver that takes into account the dependence structure should also be studied in order to improve the performance. But first of all it would be essential to be able to show what type of dependence it is important to represent in the interference. If simulations can be an interesting approach, the needed assumptions have to be carefully examined. Consideration about electromagnetic pollutions are raising everywhere and we should see available soon some numerous measurement on this topic. this could be the way to get a significant amount of measurements to study the dependence structure.

# General conclusion

In this thesis, a perspective on Internet of Things and sensor networks is investigated.

We first show the independent case of wireless network interference model in spatial random fields. Differently from the popular Gaussian approximation, which is from the central limit theorem, we find that the interferences of the wireless network present an impulsive behavior in several scenarios, for example, when the number of interferers is large but there are dominant interferers. We then review the different impulsive interference models that we can classify under two different approaches, the theoretical approaches and the empirical approaches. In the first approach, we include the Middleton model and the $\alpha$-stable model. In the second one, we have Gaussian-mixture model, generalized Gaussian model, and $\epsilon$-contaminated model. We give their definitions, generation method and for $\alpha$-stable model, we give also the estimation method. A careful study of all the proposed models shows that distributions with a heavier tail can better capture the impulsive behavior than the traditional Gaussian model.

We then propose a transmission structure where a frame consisting of several data symbols is transmitted over wireless channels and several versions of each symbol are received. This transmission structure can be motivated by many different practical wireless communication systems like an impulse radio Ultra Wide Band transmission, MIMO or a cooperative scheme with several relays. We show the impact of impulsive interference noise on optimal decision regions. It results in non-linear decision boundaries, which are not even contiguously joined. It proves that the popular Gaussian approximation is not adequate for dealing with interference exhibiting an impulsive behavior. That leads to our 3 approaches of receiver designs: linear receivers, noise distribution approximation and log-likelihood ratio approximation. We propose several receiver designs such as Linear Combiner, Cauchy, Myriad, Normal Inverse Gaussian, Soft-limiter, Hole-puncher and $p$-norm. We give their design principles and decision statistic. For some of them, we derive also the algorithm necessary for the parameter estimation. We compare their performance from their theoretical PDF, CDF and their log-likelihood ration function. And after we give the simulation result of different receivers' performance in different condition of interference. We find that the Myriad, $p$-norm and NIG receivers exhibit a good robustness to a variety of impulsive noises. The hole-puncher and soft-limiter receivers can have good performance in some cases if well configured. The MRC receiver

performs poorly in the impulsive case.

In the third chapter of this manuscript, we study the dependence in the *repetition* dimension and in the time dimension. The *repetition* dimension is the dimension of the received vectors, one vector being composed of all the values received corresponding to a single information bit. The time dimension represent the ergodic or non ergodic cases. Ergodic means that the environment is changing rapidly on single transmitted packet whereas is is quasi fixed in the non Ergodic case. We observe that the dependence structure may arise from a number of different mechanisms. We give two examples: an UWB transmission with narrow band interferer and a SIMO case with two receive antennas. These examples show that independence assumption is, in many cases, not realistic. We first introduce the sub-Gaussian model and compare the isotropic case using Sub-Gaussian model and anisotropic case samples using independent $\alpha$-stable model. We then propose a very general framework to model the dependence: the copulas. Relying on Sklar's theorem, this approach allows to separately model the dependence structure and the marginal distributions. We focus on a particular flexible class of models based on the skewed-t copula family. It allows us to capture interesting dependence features based on extreme concordance. We give the generation and estimation algorithm and compare the parameters' impact on Dependence structure. We finally study the impact of these dependences on the receivers' performance when they are designed assuming i.i.d. signals. The simulation results show that dependence affects the receiver's performance and the tail dependence has a strong effect on the performance. It shows the need of efficient and accurate dependence structure modelling.

For the future work, new receiver designed can be considered, especially based on LLR inspired design. The complexity of parameters estimation as well as the implementation issues should also be taken into account. Other extensions of this work can concern asymmetric interference, which the NIG could handle. For the dependence of interference part, future works include several aspects. Firstly how to choose the good parameters? The parameters' estimation of copula directly from its marginal samples should be further studied. And how to develop a receiver that takes dependence structure into account to improve its performance?

Appendix A

# The $\alpha$-stable case

We define the characteristic function (CF) of the interference $Y$ defined in (1.9):

$$\varphi_{Y_I^{(i)},Y_Q^{(i)}}\left(\omega_I^{(i)},\omega_Q^{(i)}\right)=\mathbb{E}_{Y_I^{(i)},Y_Q^{(i)}}\left[\exp\left(j\omega_I^{(i)}Y_I^{(i)}+j\omega_Q^{(i)}Y_Q^{(i)}\right)\right]. \tag{A.1}$$

We can now express the CF for the total interference generated by $N$ independent interferers:

$$\begin{aligned}\varphi_{Y_I,Y_Q}\left(\omega_I,\omega_Q\right)=\mathbb{E}_{\mathbf{R},\boldsymbol{c},\mathbf{A},\boldsymbol{\Phi},N}\Bigg[\exp\Bigg(j\sqrt{\left(\omega_I\right)^2+\left(\omega_Q\right)^2}\\ \times\sum_{i=1}^{N}(R^{(i)})^{-\sigma/2}A^{(i)}c^{(i)}\cos\left(\Phi^{(i)}-\arctan\left(\frac{\omega_Q}{\omega_I}\right)\right)\Bigg)\Bigg].\end{aligned} \tag{A.2}$$

The steps we take next are best summarised as follows:

1. marginalize over the number of interferers in region $A_{\mathcal{R}}$,

2. use the independence between the channels and signals from different interferers

3. and use the Taylor series representation of an exponent

to obtain:

$$\begin{aligned}
&\varphi_{Y_I,Y_Q}(\omega_I,\omega_Q) \\
&\quad= \sum_{N=0}^{\infty} \mathbb{P}(N(A_{\mathcal{R}}))\, \mathbb{E}_{\mathbf{R},\mathbf{A},\boldsymbol{c},\boldsymbol{\Phi}}\left[\prod_{i=1}^{N} \exp\left(j\sqrt{(\omega_I)^2+(\omega_Q)^2}\right.\right. \\
&\qquad\qquad \left.\left.\times (R^{(i)})^{-\sigma/2} A^{(i)} c^{(i)} \cos\left(\Phi^{(i)} - \arctan\left(\frac{\omega_Q}{\omega_I}\right)\right)\right) \mid N\right] \\
&\quad= \exp\left(-\lambda\pi \mathbf{r}_T^2 + \lambda\pi \mathbf{r}_T^2 \mathbb{E}_{\mathbf{R},\boldsymbol{c},\mathbf{A},\boldsymbol{\Phi}}\left[\exp\left(jR^{-\sigma/2} Ac\sqrt{(\omega_I)^2+(\omega_Q)^2}\right.\right.\right. \\
&\qquad\qquad \left.\left.\left.\times \cos\left(\Phi - \arctan\left(\frac{\omega_Q}{\omega_I}\right)\right)\right)\right]\right).
\end{aligned} \tag{A.3}$$

We rewrite the CF in the $\log$ domain, according to:

$$\begin{aligned}
\psi_{Y_I,Y_Q}(\omega_I,\omega_Q) &\triangleq \log\left(\varphi_{Y_I,Y_Q}(\omega_I,\omega_Q)\right) \\
&= \lambda\pi r_T^2 \left(\mathbb{E}_{\mathbf{R},\boldsymbol{c},\mathbf{A},\boldsymbol{\Phi},}\left[\exp\left(jR^{-\sigma/2} Ac\sqrt{(\omega_I)^2+(\omega_Q)^2}\right.\right.\right. \\
&\qquad \left.\left.\left.\times \cos\left(\Phi - \arctan\left(\frac{\omega_Q}{\omega_I}\right)\right)\right)\right] - 1\right).
\end{aligned} \tag{A.4}$$

The next step is to marginalize the random variable $\Phi$. We first use the complex series expansion based on Bessel functions, given by [1]

$$\exp(ja\cos(\theta)) = \sum_{s=1}^{\infty} j^s \epsilon_s J_s(a)\cos(s\theta) \tag{A.5}$$

where $\epsilon_0 = 1$ and $\epsilon_s = 2$ for all $s \geq 1$, and $J_s$ is the Bessel function of order $s$ defined by:

$$J_s(x) = \frac{1}{2\pi}\int_{-\pi}^{\pi} \exp(-j(s\tau - x\sin(\tau)))\, d\tau. \tag{A.6}$$

Applying this identity to (A.4) we have:

$$\begin{aligned}
\psi_{Y_I,Y_Q}(\omega_I,\omega_Q) = \lambda\pi r_T^2 \left(\mathbb{E}_{\mathbf{R},\boldsymbol{c},\mathbf{A},\boldsymbol{\Phi}}\left[\sum_{s=0}^{\infty} j^s \epsilon_s J_s\left(R^{-\frac{\sigma}{2}} Ac\sqrt{(\omega_I)^2+(\omega_Q)^2}\right)\right.\right. \\
\left.\left.\times \cos\left(s\Phi - s\arctan\left(\frac{\omega_Q}{\omega_I}\right)\right)\right] - 1\right).
\end{aligned} \tag{A.7}$$

The random variable $\Phi$ is uniformly distributed in $[0, 2\pi]$. Therefore:

$$\begin{aligned}\psi_{Y_I,Y_Q}(\omega_I,\omega_Q) &= \lambda\pi r_T^2\left(\sum_{s=0}^{\infty} j^s\epsilon_s\mathbb{E}_{\mathbf{R},\boldsymbol{c},\mathbf{A}}\left[J_s\left(R^{-\sigma/2}Ac\sqrt{(\omega_I)^2+(\omega_Q)^2}\right)\right]\right.\\ &\quad\left.\times\mathbb{E}_{\mathbf{\Phi}}\left[\cos\left(s\Phi - s\arctan\left(\frac{\omega_Q}{\omega_I}\right)\right)\right]-1\right)\\ &= \lambda\pi r_T^2\left(\mathbb{E}_{\mathbf{R},\boldsymbol{c},\mathbf{A}}\left[J_0\left(R^{-\sigma/2}Ac\sqrt{(\omega_I)^2+(\omega_Q)^2}\right)\right]-1\right),\end{aligned} \tag{A.8}$$

which holds due to the observation that $\mathbb{E}_{\mathbf{\Phi}}\left[\cos\left(s\Phi - s\arctan\left(\frac{\omega_Q}{\omega_I}\right)\right)\right] = 0$ for $s \geq 1$.

Conditional on any given number of potential interferers, in $\Omega(A_{\mathcal{R}})$, we can marginalize the CF with respect to the unknown spatial locations of the interferers. To achieve this we utilise the assumption on the spatial distribution of these interferers given in model assumptions in Section 1.1. Hence, we integrate the log CF as follows:

$$\begin{aligned}&\psi_{Y_I,Y_Q}(\omega_I,\omega_Q)\\ &\quad= \lambda\pi r_T^2\left(\int_0^{r_T}\mathbb{E}_{\boldsymbol{c},\mathbf{A}}\left[J_0\left(r^{-\sigma/2}Ac\sqrt{(\omega_I)^2+(\omega_Q)^2}\right)\right]\frac{2r}{r_T^2}\mathrm{d}r-1\right)\\ &\quad= \lambda\pi r_T^2\left(\int_0^{r_T}\left(\mathbb{E}_{\boldsymbol{c},\mathbf{A}}\left[J_0\left(r^{-\sigma/2}Ac\sqrt{(\omega_I)^2+(\omega_Q)^2}\right)-1\right]\right)\frac{2r}{r_T^2}\mathrm{d}r\right).\end{aligned} \tag{A.9}$$

Next we integrate by parts:

$$\begin{aligned}&\psi_{Y_I,Y_Q}(\omega_I,\omega_Q)\\ &\quad= \lambda\pi r_T^2\left(\mathbb{E}_{\boldsymbol{c},\mathbf{A}}\left[J_0\left(r_T^{-\sigma/2}Ac\sqrt{(\omega_I)^2+(\omega_Q)^2}\right)-1\right]\right.\\ &\qquad\left.-\int_0^{r_T}\frac{d}{dr}\mathbb{E}_{\boldsymbol{c},\mathbf{A}}\left[J_0\left(r^{-\sigma/2}Ac\sqrt{(\omega_I)^2+(\omega_Q)^2}\right)\right]\mathrm{d}r\right).\end{aligned} \tag{A.10}$$

To proceed, we expand the region in which the interferers are distributed via the limit $r_T \to \infty$. We obtain:

$$\begin{aligned}&\psi_{Y_I,Y_Q}(\omega_I,\omega_Q)\\ &\quad= \lim_{r_T\to\infty}\lambda\pi r_T^2\mathbb{E}_{\boldsymbol{c},\mathbf{A}}\left[J_0\left(r_T^{-\sigma/2}Ac\sqrt{(\omega_I)^2+(\omega_Q)^2}\right)-1\right]\\ &\qquad- \lim_{r_T\to\infty}\lambda\pi r_T^2\int_0^{r_T}\frac{d}{dr}\mathbb{E}_{\boldsymbol{c},\mathbf{A}}\left[J_0\left(r^{-\sigma/2}Ac\sqrt{(\omega_I)^2+(\omega_Q)^2}\right)\right]\mathrm{d}r.\end{aligned} \tag{A.11}$$

We can now evaluate the limits in each term in (A.11). Starting with the first one, we utilize the result from [83, eq. (12)] which allows us to state the following equivalent limit expression for the CF for the total interference at two extremes:

$$\begin{aligned}&\lim_{r_T\to\infty} r_T^2\mathbb{E}_{\boldsymbol{c},\mathbf{A}}\left[J_0\left(r_T^{-\sigma/2}Ac\sqrt{(\omega_I)^2+(\omega_Q)^2}\right)-1\right]\\&=\lim_{r_T\to 0} r_T^{-2}\mathbb{E}_{\boldsymbol{c},\mathbf{A}}\left[J_0\left(r_T^{\sigma/2}Ac\sqrt{(\omega_I)^2+(\omega_Q)^2}\right)-1\right].\end{aligned} \tag{A.12}$$

Since $\lim_{r_T\to 0} r_T^2 = 0$ and
$\lim_{r_T\to 0}\mathbb{E}_{\boldsymbol{c},\mathbf{A}}\left[J_0\left(r_T^{\sigma/2}Ac\sqrt{(\omega_I)^2+(\omega_Q)^2}\right)-1\right]=0$, we can apply L'Hopitals rule and the identity $\frac{\mathrm{d}}{\mathrm{d}x}J_0(x) = -J_1(x)$ given in [1] in conjunction with the chain rule to obtain

$$\begin{aligned}&\lim_{r_T\to 0} r_T^{-2}\mathbb{E}_{\boldsymbol{c},\mathbf{A}}\left[J_0\left(r_T^{\sigma/2}Ac\sqrt{(\omega_I)^2+(\omega_Q)^2}\right)-1\right]\\&=\lim_{r_T\to 0}\sigma r_T^{\frac{\sigma}{2}-2}\mathbb{E}_{\boldsymbol{c},\mathbf{A}}\left[-J_1\left(r_T^{\frac{\sigma}{2}}Ac\sqrt{(\omega_I)^2+(\omega_Q)^2}\right)Ac\sqrt{(\omega_I)^2+(\omega_Q)^2}\right].\end{aligned} \tag{A.13}$$

For $\sigma > 2$ this limit converges to $0$.

We can then work with the second term. We need to use a representation of an isotropic bivariate $\alpha$-stable distribution [46, Identity 3.12, p.152] given by:

$$\lim_{a\to\infty} a^2\left(\int_0^a \frac{2r}{a^2}\exp\left(j\omega l(r)\right)dr - 1\right) = \int_0^\infty \left(l^{-1}(x)\right)^2 j\omega\exp\left(j\omega x\right)dx \tag{A.14}$$

We have the following:

$$\begin{aligned}&\lim_{r_T\to\infty}\lambda\pi r_T^2\int_0^{r_T}\frac{d}{dr}\mathbb{E}_{\boldsymbol{c},\mathbf{A}}\left[J_0\left(r^{-\sigma/2}Ac\sqrt{(\omega_I)^2+(\omega_Q)^2}\right)\right]\mathrm{d}r\\&=\lim_{r_T\to\infty}\lambda\pi r_T^2\int_0^{r_T}\mathbb{E}_{\boldsymbol{c},\mathbf{A}}\left[J_1\left(r^{-\sigma/2}Ac\sqrt{(\omega_I)^2+(\omega_Q)^2}\right)\right.\\&\qquad\left.\times\frac{\sigma}{2}r^{-\sigma/2-1}Ac\sqrt{(\omega_I)^2+(\omega_Q)^2}\right]\mathrm{d}r.\end{aligned} \tag{A.15}$$

Using (A.14) and noting the result of [45, Equation 17, pp. 8], we obtain

$$\psi_{Y_I,Y_Q}(\omega_I,\omega_Q) = -\lambda\pi\left((\omega_I)^2+(\omega_Q)^2\right)^{\frac{2}{\sigma}}\mathbb{E}_{\boldsymbol{c},\mathbf{A}}\left[(Ac)^{\frac{4}{\sigma}}\right]\int_0^\infty\frac{J_1(x)}{x^{\frac{4}{\sigma}}}\mathrm{d}x. \tag{A.16}$$

Eq. (A.16) is the $\log$ CF of an isotropic bivariate symmetric $\alpha$-stable distribution, where

the characteristic exponent $\alpha = \frac{4}{\sigma}$, and the dispersion parameter :

$$\gamma = \lambda\pi\mathbb{E}_{\boldsymbol{c},\mathbf{A}}\left[(Ac)^{\frac{4}{\sigma}}\right]\int_0^\infty \frac{J_1(x)}{x^{\frac{4}{\sigma}}}\mathrm{d}x. \tag{A.17}$$

# Bibliography

[1] M. Abramowitz and I.A. Stegun. *Handbook of mathematical functions with formulas, graphs, and mathematical tables*. Dover Publications, 1964.

[2] D. Allen and S. Satchell. *The Four Horsemen: Heavy-tails, Negative Skew, Volatility Clustering, Asymmetric Dependence*. Tech. rep. Discussion Paper: 2014-004 - Business School, Discipline of Finance, The University of Sydney, 2014.

[3] S. Ambike, J. Ilow, and D. Hatzinakos. "Detection for binary transmission in a mixture of Gaussian noise and impulsive noise modeled as an alpha-stable process". In: *Signal Processing Letters, IEEE* 1.3 (Mar. 1994), pp. 55 –57.

[4] J.G. Andrews et al. "Random Access Transport Capacity". In: *IEEE Trans. Wireless Commun.* 9.6 (June 2010), pp. 2101–2111.

[5] T.C. Aysal and K.E. Barner. "Generalized Mean-Median Filtering for Robust Frequency-Selective Applications". In: *IEEE Trans. Signal Processing* 55.3 (Mar. 2007), pp. 937–948.

[6] A. Azzalini and A. Capitanio. "Distributions generated by perturbation of symmetry with emphasis on a multivariate skew t-distribution". In: *Journal of the Royal Statistical Society Series B-Statistical Methodology* 65 (2003), pp. 367–389.

[7] F. Baccelli and B. Blaszczyszyn. "Stochastic Geometry and Wireless Networks: Volume I Theory". In: *Foundations and Trends in Networking* 3.3-4 (2010), pp. 249–449.

[8] F. Baccelli and B. Blaszczyszyn. “Stochastic Geometry and Wireless Networks: Volume II Applications”. In: *Foundations and Trends in Networking* 4.1-2 (2010), pp. 1–312.

[9] O. E. Barndorff-Nielsen. “Normal inverse Gaussian distributions and stochastic volatility modelling”. In: *Scandinavian Journal of statistics* 24.1 (1997), pp. 1–13.

[10] O. E. Barndorff-Nielsen. “Processes of normal inverse Gaussian type”. In: *Finance and stochastics* 2.1 (1997), pp. 41–68.

[11] O.E. Barndorff-Nielsen and Blaesid. “Hyperbolic distributions and ramifications: Contributions to theory and application”. In: *Statistical Distributions in Scientific Work* 4 (1981).

[12] Ole E. Barndorff-Nielsen and Neil Shephard. *Normal Modified Stable Processes*. Economics Series Working Papers 072. University of Oxford, Department of Economics, 2001.

[13] N. C. Beaulieu, H. Shao, and J. Fiorina. “P-order metric UWB receiver structures with superior performance”. In: *IEEE Trans. Commun.* 56 (Oct. 2008), pp. 1666–1676.

[14] N. C. Beaulieu and D. J. Young. “Designing Time-Hopping Ultrawide Bandwidth Receivers for Multiuser Interference Environments”. In: *Proceedings of the IEEE*. Vol. 97. 2. Feb. 2009, pp. 255–284.

[15] N.C. Beaulieu and S. Niranjayan. “UWB receiver designs based on a gaussian-laplacian noise-plus-MAI model”. In: *Communications, IEEE Transactions on* 58.3 (Mar. 2010), pp. 997–1006.

[16] M.D. Branco and D.K. Dey. “A general class of multivariate skew-elliptical distributions”. In: *Journal of Multivariate Analysis* 79 (2001), pp. 99–113.

[17] G. Bresler, A. Parekh, and D.N.C. Tse. “The Approximate Capacity of the Many-to-One and One-to-Many Gaussian Interference Channels”. In: *IEEE Trans. Inform. Theory* 56.9 (2010), pp. 4566–4592.

[18] B.W. Brorsen and S. Yang. “Maximum likelihood estimates of symmetric stable distribution parameters”. In: *Communications in statistics. Simulation and computation* 19.4 (1990), pp. 1459–1464.

[19] P. Cardieri. “Modeling Interference in Wireless Ad Hoc Networks”. In: *IEEE Communications Surveys Tutorials* 12.4 (Oct. 2010), pp. 551–572.

[20] A. B. Carleial. “Interference channels”. In: *IEEE Trans. Inform. Theory* 24.1 (Jan. 1978), pp. 60–70.

[21] A. Charpentier. “Tail distribution and dependence measures”. In: *XXXIV International Astin Colloquium, Berlin, August*. 2003, pp. 24–27.

[22] Jiejia Chen et al. “Alpha-stable Interference Modelling and Relay Selection for Regenerative Cooperative IR-UWB Systems”. In: *European Wireless Technology Conference (EuWiT)*. 2010.

[23] A. Chopra and B.L. Evans. “Outage Probability for Diversity Combining in Interference-Limited Channels”. In: *IEEE Trans. Wireless Commun.* 12.2 (Feb. 2013), pp. 550–560.

[24] A. Chopra et al. “Performance bounds of MIMO receivers in the presence of radio frequency interference”. In: *IEEE International Conference on Acoustics, Speech and Signal Processing, ICASSP 2009*. Apr. 2009, pp. 2817–2820.

[25] R. Dabora, I. Maric, and A. Goldsmith. “Relay strategies for interference-forwarding”. In: *IEEE Information Theory Workshop ITW ’08*. 2008, pp. 46–50.

[26] G. De Luca and G. Rivieccio. “Multivariate tail dependence coefficients for Archimedean Copulae”. In: *Advanced Statistical Methods for the Analysis of Large Data-Sets*. Springer, 2012, pp. 287–296.

[27] Stefano Demarta and Alexander J McNeil. “The t copula and related copulas”. In: *International Statistical Review* 73.1 (2005), pp. 111–129.

[28] W. DuMouchel. “On the Asymptotic Normality of the Maximum-Likelihood Estimate when Sampling from a Stable Distribution”. In: *Annals of Statistics* 3 (1973), pp. 948–957.

[29] Anders Eriksson, Lars Forsberg, and Eric Ghysels. “Approximating the probability distribution of functions of random variables: A new approach”. In: *Working Paper* (2004).

[30] T. Erseghe, V. Cellini, and G. Dona. “On UWB Impulse Radio Receivers Derived by Modeling MAI as a Gaussian Mixture Process”. In: *Wireless Communications, IEEE Transactions on* 7.6 (June 2008), pp. 2388–2396.

[31] E. F. Fama and R. Roll. “Parameter estimates for symmetric stable distributions”. In: *Journal of the American Statistical Association* 66.334 (1971), pp. 331–338.

[32] D. Fertonani and G. Colavolpe. “A robust metric for soft-output detection in the presence of class-A noise”. In: *IEEE Trans. Commun.* 57.1 (Jan. 2009), pp. 36–40.

[33] D. Fertonani and G. Colavolpe. “On reliable communications over channels impaired by bursty impulse noise”. In: *IEEE Trans. Commun.* 57.7 (July 2009), pp. 2024–2030.

[34] M.C. Filippou, D. Gesbert, and G.A. Ropokis. “Optimal Combining of Instantaneous and Statistical CSI in the SIMO Interference Channel”. In: *IEEE 77th Vehicular Technology Conference (VTC Spring)*. June 2013, pp. 1–5.

[35] J. Fiorina. “A simple IR-UWB receiver adapted to Multi-User Interferences”. In: *IEEE Global Telecommunications Conf., GLOBECOM 2006*. Nov. 2006, pp. 1–4.

[36] J. Fiorina and W. Hachem. “On the asymptotic distribution of the correlation receiver output for time-hopped UWB signals”. In: *IEEE Trans. Signal Processing* 54.7 (July 2006), pp. 2529–2545.

[37] K. Furutsu and T. Ishida. “On the theory of amlitude distribution of impulsive random noise and its application to the atmospheric noise”. In: *Journal of the radio research laboratories (Japan)* 7.32 (1960).

[38] R.K. Ganti, F. Baccelli, and J.G. Andrews. “Series Expansion for Interference in Wireless Networks”. In: *IEEE Trans. Inform. Theory* 58.4 (Apr. 2012), pp. 2194 –2205.

[39] H. E. Ghannudi et al. "$\alpha$-stable interference modeling and Cauchy receiver for an IR-UWB *ad hoc* network". In: *IEEE Trans. Commun.* 58 (June 2010), pp. 1748–1757.

[40] A.A Giordano and F. Haber. "Modeling of atmospheric noise". In: *Radio Science* 7 (1972), pp. 1011–1023.

[41] J.G. Gonzalez and G.R. Arce. "Optimality of the myriad filter in practical impulsive-noise environments". In: *IEEE Trans. Signal Process.* 49.2 (Feb. 2001), pp. 438–441.

[42] Wei Gu and L. Clavier. "Decoding Metric Study for Turbo Codes in Very Impulsive Environment". In: *Communications Letters, IEEE* 16.2 (Feb. 2012), pp. 256 –258.

[43] Wei Gu et al. "Receiver study for cooperative communications in convolved additive alpha-stable interference plus Gaussian thermal noise". In: *Wireless Communication Systems (ISWCS), 2012 International Symposium on*. Aug. 2012, pp. 451–455.

[44] K. Gulati, B.L. Evans, and S. Srikanteswara. "Joint Temporal Statistics of Interference in Decentralized Wireless Networks". In: *IEEE Trans. Signal Processing* 60.12 (Dec. 2012), pp. 6713–6718.

[45] K. Gulati et al. "Statistics of Co-Channel Interference in a Field of Poisson and Poisson-Poisson Clustered Interferers". In: *IEEE Trans. Signal Processing* 58.12 (Dec. 2010), pp. 6207–6222.

[46] M. Haenggi and R.K. Ganti. *Interference in large wireless networks*. Now Publishers Inc, 2009.

[47] T. S. Han and K. Kobayashi. "A new Achievable Rate Region for the Interference Channel". In: *IEEE Trans. Inform. Theory* 27.1 (Jan. 1981), pp. 49–60.

[48] B.E. Hansen. "Autoregressive conditional density estimation". In: *International Economic Review* 35 (1994), pp. 705–730.

[49] G. R. Hossack, G. W. Peters, and K. Hayes. “Estimating nonlinear ecological state space models with flexibleobservation error.” In: *Methods in Ecology and Evolution* (2012).

[50] B. Hu and N. C. Beaulieu. “On characterizing multiple access interference in TH-UWB systems with impulsive noise models”. In: *Proc. IEEE Radio Wireless Symp.* Orlando, FL, Jan. 2008, pp. 879–882.

[51] Guido Imbens, Phillip Johnson, and Richard H Spady. *Information theoretic approaches to inference in moment condition models*. National Bureau of Economic Research Cambridge, Mass., USA, 1995.

[52] H. Ishikawa, M. Itami, and K. Itoh. “A Study on Adaptive Modulation of OFDM under Middleton’s Class-A Impulsive Noise Model”. In: *Digest of Technical Papers. International Conference on Consumer Electronics, 2007. ICCE 2007.* Jan. 2007, pp. 1–2.

[53] C.L. Mallows J.M. Chambers and B.W. Stuck. “A method for simulating stable random variables”. In: *Journal of the American Statistical Association* 71 (1976), pp. 340–344.

[54] D.H. Johnson. “Optimal Linear Detectors for Additive Noise Channels”. In: *IEEE Trans. Signal Processing* 44.12 (Dec. 1996), pp. 3079–3084.

[55] F. Kharrat-Kammoun, C.J. Le Martret, and P. Ciblat. “Performance analysis of IR-UWB in a multi-user environment”. In: *IEEE Trans. Wireless Commun.* 8.11 (Nov. 2009), pp. 5552–5563.

[56] I. A. Koutrouvelis. “Regression-type estimation of the parameters of stable laws”. In: *Journal of the American Statistical Association* 75 (1980), pp. 918–928.

[57] S. Kundu and S. Chakrabarti. “Outage and BER Analysis of Cellular CDMA for Integrated Services With Correlated Signal and Interference”. In: *IEEE Commun. Lett.* 7.10 (Oct. 2003), pp. 478–480.

[58] Haijun Li. “Orthant tail dependence of multivariate extreme value distributions”. In: *Journal of Multivariate Analysis* 100.1 (2009), pp. 243–256.

[59] H.B. Maad et al. “Clipping Demapper for LDPC Decoding in Impulsive Channel”. In: *IEEE Commun. Lett.* 17.5 (May 2013), pp. 968–971.

[60] A. Mahmood, M. Chitre, and M.A. Armand. “PSK Communication with Passband Additive Symmetric $\alpha$-Stable Noise”. In: *IEEE Trans. Commun.* 60.10 (Oct. 2012), pp. 2990–3000.

[61] J. H. McCulloch. “Simple Consistent Estimators of Stable distribution Parameters”. In: *Communications on Satatistical Simulations* 15.4 (1986), pp. 1109–1136.

[62] A. McNeil, R. Frey, and P. Embrechts. “Quantitative Risk Management: Concepts, Techniques and Tools”. In: *Princeton University Press* (2005).

[63] D. Middleton. “Non-Gaussian noise models in signal processing for telecommunications: New methods and results for class A and class B noise models”. In: *IEEE Trans. Inf. Theory* 45.4 (May 1999), pp. 1129–1149.

[64] D. Middleton. “Statistical-Physical Models of Electromagnetic Interference”. In: *IEEE Transactions on Electromagnetic Compatibility* EMC-19.3 (Aug. 1977), pp. 106–127.

[65] S. Nammi et al. “Effects of impulse noise on the performance of multidimensional parity check codes”. In: *IEEE Wireless Communications and Networking Conference, WCNC 2006*. Vol. 4. Apr. 2006, pp. 1966–1971.

[66] B. Nikfar, T. Akbudak, and A.J.H. Vinck. “MIMO capacity of class A impulsive noise channel for different levels of information availability at transmitter”. In: *18th IEEE International Symposium on Power Line Communications and its Applications (ISPLC)*. Mar. 2014, pp. 266–271.

[67] C. L. Nikias and M. Shao. *Signal processing with $\alpha$-stable distributions and applications*. Ed. by Wiley inter science. J.Wiley, 1995.

[68] Chrysostomos L. Nikias and Min. Shao. *Signal Processing with Alpha-Stable Distributions and Applications*. JOHN WILEY and SONS, INC, 1995.

[69] S. Niranjayan and N.C. Beaulieu. “A Myriad Filter Detector for UWB Multiuser Communication”. In: *IEEE International Conference on Communications, ICC ’08*. May 2008, pp. 3918–3922.

[70] S. Niranjayan and N.C. Beaulieu. “BER optimal linear combiner for signal detection in symmetric alpha-stable noise: small values of alpha”. In: *Wireless Communications, IEEE Transactions on* 9.3 (Mar. 2010), pp. 886 –890.

[71] S. Niranjayan and N.C. Beaulieu. “The BER optimal linear rake receiver for signal detection in symmetric alpha-stable noise”. In: *IEEE Trans. Commun.* 57.12 (Dec. 2009), pp. 3585–3588.

[72] A. Patton. “On the out-of-sample importance of skewness and asymmetric dependence for asset allocation”. In: *Journal of Financial of Econometrics* 2 (2004).

[73] Duc Son Pham et al. “On the computational aspect of robust multiuser detection”. In: *Proceedings of the 3rd IEEE International Symposium on Signal Processing and Information Technology, 2003. ISSPIT 2003.* 2003, pp. 22–25.

[74] P.C. Pinto and M.Z. Win. “Communication in a Poisson Field of Interferers–Part I: Interference Distribution and Error Probability”. In: *IEEE Trans. Wireless Commun.* 9.7 (July 2010), pp. 2176–2186.

[75] P.C. Pinto and M.Z. Win. “Communication in a Poisson Field of Interferers-Part II: Channel Capacity and Interference Spectrum”. In: *IEEE Trans. Wireless Commun.* 9.7 (July 2010), pp. 2187–2195.

[76] T.S. Saleh, I. Marsland, and M. El-Tanany. “Suboptimal Detectors for Alpha-Stable Noise: Simplifying Design and Improving Performance”. In: *IEEE Trans. Commun.* 60.10 (Oct. 2012), pp. 2982 –2989.

[77] G. Samorodnitsky and M.S. Taqqu. *Stable Non-Gaussian Random Processes : Stochastic Models with Infinite Variance*. Chapmann and Hall, 1994.

[78] H. Sato. “The capacity of the Gaussian interference channel under strong interference”. In: *IEEE Trans. Inform. Theory* 27.6 (Nov. 1981), pp. 786–788.

[79] Marco Scarsini. “On measures of concordance.” In: *Stochastica: revista de matemática pura y aplicada* 8.3 (1984), pp. 201–218.

[80] U. Schilcher, C. Bettstetter, and G. Brandner. “Temporal Correlation of Interference in Wireless Networks with Rayleigh Block Fading”. In: *IEEE Trans. Mob. Comput.* 11.12 (2012), pp. 2109–2120.

[81] Lee Seoyoung and J. Dickerson. “Least Lp-norm interference suppression for DS/CDMA systems in non-Gaussian impulsive channels”. In: *IEEE International Conference on Communications, ICC ’99*. Vol. 2. 1999, pp. 907–911.

[82] A. Sklar. *Fonctions de répartition à n dimensions et leurs marges*. Inst. Statist. Univ. Paris 8, 1959.

[83] E.S. Sousa. “Performance of a Spread Spectrum Packet Radio Network in a Poisson Field of Interferers”. In: *IEEE Trans. Inform. Theory* 38.6 (Nov. 1992), pp. 1743–1754.

[84] E.S. Sousa. “Performance of a spread spectrum packet radio network link in a Poisson field of interferers”. In: *IEEE Trans. Inform. Theory* 38.6 (Nov. 1992), pp. 1743–1754.

[85] G. A. Tsihrintzis and C. L. Nikias. “Performance of optimum and suboptimum receivers in the presence of impulsive noise modeled as an $\alpha$-stable process”. In: *IEEE Tran. Commun.* 43 (1995), pp. 904–914.

[86] K.S Vastola. “Threshold Detection in Narrow-Band Non-Gaussian Noise”. In: *IEEE Trans. Commun.* 32.2 (Feb. 1984), pp. 134–139.

[87] S. Verdu. *Multiuser Detection*. Cambridge University Press, 1998.

[88] S. Weber and J.G. Andrews. “Transmission capacity of wireless networks”. In: *Foundations and Trends in Networking*. Vol. 5. 2-3. NOW Publishers, 2012.

[89] M.Z. Win, P.C. Pinto, and L.A. Shepp. “A Mathematical Theory of Network Interference and Its Applications”. In: *Proc. IEEE* 97.2 (Feb. 2009), pp. 205–230.

[90] S. Zozor, J.M. Brossier, and P.O. Amblard. “A Parametric Approach to Suboptimal Signal Detection in $\alpha$-stable Noise”. In: *IEEE Trans. Signal Processing* 54.12 (Dec. 2006), pp. 4497–4509.

# Publications

## Journal papers (Submitted)

- **Robust Receiver Design in Impulsive Subexponential or Gaussian Noises**

  Wei GU, Xin YAN, Gareth W. PETERS, Laurent CLAVIER, François SEPTIER, Ido NEVAT

  Submitted to IEEE transaction on wireless communications

## Conference papers

- **Skew-t copula for dependence modelling of impulsive ($\alpha$-stable) interference**

  Xin YAN, Laurent CLAVIER, Gareth W. PETERS, Nourddine AZZAOUI, François SEPTIER, Ido NEVAT

  2015 IEEE International Conference on Communications (ICC), London, UK, June 8-12, 2015

## COST IC 1004

- **Questions about Interference and Space dependence.**

  Laurent CLAVIER, Xin YAN, François SEPTIER, Gareth PETERS, Ido NEVAT

  IC1004 TD(14)10038, Aalborg, Danemark, May 26-28, 2014

- **Modeling dependence in impulsive interference and impact on receivers**

  Xin YAN, Laurent CLAVIER, Gareth PETERS, François SEPTIER, Ido NEVAT

IC1004 (14)11039, Krakow, Poland, September 24-26, 2014